

UNIVERSITY OF CALGARY

Robust Gain Scheduled Control of a Hydrokinetic Turbine

by

Vincent J. Ginter

A THESIS

SUBMITTED TO THE FACULTY OF GRADUATE STUDIES
IN PARTIAL FULFILMENT OF THE REQUIREMENTS FOR THE
DEGREE OF MASTER OF SCIENCE

DEPARTMENT OF MECHANICAL AND MANUFACTURING ENGINEERING

CALGARY, ALBERTA

June, 2009

© Vincent J. Ginter 2009



Library and Archives
Canada

Published Heritage
Branch

395 Wellington Street
Ottawa ON K1A 0N4
Canada

Bibliothèque et
Archives Canada

Direction du
Patrimoine de l'édition

395, rue Wellington
Ottawa ON K1A 0N4
Canada

Your file Votre référence
ISBN: 978-0-494-54372-6
Our file Notre référence
ISBN: 978-0-494-54372-6

NOTICE:

The author has granted a non-exclusive license allowing Library and Archives Canada to reproduce, publish, archive, preserve, conserve, communicate to the public by telecommunication or on the Internet, loan, distribute and sell theses worldwide, for commercial or non-commercial purposes, in microform, paper, electronic and/or any other formats.

The author retains copyright ownership and moral rights in this thesis. Neither the thesis nor substantial extracts from it may be printed or otherwise reproduced without the author's permission.

In compliance with the Canadian Privacy Act some supporting forms may have been removed from this thesis.

While these forms may be included in the document page count, their removal does not represent any loss of content from the thesis.

AVIS:

L'auteur a accordé une licence non exclusive permettant à la Bibliothèque et Archives Canada de reproduire, publier, archiver, sauvegarder, conserver, transmettre au public par télécommunication ou par l'Internet, prêter, distribuer et vendre des thèses partout dans le monde, à des fins commerciales ou autres, sur support microforme, papier, électronique et/ou autres formats.

L'auteur conserve la propriété du droit d'auteur et des droits moraux qui protègent cette thèse. Ni la thèse ni des extraits substantiels de celle-ci ne doivent être imprimés ou autrement reproduits sans son autorisation.

Conformément à la loi canadienne sur la protection de la vie privée, quelques formulaires secondaires ont été enlevés de cette thèse.

Bien que ces formulaires aient inclus dans la pagination, il n'y aura aucun contenu manquant.


Canada

Abstract

The main objective of this thesis work is to produce a vertical-axis hydrokinetic turbine speed control system that guarantees stability and performance properties for the entire range of operation including tracking of the maximum power point below rated speeds and power regulation above rated speed. Secondary objectives include the ability to explicitly incorporate a tuning method to adjust the important trade-off between reference tracking and load transients as well as ensuring the use of an advanced control methodology with a high probability of industry acceptance.

To facilitate this, an H_∞ linear parameter varying controller was developed based on a physical model of the system and iterative simulation based testing. The final version of the controller was field tested on a 5kW turbine with results compared to a PI controller tuned for reference tracking considerations only. The robust gain scheduled controller performed very well with notably smooth load transitions and good reference tracking characteristics.

Acknowledgements

I would like to thank the following people for their contribution to this thesis work:

My supervisor, Dr. Jeff Pieper, for his advice, guidance, and teaching.

New Energy Corporation Inc. for their incredible support of this work (special thanks to Clayton Bear and Bob Moll).

The University of Manitoba and Manitoba Hydro for their support at the hydrokinetic test site located in Pointe du Bois, Manitoba, Canada.

Dedication

To my family for their patience, encouragement, and unfailing support.

Table of Contents

Approval Page	ii
Abstract	iii
Acknowledgements	iv
Dedication	v
Table of Contents	vi
List of Figures and Illustrations	ix
List of Symbols and Abbreviations	xii
CHAPTER ONE: INTRODUCTION	1
1.1 General Introduction	1
1.2 Motivation for Research.....	3
1.3 Scope.....	3
1.4 Contributions	5
1.5 Outline of Dissertation.....	6
CHAPTER TWO: LITERATURE REVIEW	8
2.1 Introduction	8
2.2 Hydrokinetic Turbine Literature Review	8
2.3 Related Technologies.....	10
2.4 Wind Turbine Control System Research.....	11
2.4.1 Control Using Nonlinear Models	12
2.4.1.1 Perturb and Observe Methods	12
2.4.1.2 Sliding Mode Control	13
2.4.1.3 Direct Imposition of Maximum Power Output	14
2.4.2 Control Using Linear Models.....	15
2.4.2.1 Torque, Power, and Tip Speed Ratio Control Using P, PI and PID.....	15
2.4.2.2 Modern and Intelligent Methods of Torque, Power and TSR Control..	17
2.5 Literature Summary	21
CHAPTER THREE: TURBINE TEST SYSTEM	24
3.1 General Technology Introduction.....	24
3.2 Introduction to Hydrodynamic Operation.....	29
3.3 5kW Test Turbine and Floatation System.....	31
3.4 Power Electronics System.....	34
3.5 Control Hardware and Instrumentation.....	36
3.6 Control Software and Data Processing	39
3.7 Test Site.....	40
CHAPTER FOUR: SYSTEM MODELING.....	44
4.1 Introduction	44
4.2 Turbine Performance Characteristics.....	44
4.3 Physical System Model.....	48
4.4 Linearization of the Equation of Motion.....	51
4.5 LPV model	54

CHAPTER FIVE: CONTROLLER DESIGN	56
5.1 Introduction	56
5.2 General Control Problem	56
5.2.1 Open Loop Stability.....	56
5.2.2 Nonlinearities	59
5.2.3 Time Varying Plant.....	59
5.3 Control Objectives	61
5.4 Control strategy	65
5.5 Controller Synthesis.....	68
5.5.1 Introduction to Gain Scheduled Control for LPV Plants	69
5.5.2 H_{∞} LPV Controller Synthesis	74
5.5.3 PI Controller Synthesis	86
5.5.4 Simulation Results	86
5.5.4.1 Step Response (Region 2).....	87
5.5.4.2 Tracking Response (Region 2).....	90
5.5.4.3 Power Regulation (Region 4).....	94
CHAPTER SIX: IMPLEMENTATION.....	98
6.1 Introduction	98
6.2 Turbine Installation.....	98
6.3 Control Hardware Installation	101
6.3.1 Hardware Enclosures	101
6.3.2 Supervisory Control Levels.....	103
6.4 Problems Encountered During Field Testing	104
6.4.1 Coupling Failure	105
6.4.2 Test Platform Problems.....	106
CHAPTER SEVEN: FIELD TEST RESULTS	108
7.1 Introduction	108
7.2 H_{∞} LPV Controller Test Results.....	108
7.3 PI Controller Test Results	114
CHAPTER EIGHT: SUMMARY AND RECOMMENDATIONS.....	119
8.1 Introduction	119
8.2 Summary of Work	119
8.3 Summary of Results.....	121
8.4 Recommendations for Future Work	122
8.4.1 Quantify Range of Turbulence Levels	123
8.4.2 Generate, Verify and Validate a Higher Order Model.....	123
8.4.3 Revise Control Problem Setup	123
8.4.4 Reduce Required Instrumentation	124
8.4.5 Revise Turbine Speed Reference Generator	126
8.4.6 Field Testing for Power Regulation.....	127
APPENDIX A: TEST TURBINE SPECIFICATION	128
APPENDIX B: PWM AMPLIFIER SPECIFICATION.....	130

APPENDIX C: THREE PHASE RECIFIER AND FILTER SPECIFICATION	131
APPENDIX D: ELECTRICAL LOAD SPECIFICATION.....	132
APPENDIX E: CONTROL HARDWARE	133
APPENDIX F: INSTRUMENTATION SPECIFICATION.....	135
APPENDIX G: SIMULINK CODE	137
REFERENCES.....	138

List of Figures and Illustrations

Figure 3.1: Horizontal and vertical axis turbines (left from [41], right from [76]).....	25
Figure 3.2: Floating, ducted, vertical-axis turbine (from [29]).....	26
Figure 3.3: Floating, unducted, vertical-axis turbine (from [29]).....	27
Figure 3.4: Vertical axis turbine rotor configurations (from [3]).....	28
Figure 3.5: Hydrodynamic force vector diagram (shown from top of rotor).....	29
Figure 3.6: Angle of attack versus rotor azimuth angle.....	30
Figure 3.7: 5kW turbine test system (drive train)	32
Figure 3.8: Turbine, floatation system and trailer	33
Figure 3.9: Electrical system schematic	35
Figure 3.10: Electrical system.....	36
Figure 3.11: Control system architecture (from www.ni.com).....	37
Figure 3.12: Custom tone wheel and Hall sensor for turbine rpm.....	38
Figure 3.13: Laptop human machine interface for control testing.....	40
Figure 3.14: Pointe du Bois, hydrokinetic turbine test site (drawing from the University of Manitoba).....	41
Figure 3.15: 5kW test turbine system mounted behind 25kW system.....	42
Figure 4.1: Coefficients of performance and torque versus tip speed ratio.....	47
Figure 4.2: Hydraulic torque ripple example.....	48
Figure 4.3: Generalized system (left), FBD low speed system (center), FBD high speed system (right).....	49
Figure 4.4: Comparison of quadratic approximation for C_t and test data.....	53
Figure 5.1: Turbine torque versus rpm for different free stream velocities.....	57
Figure 5.2: Turbine power versus rpm for different free stream velocities.....	57
Figure 5.3: Power regulation by reducing turbine rpm to reduce system efficiency	62

Figure 5.4: Four regions of turbine operation (power versus water velocity)	66
Figure 5.5: Control strategy example for turbine power versus rpm	66
Figure 5.6: General augmented LPV plant	72
Figure 5.7: General interconnected system.....	75
Figure 5.8: Two port diagram with weighting functions.....	76
Figure 5.9: Frequency response for error and control weighting functions.....	78
Figure 5.10: Convex region of possible operating points.....	80
Figure 5.11: Closed loop implementation of the H_∞ LPV controller	81
Figure 5.12: H_∞ LPV, 15 step responses for 15 frozen parameter sets	82
Figure 5.13: Fifteen parameter sets $\theta = [\bar{\Omega}_R, \bar{V}_\infty]$ chosen for step response	82
Figure 5.14: Fixed point control, 15 step responses for 15 frozen parameter sets.....	83
Figure 5.15: H_∞ LPV closed loop magnitude and phase plots for $\theta = [69.1, 2.25]$	84
Figure 5.16: Twenty second time varying parameter trajectory shown inside polytope...85	
Figure 5.17: H_∞ LPV step response for time varying parameters	85
Figure 5.18: Simulation PI controller step response	88
Figure 5.19: Simulation H_∞ LPV step response	89
Figure 5.20: Simulation PI tracking response results.....	92
Figure 5.21: Simulation H_∞ LPV tracking response results.....	93
Figure 5.22: PI tracking response under power regulation	96
Figure 5.23: H_∞ LPV tracking response under power regulation.....	97
Figure 6.1: Turbine initially deployed behind larger 25kW test platform.....	98
Figure 6.2: Log removal	99
Figure 6.3: Rebuild of turbine drive system	100
Figure 6.4: Weather proof control testing hardware on test platform.....	102
Figure 6.5: Laptop placement in metal instrumentation enclosure	103

Figure 6.6: Turbine Stall Test	104
Figure 7.1: H_{∞} LPV Step and auto response rpm versus time	109
Figure 7.2: H_{∞} LPV Step and auto response load current versus time	109
Figure 7.3: H_{∞} LPV Step and auto response flow speed versus time.....	110
Figure 7.4: H_{∞} LPV Step response rpm versus time	111
Figure 7.5: H_{∞} LPV Step response load current versus time	111
Figure 7.6: H_{∞} LPV Step response flow speed versus time.....	112
Figure 7.7: H_{∞} LPV Auto tracking response rpm versus time	113
Figure 7.8: H_{∞} LPV Auto tracking response load current versus time.....	114
Figure 7.9: H_{∞} LPV Auto tracking response flow speed versus time	114
Figure 7.10: PI Step response rpm versus time.....	115
Figure 7.11: PI Step response load current versus time.....	115
Figure 7.12: PI Step response water speed versus time.....	116
Figure 7.13: PI Auto tracking response rpm versus time	117
Figure 7.14: PI Auto tracking response load current versus time	117
Figure 7.15: PI Auto tracking response flow speed versus time.....	118

List of Symbols and Abbreviations

$\hat{}$	Denotes deviation of a variable with respect to steady state
$\bar{}$	Denotes the steady state value of a variable
A, B, C, D	System state space matrices
A_t	Turbine cross sectional area
c	Gearbox ratio
C_P	Coefficient of performance
C_T	Torque coefficient
e	error
\tilde{e}	Weighted error
g	Gravitational constant
h	Height of rotor
H_2	Hardy space of square integrable functions
H_∞	Hardy space of bounded functions
i_q	Portion of stator current due to real power
J	Equivalent polar moment of inertia of turbine system reflected to low speed shaft
J_{HS}	Rotating inertia of high speed system
J_{LS}	Rotating inertia of low speed system
K_G	Generator torque constant
k_V	Linearization constant of hydraulic torque with respect to water speed
k_ω	Linearization constant of hydraulic torque with respect to rotor speed
M_s	Peak sensitivity magnitude

M_u	Peak control sensitivity magnitude
n	Number of generator pole pairs
P_T	Turbine power
Q	Flow rate
R	Turbine rotor radius
T_G	Generator torque
T_H	Hydraulic torque
T_{zw}	General input, output transfer matrix
u	General control input
\tilde{u}	Weighted control input
V	Flow velocity
V_∞	Undisturbed free stream velocity
w	Disturbance
W_e	Error weighting function
W_u	Control weighting function
z	Performance output
β	Drive system loss proportionality constant
γ	Performance level
Δ_H	Total head differential
ε	Maximum steady state error
η	Hydraulic efficiency
θ	Parameter vector
λ	Tip speed ratio
ρ	Density of water
Φ	Permanent magnet flux
ω_b	Error weight bandwidth
ω_{bc}	Controller bandwidth
Ω_G	Angular velocity of generator
Ω_R	Angular velocity of turbine rotor

$\dot{\Omega}_G$	Generator angular acceleration
$\dot{\Omega}_R$	Rotor angular acceleration
AC, DC	Alternating current, direct current
DAQ	Data acquisition
FBD	Free body diagram
FPGA	Field programmable gate array
HSS	High speed shaft
IGBT	Insulated gate bipolar transistor
LMI	Linear matrix inequality
LQG	Linear Quadratic Gaussian
LPV	Linear parameter varying
LSS	Low speed shaft
LTI	Linear time invariant
MPPT	Maximum power point tracking
NEMA	National Electric Manufacturers Association
P, PI, PID	Single, two or three term controller (proportional, integral derivate)
PDQ stability	Parameter dependent quadratic stability
PMG	Permanent magnet generator
PWM	Pulse width modulation

Chapter One: Introduction

1.1 General Introduction

With rising concern over greenhouse gas emissions, the environment, depletion of fossil fuels and rising electricity demand; sustainable sources and environmentally friendly methods to meet this demand are being considered. One such source is kinetic energy stored in moving water such as rivers, tidal streams, and ocean currents (created by salinity or thermal gradients). The leading technology for exploitation of this resource is the hydrokinetic turbine (also known as in-stream, or zero head turbines). These turbines do not require barrages or dams. They also maintain very low rotor pressure drops and rotor speeds compared to traditional hydro installations giving them a considerably smaller environmental footprint. They maintain higher capacity factors than other renewable sources such as wind (generally 42% compared to about 32% for wind) and are a much more predictable resource making integration into existing generation portfolios much easier.

The majority of the development of this technology is quite recent (over approximately the last five to eight years) though original patents go as far back as 1931 (the original Darrieus patent). A brief development period in the early 1970's was carried out (most notably with the Coriollis Project in the United States) and a significant effort was carried out by the National Research Council of Canada and Natural Resources Canada through the 1980's. With such close relation to wind turbine technology, hydrokinetic systems have benefited from the many years of advancement in the wind industry including the variable speed nature of the turbine for optimal energy extraction.

However, purpose built power conversion systems and turbine speed controllers are not available off-the-shelf.

One local company from Calgary, Alberta, called New Energy Corporation Inc. is developing this turbine technology with existing products of 5 kW, 10 kW and 25 kW. Larger 125 kW and 250 kW systems are currently in development. These systems utilize off-the-shelf small-wind power conversion packages with integrated turbine speed control systems. While these systems provide reasonable operational characteristics, a purpose built power electronics package and turbine speed controller would significantly improve all aspects of operation.

This thesis work addresses the problem of turbine speed control over the entire operating envelope for an unducted, fixed pitch, variable-speed, vertical axis, 5 kW hydrokinetic turbine. Due to the early nature of development, little published work on hydrokinetic turbine control is available. Thus, wind turbine control research was investigated to find the most promising control synthesis procedure applicable to this new turbine technology with an emphasis on industrial application and operator acceptance of the control methodology. This is a very complex problem involving a highly nonlinear plant with a wide operating range that is open loop unstable and non-minimum phase over a significant portion of the operating envelope. A mathematical model of the plant was generated from physical principles. An H_∞ LPV (linear parameter varying) controller was developed for a 5kW hydrokinetic turbine, including identification of control objectives and generation of a control strategy which were thoroughly tested with a simulation model developed specifically for the field test unit. The test turbine was supplied by New Energy Corporation Inc who also provided funding for the assembly of

a rapid prototyping test platform which was used for field testing of the turbine speed control algorithm. The hydrokinetic turbine test site located at Pointe du Bois, Manitoba, was provided by the University of Manitoba with the support of Manitoba Hydro (currently the only hydrokinetic turbine test site in Canada).

1.2 Motivation for Research

The motivation for this research is the recent development of hydrokinetic turbine technology (facilitated by favourable political and economic climates due to concern for the environment), for which a purpose built control system simply does not exist. To enable wide spread adoption of this technology it must attain a comparable cost of electricity to that of traditional sources, while maintaining ease of use and reliability. Thus, lean design methods, high system efficiency and long system life are essential to meeting these requirements which are made possible in a large part to an advanced control system. The control system has the ability to;

1. reduce load transients (which facilitates lean design methodology) and increase life of mechanical and electrical components
2. maintain high overall efficiencies by forcing operation to the optimal energy extraction point for a large range of operating conditions
3. allow system monitoring and adaptation as required to account for plant changes and prevent or minimize system damage

1.3 Scope

The scope of this research work is limited to development of a turbine speed control algorithm suitable for the entire range of operation, but not including system start-

up, shutdown, or supervisory control. It is assumed that the required load is always available for control purposes as is the case when distributed resources are used in conjunction with much larger generation sources on a common grid (i.e.: the grid acts as an infinite sink). This differs from stand alone generation systems or central power generation where this assumption does not apply. It also does not address implementation concerns directly but discusses some related points due to the nature of the testing carried out. Thus, system monitoring, proper enclosures, processor power, required memory and related concerns are not addressed. The following are in the scope of the project;

- Derivation of a mathematical model of the system for use in both control synthesis and simulation based testing.
- Perform a literature search to provide reasonable background on previous work as well as informed choice of a control synthesis procedure.
- Outline control objectives and define a control strategy.
- Carry out controller synthesis meeting all the requirements for the H_∞ LPV control algorithm.
- Generate a PI controller for comparative results generated during simulation and field tests.
- Specify, acquire, build and integrate all necessary hardware, software, and instrumentation to produce a control algorithm rapid prototyping platform to facilitate field testing of the control algorithms.
- Locate a suitable test site, attain required permissions, schedule testing and coordinate logistics for test turbine and control hardware.

- Field test controller. Perform all equipment assembly, maintenance, installation, removal and decommissioning tasks associated with field testing.
- Generate a comprehensive report meeting all stake holders' requirements (University of Calgary as well as the industry partner New Energy Corporation Inc).

1.4 Contributions

This thesis is a preliminary work at the early stages of development for a new electric power generation technology. Contributions include;

- A complete review of published work reveals that this thesis work involves an application of a relatively new control methodology to a new field of application (hydrokinetic turbines).
- A linear parameter varying model of the turbine system was derived from first principles and based on performance information gathered from the industry partner.
- A set of control objectives and a control strategy were defined.
- An H_∞ LPV controller was synthesized and tuned through iterative simulation based testing to achieve the desired tradeoff between reference tracking and load transient magnitude.
- A fixed point PI controller was generated and tuned for the small range of flows realized at the field test site. This was used for comparative testing of a controller designed for good tracking response without considering destructive load transients.

- Field testing of the H_{∞} LPV controller as well as the PI controller was carried out and demonstrated the superior characteristics of smooth load transitions for the gain scheduled controller while maintaining excellent reference tracking performance.
- Propose six important recommendations for future work based on results of this testing.

1.5 Outline of Dissertation

The thesis material is presented as follows;

- **Chapter Two** contains a literature review on hydrokinetic turbine speed control systems. Due to the small number of papers located for this topic, another search for the closely related technology of wind turbine variable speed control is presented. This allowed results of a much better developed field of work to be directly applied to the current problem significantly accelerating the research process.
- **Chapter Three** provides a general technical introduction to the field of hydrokinetic turbines (including basic hydrodynamic operation). The research turbine and related control hardware (power conversion hardware and industrial real-time controller) used for the field work portion of this research are also outlined followed by details of the test site.
- **Chapter Four** details the methods used to produce the turbine system model. Turbine performance information and special operational considerations are also discussed.

- **Chapter Five** discusses the general control problem and provides a high level introduction to the general H_∞ LPV control synthesis procedure. Control objectives are developed and a control strategy chosen. Control synthesis for both the H_∞ LPV controller and PI controller are carried out. Simulation based results are presented and discussed.
- **Chapter Six** outlines the implementation details associated preparation of all equipment and hardware setup as well as operational problems encountered during the field testing portion of this work.
- **Chapter Seven** presents and discusses field testing results for both control systems.
- **Chapter Eight** provides a summary of all work, summary of results and a set of recommendations for future work.

Chapter Two: Literature Review

2.1 Introduction

This chapter outlines previous work completed on hydrokinetic turbine speed and load control systems. Though there is much development on these types of control systems being carried out in industry today, little work has been published. Since wind turbine control systems are a much more mature technology, and closely related in operating principles and system dynamics, they have been identified as a reasonable starting point for control system work. Literature relating to hydrokinetic turbine control systems is reviewed first, followed by a discussion of related control technologies and the state-of-the-art of wind turbine control systems.

2.2 Hydrokinetic Turbine Literature Review

A search was performed to identify control system research carried out for both horizontal and vertical-axis hydrokinetic turbines. Most of the published work for hydrokinetic turbines is concerned with hydrodynamic rotor design ([43], [44], [76], and [81]); duct design ([45], [71], and [78]); mechanical design ([30] and [87]); and fluid dynamic modelling ([33] and [93]). Only four papers were located that discuss control systems for this technology. The first two papers ([19] and [60]) discuss condition monitoring, high level implementation concerns and plant management concepts without disclosing any turbine load control system information. The third paper [48] focuses more on the power electronics system and its control, again without discussing the turbine variable speed control in any detail. In the fourth paper [88], Tuckey outlines a fixed PID controller used for tracking the maximum power point of the system using the

tip speed ratio approach. In this approach a water speed measurement and the optimal tip speed ratio value are used to calculate the turbine speed reference. Since the maximum power point of the turbine was known to occur at a fixed tip speed ratio, it could be used to calculate the turbine speed setpoint corresponding to peak extraction efficiency which is then fed into the PID controller. In this case load current was the control variable. This control was used for the range of velocities found at the tidal site and was satisfactory over a limited tip speed ratio and operating range.

One last academic work found at Memorial University of Newfoundland is currently in progress and thus no associated publication is yet available. Discussions with the PhD candidate carrying out the work outlined that this thesis work is based on developing a fuzzy logic load controller for variable-speed, vertical-axis, hydrokinetic turbine speed control [42]. The controller design and experimental work have been completed but the thesis write up is not scheduled for completion until mid 2009.

Finally, there is much work being carried out in industry. Marine Current Turbines [59] has completed the *Seaflow* demonstration project off Foreland Point, near Lynmouth, on the North Devon coast of England, part of which was extensive variable speed control system work. The details of this work have not been made public. Both Verdant Power LLC [91] and Clean Current Power Systems Inc [20], are presently field-testing variable speed kinetic turbine systems in the New York East River, and Race Rocks, British Columbia respectively. Again the results are proprietary and have not been made public. New Energy Corporation Inc (NECI) [65] has developed a variable speed turbine system using an off-the-shelf small wind turbine controller and power electronics system that functions reasonably well over the operating range, but lacks

desired functionality. Specifically, the system lacks power regulation ability and stability in the immediate region of peak efficiency operation. The controller uses a lookup table of applied load versus inverter DC input voltage to modify turbine speed. Since the generator is a brushless permanent magnet type, the output voltage is linear with generator speed. Thus the passively rectified DC voltage is also proportional to generator speed allowing control based on the DC inverter input voltage.

Little published work on hydrokinetic turbines is available. Knowledge of control objectives, challenges (regarding strategies as well as implementation issues) and respective solutions is not available.

2.3 Related Technologies

Due to the lack of published material available for hydrokinetic turbine control systems, and a desire to speed the evolution of a control system for hydrokinetic turbines, control system work from a related but better developed technology was sought.

A reasonable starting point would seem to be traditional hydro turbine controllers, but these systems have significant differences from hydrokinetic schemes. Traditional hydro systems are constant speed, with direct grid-connected synchronous generators, flatter torque curves, and smaller flow parameter variations. The operational principles and environments are considerably different. They use linear PI or PID control and assume one fixed set of parameters for all operating conditions. Despite the simple control structure, this type of control is usually adopted because it provides reasonable performance and is well known among industrial operators [101].

Wind turbine systems have much more in common with hydrokinetic turbines as they are both derived from common physical principles of operation, have similar drive and electrical systems and share similar performance characteristics ([6], [7], [24] and [60]). Since wind turbine, variable-speed load control systems benefit from approximately twenty five years more development time, a thorough literature search was performed to define its state-of-the-art and thus serve as a starting point for variable speed, hydrokinetic turbine control considerations.

2.4 Wind Turbine Control System Research

Research for wind turbine variable speed control systems is very well developed with a great deal of research carried out from the early 1980's to present. The literature search is restricted to fixed-pitch, variable speed wind turbines to coincide with the fixed pitch variable speed hydrokinetic turbine with which this thesis work is concerned. Generally controller synthesis for two control regions is discussed. The first regards control for below rated wind speed. The rated wind speed is the wind speed that corresponds to the rated power of the turbine system. In this region (we shall call this Region 2 to remain consistent with later work in this thesis in Section 5.4 on control strategies) turbine speed is adjusted to attain maximum power for a given wind speed. The second region (we shall call Region 4) is for control above rated wind speed. In this region the power output is maintained at or below the rated power of the turbine (also known as power regulation).

Literature describes two broad classes of control for both regions of operation. The first uses the nonlinear model of the system with the second using linear models ([16] and [17]).

2.4.1 Control Using Nonlinear Models

There are several approaches in literature using nonlinear models. Though this list is not exhaustive, those that do not appear are either not well developed, highly experimental or do not incorporate explicit methods for load transient mitigation and are thus not well suited for initial consideration of hydrokinetic turbine control.

2.4.1.1 Perturb and Observe Methods

Perturb and observe methods are also known as hill climbing or maximum power point tracking (MPPT) techniques. These methods have the benefit of requiring relatively little information about the plant other than general knowledge such as rated power, rotational speed range, etc. Several approaches are noted, most of which were developed for Region 2 (maximum power tracking) operation, though most can be extended to Region 4 (power regulation) as well.

First, derivative techniques rely on estimation of key variable gradients (usually active electrical power and turbine speed in order to calculate $\partial P / \partial \Omega$) and their sign in order to drive their values to zero ([23], [28], [94], and [95]). Since wind turbine power-speed curves are unimodal functions for a given wind speed, this corresponds to the maximum power for a given set of operating conditions. These methods are quite simple, but lack flexibility. The main drawbacks of these methods (caused by wind speed fluctuations and high rotating inertia) are large gradient estimation errors and power

fluctuations which in turn cause drive system reliability issues. These issues can be improved with the use of Fuzzy Logic control ([1], [83], and [84]) as well as the use of advanced estimation techniques such as neural network based wind speed estimators presented in [80], online system identification, and a Kalman filter for aerodynamic torque in [102].

A slightly different method based on extremum seeking techniques presented in [5] use sinusoidal probing signals to excite the plant thus enabling the search process. This method is adapted in [64] for variable speed wind turbine systems where it is shown that the wind turbine plant is naturally excited by random wind turbulence, which serves as a natural perturbation for the extremum search process. This method was demonstrated to have performance benefits over traditional MPPT, based on simulations (where it was assumed reliable turbine power, wind speed and rotational measurements are available). Performance of the controller increases as turbulence levels increase and it was noted that an adaptive law of the search speed increases flexibility of the system (for tuning purposes).

2.4.1.2 Sliding Mode Control

Another technique employed in both regions 2 and 4 is that of sliding mode control ([10], [16], and [26]). To increase flexibility in the tradeoff between tracking maximum power while maintaining allowable drive system transients, combined switching surfaces are used to allow multi-criteria optimization adjusted with a tradeoff coefficient. The control sliding surface cannot be the optimal operating curve itself, but must be designed to operate in the neighbourhood of this curve implicitly allowing the possibility of limiting the control effort [17]. An expression for the quantitative tradeoff

between tight tracking and drive system force/torque transients has not yet been derived for this type of control structure employed in wind turbine systems. Note that in systems where the electromagnetic torque is the control input, mechanical stresses may also increase due to chattering.

2.4.1.3 Direct Imposition of Maximum Power Output

This method is one of the first used widely in industry for medium to large wind turbine systems and is known as the $k.\Omega^2$ algorithm ([17], [36]). Essentially, the optimal torque of the wind turbine, for any static operating point, can be solved from the nonlinear model in terms of the turbine rotational speed alone, leaving all other terms constant and thus lumped into the k term. For instance, from Section 4.1 in this thesis solve Eq. 4 for the free stream velocity V_∞ and substitute the result into Eq. 3. Then solve for the hydraulic torque T_H , noting that the torque coefficient C_T and tip speed ratio λ correspond to those of peak power extraction and are therefore constant. The result is

$$T_H = \frac{1}{2} C_T \rho A_t R^3 \left(\frac{\Omega}{\lambda}\right)^2 = k \Omega^2$$

where

$$k = \frac{1}{2} C_T \rho A_t R^3 / \lambda^2$$

A_t = turbine area

R = turbine rotor radius

ρ = density of flow medium

Ω = angular velocity of the turbine rotor.

Thus, the turbine rotational speed is measured, squared and multiplied by the gain k to find the generator torque demand (which in this case is the control input). This of course

assumes a great deal of knowledge about the particular plant (torque, speed characteristics, etc). The benefit of this control is that it is simple to employ and only requires a measurement of rotational speed (not wind, power measurements, or estimates). The drawbacks are that it does not work well with high inertia systems where a great deal of time is spent off the theoretical maximum operating curve as well as inflexibility in adjusting the tradeoff between tracking performance and torsional transients.

A variant of this control structure is also used in industry for many small wind systems ([72], [85], and [98]). The control law is the same, but the implementation uses a lookup table of input voltage versus load power (essentially equivalent to generator speed and load current since they are used with permanent magnet generators [65]) instead of the traditional k value. This enables ease of entering wind turbine information by the customer since many small wind power electronics manufacturers only build inverter packages and not the wind turbine for which they might be used.

2.4.2 Control Using Linear Models

2.4.2.1 Torque, Power, and Tip Speed Ratio Control Using P, PI and PID

There are a wide range of control systems in literature using linear models. Likely the most widespread employed in industry is a variant of the $k.\Omega^2$ algorithm commonly known as *torque control* ([52] and [36]). In this case the optimal torque setpoint is again calculated based on information of static turbine performance and rotational speed, but is compared with a generator torque estimate to formulate an error signal used as input to a P, PI, or PID controller (most popular with induction generators and conversion systems

where PI controllers are commonplace). This allows adjustment of the reference tracking versus torsional transient tradeoff and has the benefit of not requiring wind speed information. However it suffers from poor overall performance since it does not allow proper tracking within mechanical load limits [17]. Note that the system is normally linearized about some fixed operating point in the middle of the parameter range and thus performance is sensitive to the operating point of the plant.

Two more popular variants of this scheme are *power control* and *tip speed ratio control*. *Power control* is very similar to *torque control* except that power is now proportional to Ω^3 (instead of Ω^2 as in torque control), with the power reference calculated in the same manner. An estimate of turbine power based on active electrical power output is compared with the calculated power reference, and the error fed to a P, PI or PID controller ([37] and [63]). This method has the same advantages and disadvantages as torque control.

Tip speed ratio control is based on the fact that optimal power or torque is realized at a unique and fixed value of the tip speed ratio for any value of wind speed in the operational envelope ([88] and [17]). Therefore, with a wind speed measurement, this value of tip speed ratio is used to calculate the turbine rpm setpoint. The turbine speed is the feedback variable and the error, formed by comparison of the turbine speed and reference, is passed into a controller (typically P, PI, or PID though other methods will be discussed in 2.4.2.2).

Though for many years, torque control with a fixed controller was used successfully, many companies are looking to employ methods to modify the controller based on the operating point. For instance, [38] uses measurements of turbine power and

wind power as the basis for a gain adaptation law within the $k.\Omega^2$ torque control scheme. In [40] a method to schedule both PI gains for *tip speed ratio* control based on the absolute error between the rpm and rpm setpoint is outlined.

2.4.2.2 Modern and Intelligent Methods of Torque, Power and TSR Control

Many modern control techniques as well as new methods of adjusting controller parameters are being researched in academia today. A large number of these projects are carried out with industry collaboration. Some methods based on optimal control techniques (such as H_2 and H_∞) and modern adaptive methods (such as direct model reference adaptive control and gain scheduling) are reasonably well developed, with intelligent adaptive techniques in earlier experimental stages. A representative set of works is presented here to demonstrate the range of control methodologies for completeness.

Novak and Ekelund [66] use Linear Quadratic Optimal control designed using a single operating point (single wind speed) for below rated operation in Region 2. While it is shown that the controller has reasonable performance within the neighbourhood of the design point, Leithead and Connor [52] reveal that performance (and even stability) outside this neighbourhood cannot be maintained. In [28] Ekelund develops a gain scheduled Linear Quadratic Gaussian (LQG) control which works well over the entire operating range. The controller uses an *ad-hoc* method to schedule the controller parameters based on an estimate of the torque (thus switching to the controller specified for a particular operating range).

In [73] a comparison of H_2 and H_∞ controllers is presented for a multivariable pitch regulated wind turbine where the generator torque and pitch angle were the control

inputs. The H_2 controller was noted to perform considerably better than the H_∞ counterpart for reference tracking, though it was noted that the latter retained superior disturbance rejection characteristics. Both controllers were linearized about a single operating point, and it was noted that the H_2 controller became unstable when operation moved too far from the linearization point. This emphasizes the need for some method of accounting for nonlinearities in the control scheme, and thus the methods presented in [73] cannot be used directly.

Advanced methods of adjusting controller parameters have been noted in many works. In [22], online parameter estimation is employed to find unknown parameters of a linear model from which the controller is calculated (the so-called one step ahead adaptive control technique). The emphasis here is on voltage and frequency stability in a standalone system, so mechanical stresses are ignored. It is also noted in [28] that this type of online parameter estimation does not respond to operating point changes quickly enough compared to other techniques such as gain scheduling. In [39] neural networks are used to modify proportional, integral and derivative coefficients for an adaptive PID controller. Neural networks are used to perform a plant identification process offline, which is then used to minimize an energy function online that is solved for the corresponding P, I and D coefficients. It was shown that as parameters varied, reasonable tracking was achieved. However, mechanical stresses are not considered at all, and no method of introducing flexibility for the tracking/stress tradeoff is obvious.

An older method to account for plant nonlinearities and increase energy extraction uses switching between two predetermined, discrete speeds [52]. As the operating point moves, the fixed turbine speed is switched to increase control performance and energy

extraction. This control is relatively simple, but does not perform as well as more advanced methods using continuously variable speed such as switched linear control [50]. Note that in [50] a nonlinear control gain is adjusted for variable pitch systems based on pitch angle demand (method is outlined in [53]) thus effectively linearizing the system and allowing linear control techniques to be employed.

In [31] a direct model reference adaptive controller is developed in which the gains of the system are adapted so the output of the plant matches that of the reference model. It was shown that while good performance is obtained for power regulation, operation for below rated power suffers due to the inability of the gains to be adjusted quickly enough.

In [49], a nonlinear model predictive controller modified with an internal linear model removes the need for quadratic criterion minimization using the nonlinear model. This saves considerable computation time for which many model predictive control schemes are notorious. The controller works well and explicitly takes into account bounds on input and output variables in the synthesis, but the issue of mechanical loading was not addressed.

Feedback linearization has also been used in [17]. While the method appears to work reasonably well, linearizing the plant in this way is quite difficult due to system uncertainty. In [90] an adaptive feedback linearization approach is employed to deal with these uncertainties, though the parameters that assign the tracking error (based on turbine speed) and torque estimator dynamics also affect the size of the region where convergence is guaranteed.

Finally, gain scheduling techniques are quite common in industry. Traditional wind turbine gain scheduling involves either introduction of a nonlinear gain in the controller (as in [53]), incorporation of an inverse function cancelling the static nonlinearity ([54] and [62]) or simply designing multiple linear control systems for various stationary operating points ([28], [51], and [68]); all of which are varied based on changes in chosen scheduling variables to provide a valid global control structure. In more general terms traditional gain scheduling techniques are related with a family of linear time invariant (LTI) controllers and an algorithm that changes the applied controller based on the operating point. While this control method is widely adopted by practicing engineers in many industries due to the intuitive approach of dealing with nonlinearities, little has been accomplished in the way of theory. Thus performance and even stability cannot be guaranteed for the nonlinear time varying closed loop system. Even worse, the issue of modifying the control structure based on the developed family of LTI controllers is seldom treated in literature, though methods involving simple switching of controllers or interpolation have been noted.

A relatively recent development in gain scheduling that is quickly gaining popularity in wind turbine control, involves the theoretical formulation of gain scheduling in an LPV framework ([12], [13] and [56]). LPV design generates a single controller (as opposed to a family of controllers in traditional gain scheduling) with guaranteed global stability and performance for arbitrarily fast parameter variations. Introducing the concepts of robust control within the LPV framework results in a synthesis procedure similar to that of H_∞ , allowing control objectives to be stated in the form of bounds on an induced norm of respective input-output functions [14]. In [67], H_∞ LPV control is shown

to perform better than traditional gain scheduling methods in both regions two and four operation with a single controller. The superior characteristics for alleviation of loading transients is also proven in [57]. Advantages of this method include a means of incorporating control objectives in the synthesis, explicit adjustment of the reference tracking versus load transient magnitude tradeoff using weighting filters, explicit incorporation of modelling uncertainty and ability to use well developed linear control techniques.

2.5 Literature Summary

Due to the relatively recent development of hydrokinetic turbine technology, only a single relevant turbine control paper was located. This outlined the use of the *tip speed ratio* method using speed feedback with a PID controller (all of which were borrowed from the wind industry). Though much work is currently being carried out in industry as confirmed by the many demonstration projects in service, little has been published due to its proprietary nature.

Research shows that wind turbines and hydrokinetic turbines share the same basic principles of operation as well as performance and operational characteristics (even sharing similar drive and electrical system layouts). It is also known that variable speed wind turbine control benefits from approximately twenty five years of research and is thus in a relatively advanced stage of development. Thus, in an effort to speed hydrokinetic control investigations using the most relevant, advanced and developed methods, a literature search for variable speed, fixed pitch wind turbine control systems was completed.

Two broad approaches are outlined. The first utilizes the nonlinear system model for popular control methods of perturb and observe, sliding mode control or direct imposition of maximum output power. All the methods in this approach aim to maximize power without consideration of mechanical loading transients. Perturb and observe as well as sliding mode control have been shown to induce considerably higher levels of mechanical loading through the naturally oscillatory nature of these control approaches. They have also demonstrated issues with unacceptable convergence time in some instances. Methods to alleviate these induced loading transients have been attempted such as the use of Fuzzy Logic and advanced estimation techniques using neural networks with various levels of success. Most of these advanced techniques are in early stages of development. Direct imposition of maximum power (or torque) output has been shown to perform poorly for tracking considerations, with significant time spent off the optimal power points and has no explicit method for adjusting load transient magnitude.

The second broad wind control approach uses linear system models. A great many synthesis procedures are discussed ranging from classical P, PI and PID, to adaptive techniques using direct model reference control with online parameter estimation, predictive control, robust control methods, feedback linearization and gain scheduling. In almost all works, the need for a method to account for nonlinearities in an effort to maintain performance and stability is obviated. While the industry standard PI torque and power control (using $k.\Omega^2$ and $k.\Omega^3$ respectively) are currently the most widely used, they demonstrate poor tracking performance since the control is significantly detuned for the system to remain within mechanical load limits.

One of the most promising control schemes is H_∞ LPV since it results in a single controller for all operating points (without the need to generate a separate scheduling algorithm), allows direct incorporation of control objectives, and utilizes tuning parameters in the form of weighting functions for adjusting importance of relative objectives. Many papers site superior tracking and load alleviation abilities compared with other techniques ([14], [57]). Though development of this control theory is relatively recent (within the last 15 years), field testing on wind turbines is already noted in literature ([67]). While many advanced control techniques suffer from technology transfer issues, H_∞ LPV control holds many similarities to traditional gain scheduling which is already widely used in industry, and is thus more likely to find industry wide acceptance.

Chapter Three: Turbine Test System

3.1 General Technology Introduction

The hydrokinetic turbine system used in the present work is a new variant of water turbine more akin to wind turbine technology than traditional high head water turbine systems. While traditional hydroelectric systems (commonly based on Kaplan, Francis or Pelton turbines) extract energy from the potential component alone, hydrokinetic turbines extract energy from the kinetic component of a flow. Due to the similarities with wind turbine technology, development of hydrokinetic turbines has benefited greatly from wind turbine research allowing significantly reduced development timelines for the near commercial systems found in various demonstration projects around the world today (Marine Current Turbines *SeaFlow* project [59], Clean Current's project at Race Rocks [20], Verdant Power's New York East River installation [92] and New Energy Corporation's Pointe du Bois project [65]). However, significant differences from wind also exist such as lower tip speed ratio ranges, cavitation limits and the requirement to deal with harsh marine environments.

Hydrokinetic turbines can be drag based (such as a Savonius rotor [41]) or reaction based (using principles of lift such as the Darrieus rotor [29]), though most systems in development now are reaction types. Generally hydrokinetic turbines are categorized by;

- orientation of rotational axis (horizontal and vertical)
- implementation (free stream or restricted flow)
- flow augmentation (ducted or unducted)

- fixed or variable speed
- fixed or variable pitch
- rotor geometry

Horizontal axis turbines (shown on the left in Fig. 3.1) operate with the rotor rotational axis parallel to the flow direction, whereas vertical axis turbines (also known as cross flow turbines and shown on the right in Fig. 3.1) have a rotational axis perpendicular to the flow.

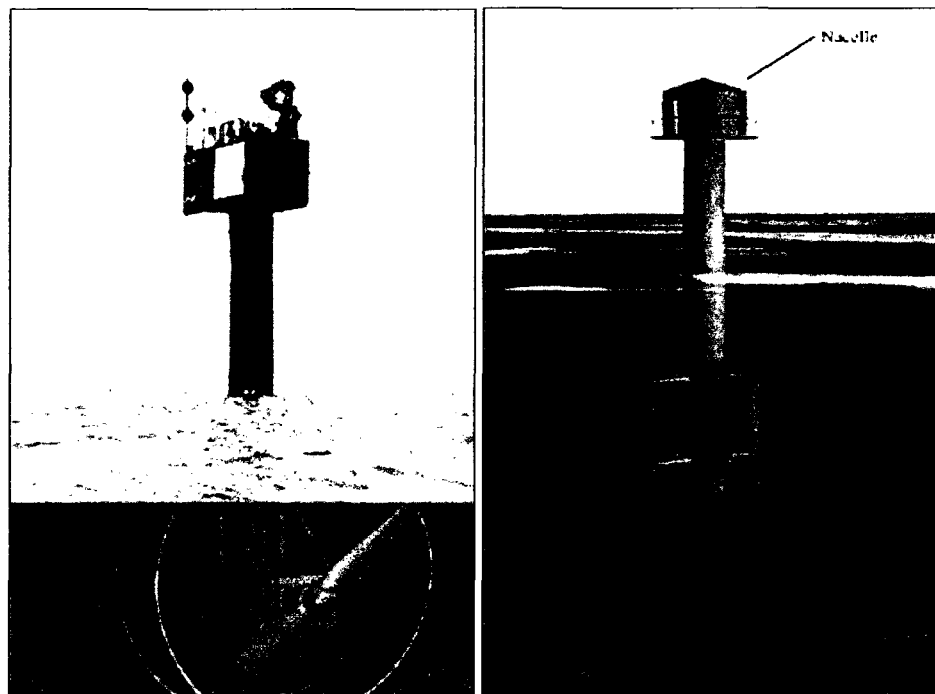


Figure 3.1: Horizontal and vertical axis turbines (left from [41], right from [76])

Horizontal axis turbines usually have higher starting torques and lower shaft torque pulsation amplitudes, though vertical axis systems have more flexible form factors and allow the opportunity for drive bearings, gearboxes and generators to be situated above the waterline increasing reliability and ease of maintenance [65].

A free stream turbine implementation is one where a potential head is not imposed across the system (for example a small turbine in a wide river or tidal stream). Conversely restricted flow implementations impose a potential head differential across the installation due to large blockage ratios (such as in a low head dam or by closely spacing turbine units in a flow).

Ducting is sometimes used to augment the flow through the rotor (especially in low velocity flows) and can allow larger power outputs with smaller rotors [45] compared to unducted units. A floating version of a ducted turbine is shown in Fig. 3.2. This was a system tested by the National Research Council of Canada in 1984 [29]. The same turbine had the ducting removed and was tested in an unducted configuration for comparative purposes (shown in Fig. 3.3) and overall hydraulic efficiencies were found to be similar. Ducted and unducted versions of a free stream turbine are equally prevalent in industry.

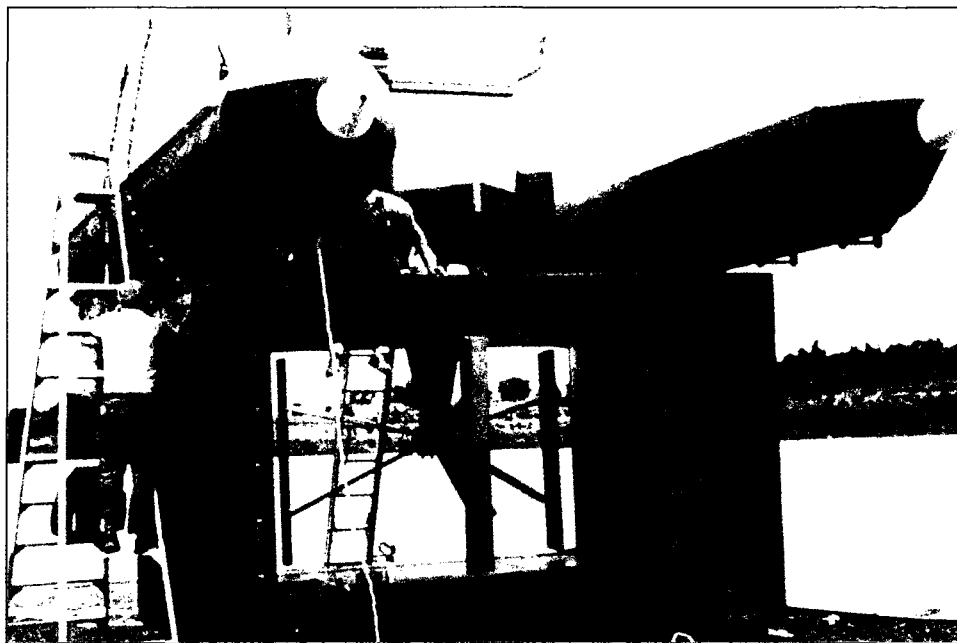


Figure 3.2: Floating, ducted, vertical-axis turbine (from [29])

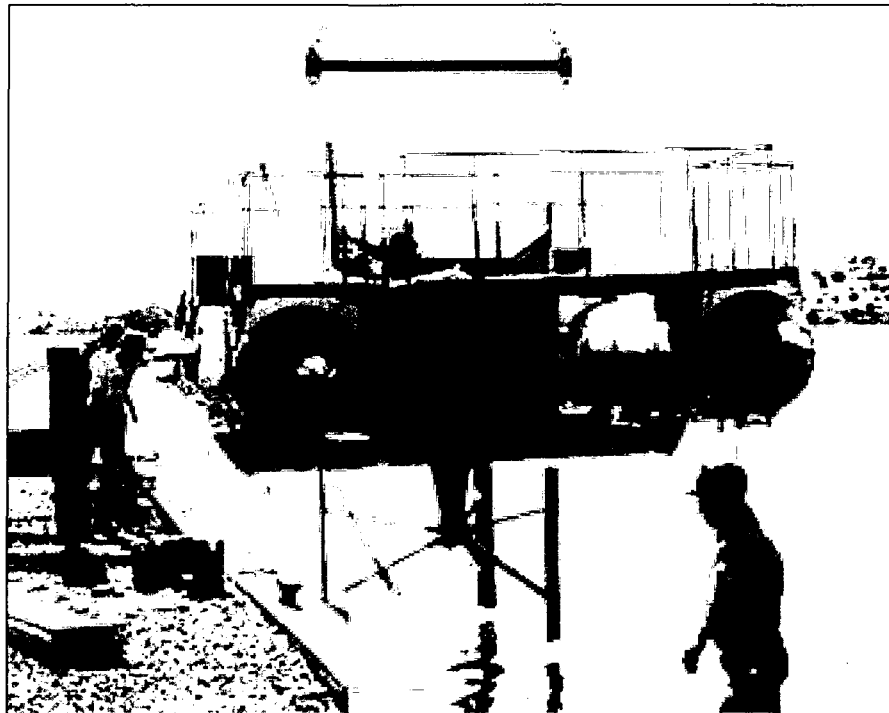


Figure 3.3: Floating, unducted, vertical-axis turbine (from [29])

Variable speed and variable pitch turbines allow the turbine rpm and hydrofoil pitch angle (respectively) to change in time. Variable speed is commonly achieved through the use of variable speed electric generators, though systems using variable speed transmissions also exist. Variable speed is desirable for maintaining maximum extraction efficiency as flow velocities change as well as introducing the potential to reduce torque transients. Variable pitch turbines permit modification of the hydrofoil pitch angle (angle between the hydrofoil chord line and a radial line passing through the center of rotor rotation at a reference point on the chord) either passively [9] or actively [76]. For horizontal axis turbines this is used mainly for power regulation in above rated speed operation. For vertical axis machines variable pitch allows smoothing of rotor torque

pulsations (at 1 or 2 times the blade passing frequency depending on the tip speed ratio), increases starting torque and raises hydraulic efficiency.

Finally, turbines are classified by rotor geometry (common vertical axis configurations are shown in Fig. 3.4).

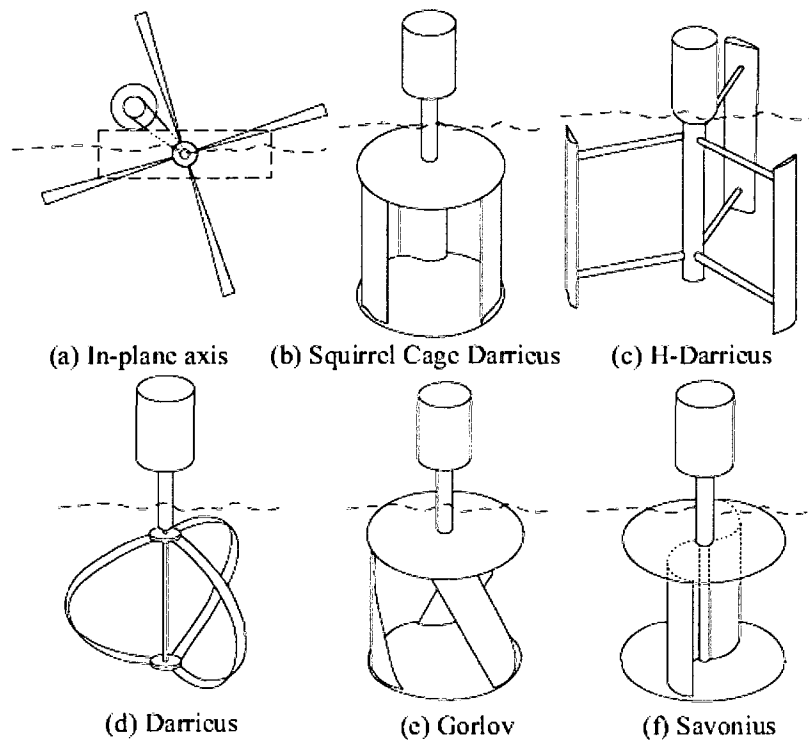


Figure 3.4: Vertical axis turbine rotor configurations (from [3])

Many versions exist with various advantages and limitations. For instance squirrel cage rotors tend to have higher drag losses associated with rotating the large surface area of the upper and lower plates through the flow, but maintain higher rotating inertia to smooth power output. Helical turbines have higher starting torques and somewhat smoother torque output at the cost of lower hydraulic efficiencies ([2], [82] and [86]).

There are many companies such as New Energy Corporation Inc, Blue Energy International, Ponte di Archimede International, GCK Technology, Alternative Hydro Solutions, Verdant Power LLC, etc, developing various versions of this vertical axis hydrokinetic technology, in mid to late stages of commercialization.

3.2 Introduction to Hydrodynamic Operation

General hydrodynamic operation of the unducted, vertical-axis turbine is shown in Fig. 3.5, which displays a four blade turbine rotor (top view). A relative water velocity vector, whose components are made up of the free stream velocity and hydrofoil tangential velocity, impacts the hydrofoil at an angle of attack with respect to the foil chord line. The net force due to components of lift and drag tangent to the pitch circle (also called the thrust vector), induces torque through the radial moment arm about the center of rotor rotation.

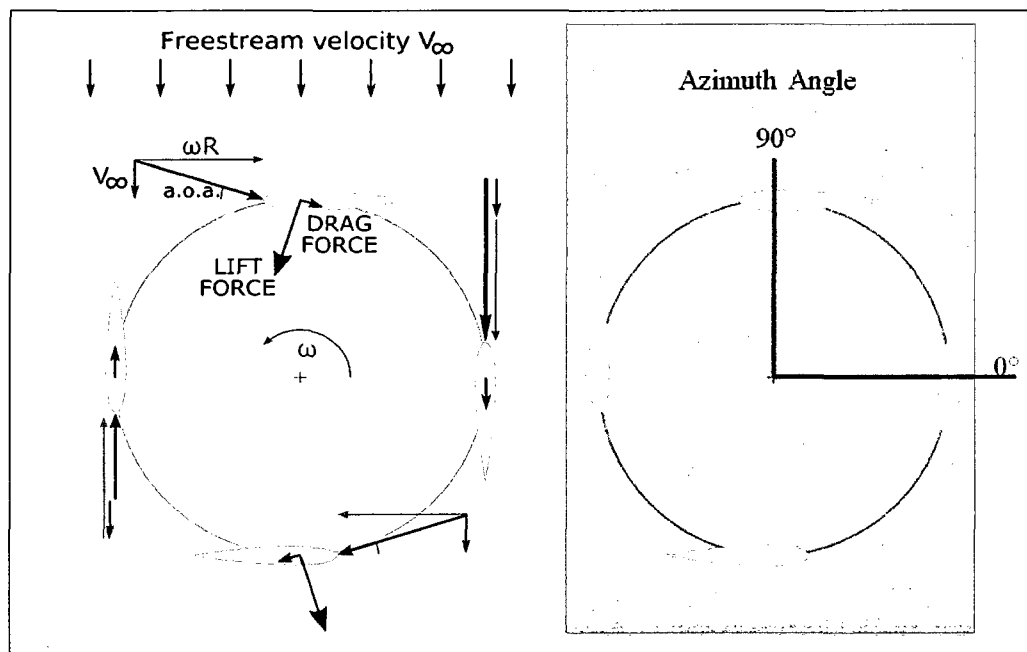


Figure 3.5: Hydrodynamic force vector diagram (shown from top of rotor)

The angle of attack cycles from 0° at a rotor azimuth angle of 0° , to some maximum and back to 0° at an azimuth angle of 180 degrees (assuming that streamlines pass straight through the rotor). The angle of attack is also dependent on the tip speed ratio (ratio of the hydrofoil tangential velocity to the free stream velocity) as seen in Fig. 3.6.

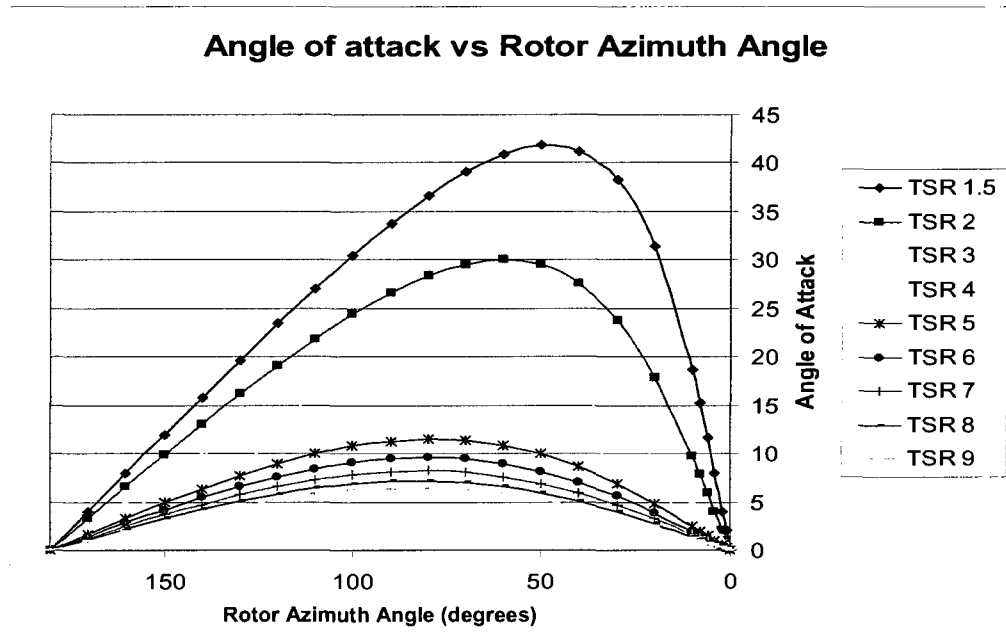


Figure 3.6: Angle of attack versus rotor azimuth angle

Since the thrust force is derived from hydrofoil lift and drag, which are dependent on a cyclic angle of attack, shaft-torque pulsations are expected twice per revolution for each blade (i.e.: the torque pulsation frequency is twice the blade passing frequency; which is the number of blades multiplied by the rotor rotation frequency). However, experimental data has verified that for many rotors these torque pulses appear at this frequency only at low tip speed ratio's with successive peaks tending to merge at higher tip speed ratio's, thus reducing the torque pulsation frequency to that of the blade passing frequency. This

is likely due to the disturbed flow passing through the downstream region of the rotor reducing hydrofoil performance and therefore rotor torque generation [25].

The free stream velocity is limited to approximately 3.5 m/s due to cavitation (highly dependent on factors such as turbine design, dissolved gas content in the flow, hydrofoil smoothness, depth of rotor submergence, etc). The turbine will operate above this limit but with considerable performance degradation and wear of components. The theoretical maximum hydraulic efficiency for free stream turbines is limited to 59.3 % and is known as the Betz limit [11]. This is very different from traditional Francis or Pelton turbines that can reach hydraulic efficiencies of 96%. This is due mainly to the fact that hydrokinetic turbines are governed by a fundamental tradeoff between energy extraction capability of the rotor and resistance to flow through the rotor. Note also that hydrokinetic turbines utilize water with much lower energy densities compared to traditional high head turbines so that any losses in the system are usually a significant portion of the total energy available.

An interesting characteristic of this vertical axis rotor is that rotational direction is independent of the direction of flow due to rotor symmetry.

3.3 5kW Test Turbine and Floatation System

The test turbine is a 5kW vertical-axis, unducted, fixed-pitch, variable speed derivative using an *H* style rotor, and is shown below in Fig. 3.7.

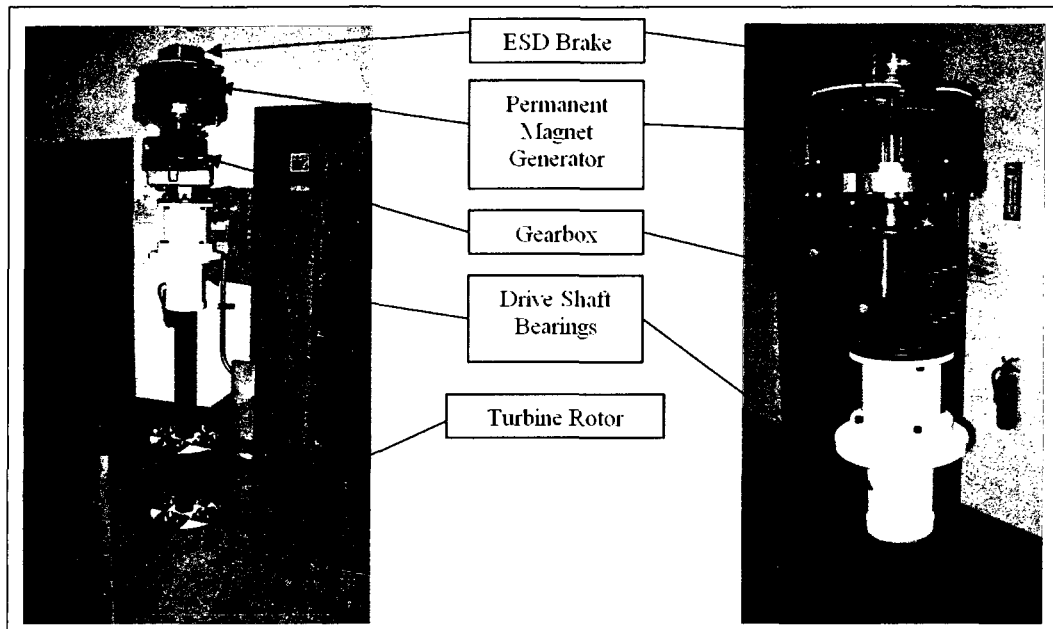


Figure 3.7: 5kW turbine test system (drive train)

Energy is extracted from the flow by the rotor and converted to shaft power. This is transmitted to a step-up gearbox which increases the shaft rotational speed (reducing shaft torque) before being passed to a variable speed, 3-phase, axial flux, permanent magnet generator. The drive system incorporates a cantilevered rotor so that the drive bearings, gearbox and generator can be mounted above the waterline. This also makes the drive system very stiff in torsion due to larger driveshaft diameters required to support bending loads caused by rotor hydrodynamic drag. For emergency shutdown purposes a spring applied, electrically released brake is mounted to the generator shaft on top of the generator.

The test turbine is supported by a pontoon style floating platform, and transported using a conventional boat trailer as shown in Fig. 3.8. The pontoons are made of

polyethylene and filled with polystyrene foam inserts. A small aluminum frame houses the pontoons and provides mounting for the turbine system.



Figure 3.8: Turbine, floatation system and trailer

The floatation system allows the turbine to be rotated out of the water 90 degrees for ease of deployment and removal. Log booms are sometimes used to deflect debris that might pass through the rotor, though in the present work the system was only deployed for brief test purposes and was therefore not used. A document from the turbine supplier outlining the technical specifications for the test turbine (model number ENC-005-F4) system is attached in Appendix A.

3.4 Power Electronics System

Power electronics are required to condition the variable speed, permanent magnet generator output (which is variable voltage and frequency) before it can be connected to useful AC or DC loads. The power electronics system normally used for this turbine is an off-the-shelf small wind package that uses AC-DC-AC conversion technology with a passive rectifier on the generator side, a DC booster, and finally an IGBT (insulated gate bipolar transistor) active bridge for the load side inverter. Both grid connected and stand alone versions of the package exist. However, the turbine speed control hardware which ties into the active inverter bridge and uses control periods of 500 ms that are too slow for closed loop turbine control. It is also integral to the system and proved difficult to modify or remove without support from the manufacturer. Therefore other off-the-shelf power electronics solutions were sought that either allowed reprogramming of the load controller, or supplied a control interface for an external control system. Since none could be located short of designing a custom system from basic principles, it was decided a system would be constructed using commercially available basic building blocks. A three phase passive rectifier and capacitive filter was acquired from Power One Inc., to convert the permanent magnet generator output to variable voltage DC. A second-hand, AMC (Advanced Motion Controls), 50 Amp, brush type DC servo amplifier was acquired and served as an active PWM bridge to control load current. This amplifier contains an internal current control loop with an external control interface of 0 to 10VDC (corresponding to 0 and full drive amperage respectively), to define the current setpoint. Since the power electronics system does not have an inverter section and is not certified

for grid connected operation (does not meet CSA C22.2 N.107.1-01, UL 1741, IEEE519 and IEEE1547), stand alone testing was the only option.

A load consisting of two 600V, 15kW, 24 ohm resistors (connected in parallel), in series with two parallel 0.8mH inductors, was connected to the servo amplifier terminals. The inductors were installed to filter current transients and to meet the minimum load inductance requirement of the amplifier. Specifications for all hardware are included in Appendices B, C and D. A functional schematic outlining the electrical and power electronics systems is shown in Fig. 3.9 along with the physical system in Fig. 3.10.

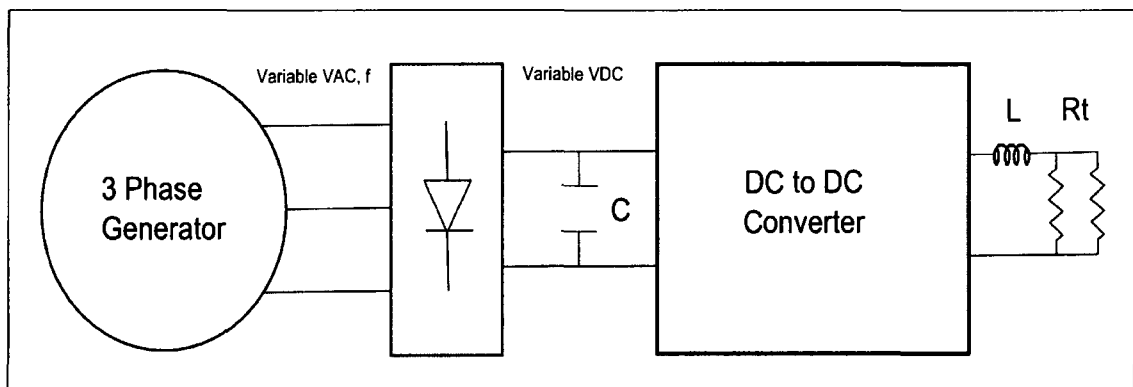


Figure 3.9: Electrical system schematic

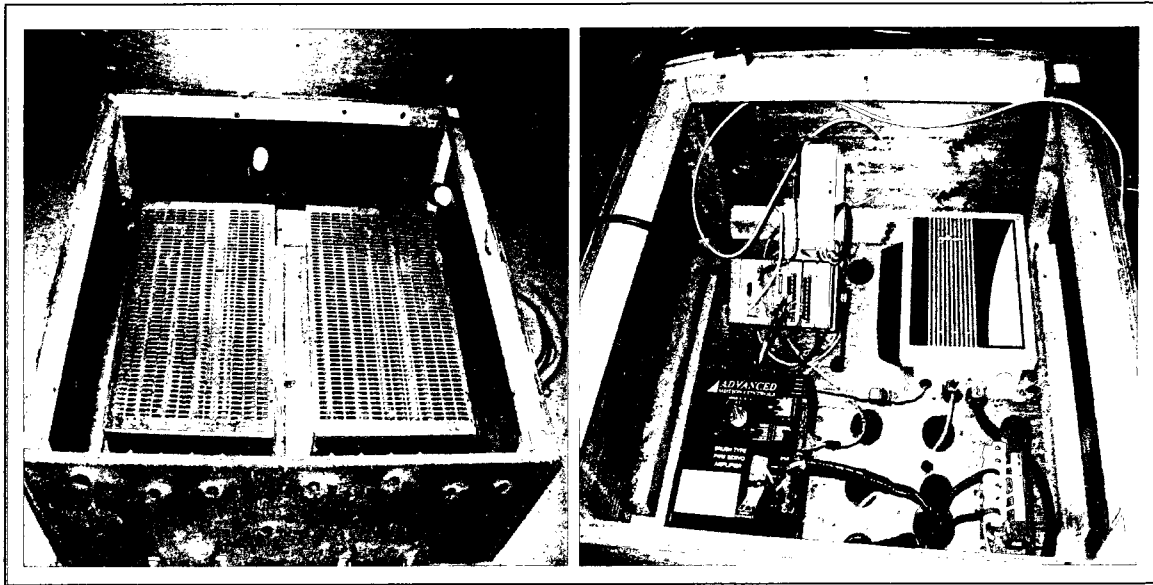


Figure 3.10: Electrical system

The left picture in Fig. 3.10 shows the two resistors. The right picture, starting from the top left and moving clockwise shows the CompactRIO real-time controller and power supply, the Aurora three phase rectifier and filter, the inductor and finally the servo amplifier (DC to DC converter).

3.5 Control Hardware and Instrumentation

An external CompactRIO real-time controller with LabVIEW development software was acquired from National Instruments to facilitate rapid prototyping of the control algorithm. This hardware uses an FPGA (field programmable gate array) chip in conjunction with a real time controller and VxWorks operating system. The controller has a 400MHz processor with 64MB DRAM, 128MB of storage, with a four slot chassis and analog input, digital input and analog output cards. The chassis incorporates a 1M gate FPGA chip which had to be programmed separately to acquire external signals, pre-process/scale data, and transmit data to the real time controller where it is stored. The

FPGA is unique in that it is completely reconfigurable and allows true parallel processing. The LabVIEW development software interfaces directly with the Simulink environment through the Simulation Interface Toolkit to generate executable code that runs on the real time controller. Though this control hardware can be run as a standalone system, a laptop computer was used to interface with the controller to aid in diagnostics and assess early test results. The control system hierarchy is shown in Fig. 3.11.

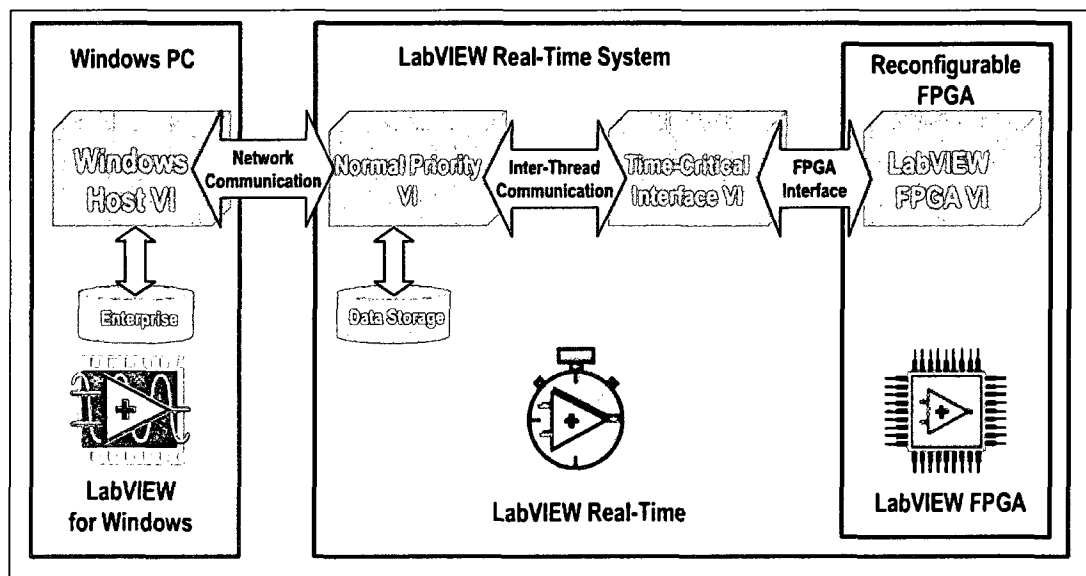


Figure 3.11: Control system architecture (from www.ni.com)

The turbine generator was retrofitted with an rpm sensing system consisting of a tone wheel and a 427012-30 Hall sensor from Magnetic Sensors Corporation. The tone wheel was made from an off-the-shelf chain sprocket welded to a homemade hub bored to fit the generator shaft (Fig. 3.12).

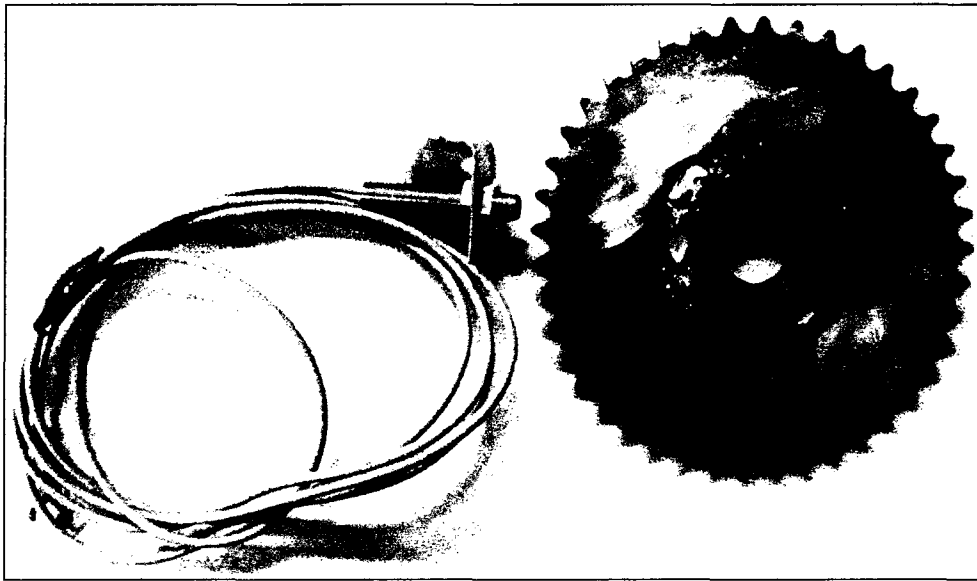


Figure 3.12: Custom tone wheel and Hall sensor for turbine rpm

The tone wheel and sensor were installed on top of the generator just below the failsafe brake assembly. The rpm sensing system was calibrated by mounting the tone wheel in a metal lathe and spinning it at discrete speeds over the entire operating range.

An aluminum mount was fabricated to attach a Swoffer Instruments, Model A2100 water velocity sensing element to the front of the floating platform to measure free stream velocity. The water velocity sensor was sent to Environment Canada for calibration. This is the same group that calibrates equipment for the Canadian Hydraulics Center in Ottawa (part of the National Research Council of Canada). The meter was tested in a tow tank at several different speeds between 1.5 m/s and 3.5 m/s to find the calibration constant and verify there is no sensitivity change with velocity.

The load current was also fed into the controller from a pre-calibrated output on the PWM amplifier that produces a voltage proportional to load current, for data logging purposes. This calibration was checked using a resistive load and external oscilloscope.

Specifications for the control hardware, water velocity sensor and turbine speed sensor are included in appendices E and F respectively.

3.6 Control Software and Data Processing

Upon completion of the control system modelling in Simulink, the code was translated into a format compatible for use on the CompactRIO hardware using built-in LabVIEW code translators. However, there was an incompatibility between the VxWorks operating system on the real-time controller and the *.out* files compiled by LabVIEW. Thus a work-around using the GNU tool chain (free download off the internet) was implemented as specified by National Instruments technical support.

The FPGA code used to acquire and pre-process the real world signals needed to be written and compiled separately then attached to the LabVIEW project. Both rpm and water velocity sensor square wave signals were acquired by the FPGA level of the system where counters were programmed to perform period measurements that were in turn fed to the real time controller. The current measurements were run through a mean filter to remove noise before the data was transferred to the real time controller.

At the real time controller the data was scaled with appropriate engineering units before being used to calculate the control value for the next period. A control period of 5 ms was implemented for all field testing which was as fast as the system could acquire the data, process the signals, calculate the new control signal and log all the data.

Application specific LabVIEW code serving as the human machine interface was written to run on the laptop computer and is shown below in Fig. 3.13. This allowed pretesting to

find zero offset and scale factors for the PWM amplifier as well as enter scale factors for the water velocity sensor.

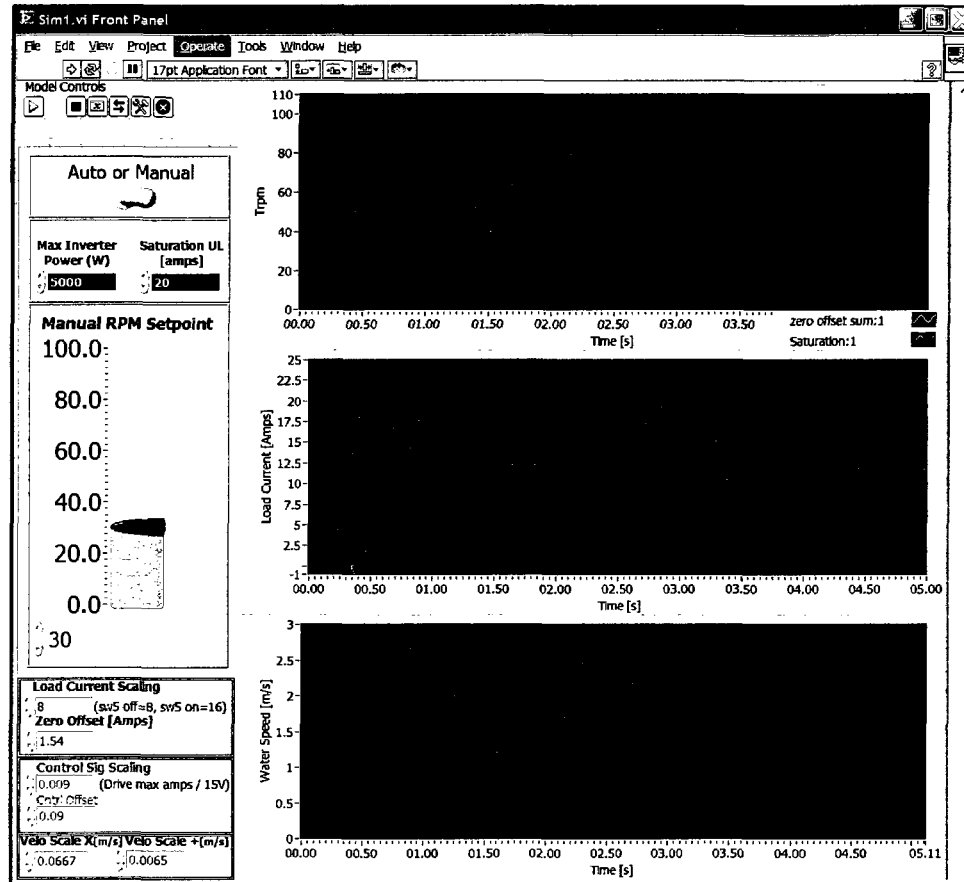


Figure 3.13: Laptop human machine interface for control testing

3.7 Test Site

The test site (shown in Fig. 3.14) is located upstream of an existing 78 MW dam in Pointe du Bois, Manitoba, and was provided by the University of Manitoba with support from Manitoba Hydro. This site is located on the Winnipeg River, approximately 160 km northeast of Winnipeg.

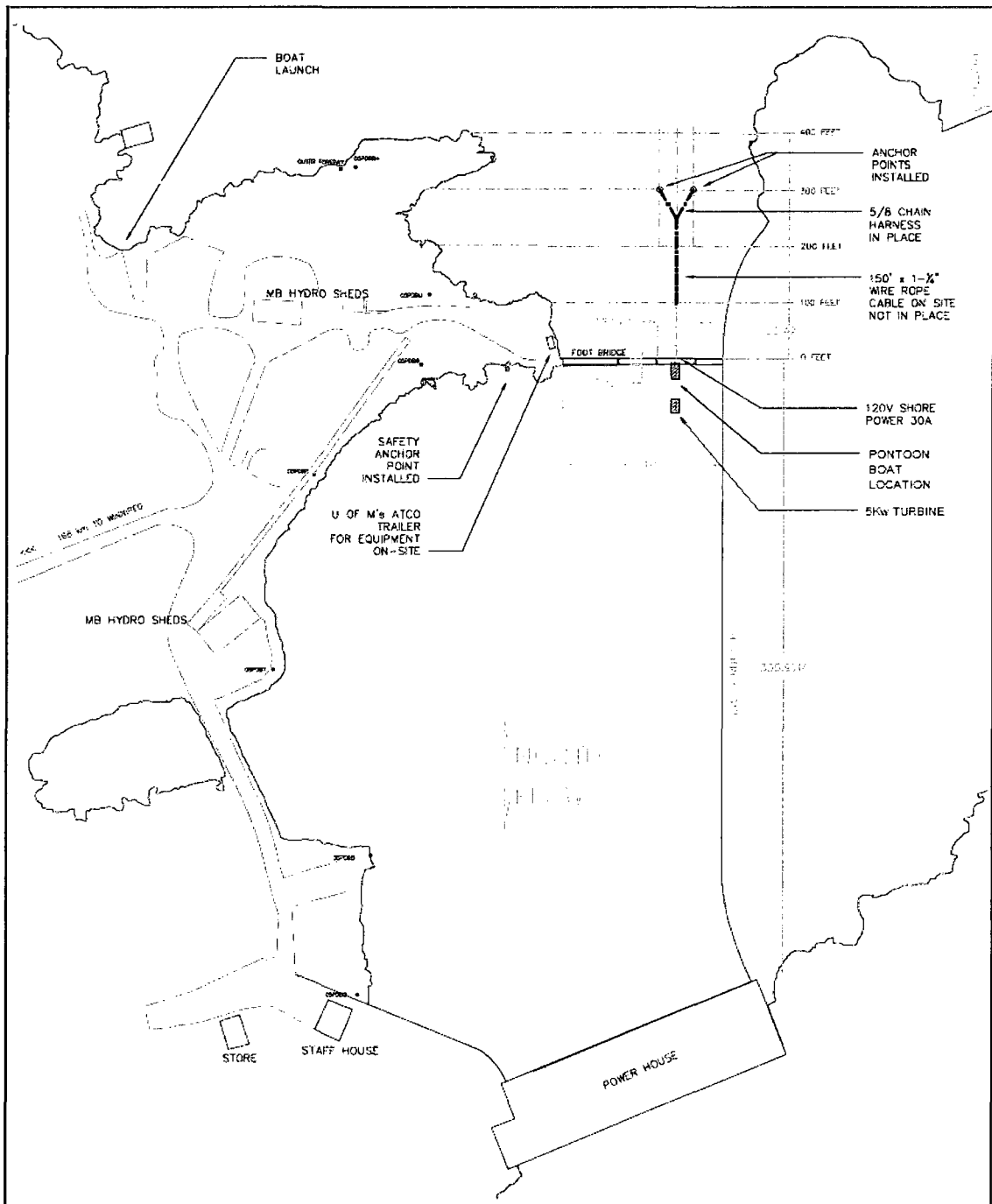


Figure 3.14: Pointe du Bois, hydrokinetic turbine test site (drawing from the University of Manitoba)

Two anchors drilled and cemented in the river-bottom bedrock facilitate turbine platform mooring. New Energy Corporation Inc and the University of Manitoba are currently testing a 25kW vertical axis turbine installed in a floating platform at this location to which the smaller 5kW test turbine used for the current work is moored (Fig. 3.15). The reason for this arrangement is that only one set of mooring lines can be attached to the submerged anchors, and testing on the larger system was not allowed to be interrupted. Note that this is currently the only hydrokinetic turbine field-test site in Canada.

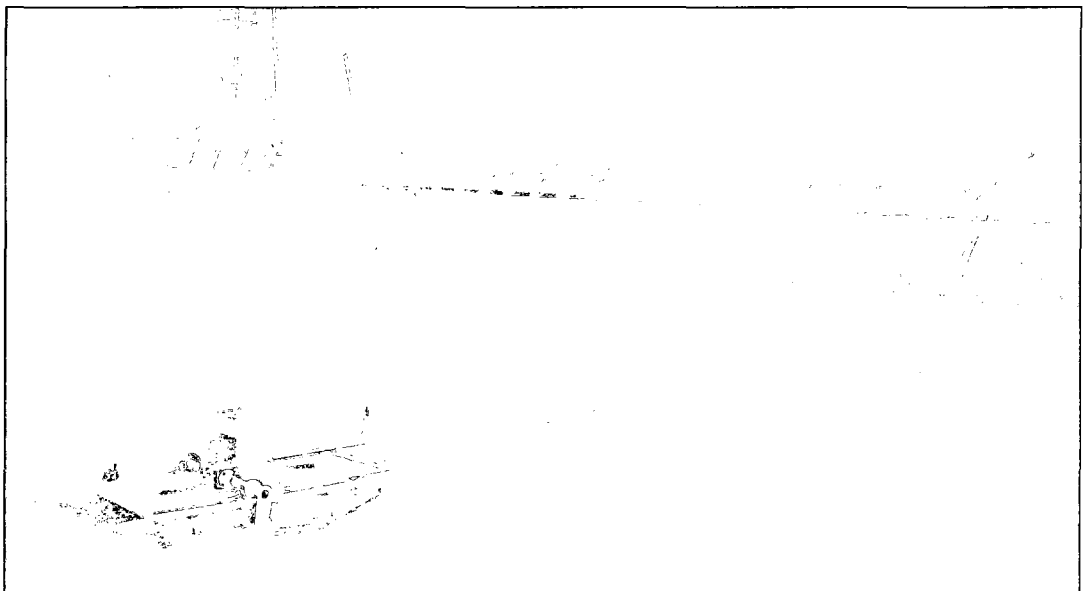


Figure 3.15: 5kW test turbine system mounted behind 25kW system

Both turbine systems were moored downstream of a footbridge which provides access to both sides of the dam, as well as the deck of the 25kW test platform (using a ladder). An ATCO trailer located at the base of the footbridge approximately 80m from the 25kW system, houses the grid tie power electronics package for the 25kW turbine as well as its DAQ system (part of which is located on the floating platform). Cables are run along the footbridge to connect the 25kW turbine with its power electronics package.

All site equipment (hand tools, multimeters, Mustang survival suites, life jackets and fall protection harnesses) is also stored in this trailer.

The power electronics package, control hardware and electric load for the 5kW test turbine were put on the stern of the 25kW turbine platform to minimize instrumentation cable lengths for the generator speed and water velocity sensors. The equipment was installed into custom designed weather proof housings consisting of the purpose built crates with which the systems were shipped to site. Water resistant cabling was used for all generator, load and instrumentation wire connections. The 5kW turbine could only be accessed by boat, so a small Zodiac (inflatable boat with a small outboard motor) was used to disable the turbine brake, make the generator and instrumentation cable connections as well as start the turbine. Note that while turbine systems 25kW and larger have no issues self-starting, this smaller system self starts only at flow speeds above 2.25 m/s. Thus a small cordless drill was used to motor the system briefly through a hex lug on top of the generator to facilitate turbine starting.

Chapter Four: System Modeling

4.1 Introduction

Typically wind energy systems use physical system models for control purposes though identification techniques have also been noted in literature. Due to the availability of detailed turbine information as well as the expense associated with physical testing in this project, a physical model was preferred.

In the interest of developing a robust gain scheduled controller, an LPV model of the system will be derived. This chapter will begin with a discussion of turbine performance characteristics followed by development of the physical model, linearized system, and LPV model.

4.2 Turbine Performance Characteristics

Turbine performance is characterized differently depending on the application and whether ducting is used, making a full analysis and presentation of all the definitions cumbersome. Therefore discussion is limited to the free stream unducted unit used for the present work.

The overall hydraulic efficiency of a turbine is the ratio of the turbine shaft power to the undisturbed fluid power passing through the area occupied by the system (i.e.; if it were removed from the flow)

$$\eta = P_T / (\rho g \Delta_H Q) = \text{hydraulic efficiency} \quad (1)$$

where

P_T = turbine shaft power

ρ = density of water

g = gravitational acceleration constant

$$\Delta_H = \left(\frac{P_1}{\rho g} + \frac{V_1^2}{2g} + Z_1 \right) - \left(\frac{P_2}{\rho g} + \frac{V_2^2}{2g} + Z_2 \right) = \text{total head across the system}$$

Q = flow rate.

By definition, free stream systems have no potential head imposed across the system. As well, only the undisturbed fluid power is considered. Therefore, the differential pressure and elevation terms are zero, and the upstream velocity is the undisturbed free stream velocity. Also, by convention the downstream velocity is set to zero [25] giving the interpretation of hydraulic efficiency based on total kinetic head available. The total head across the system simplifies to

$$\Delta_H = \frac{V_\infty^2}{2g}.$$

The undisturbed flow convention also implies the flow rate in Eq. 1 must be defined as

$$Q = A_t V_\infty$$

where

A_t = cross-sectional area of turbine rotor (blade height X rotor diameter)

V_∞ = undisturbed free stream velocity.

Thus, the hydraulic efficiency given by Eq. 1, for a free stream unducted turbine simplifies to the following expression known as the coefficient of performance

$$C_P = P_T / \left(\frac{1}{2} \rho A_t V_\infty^3 \right). \quad (2)$$

Through a similar derivation, the unducted free-stream dimensionless torque coefficient is defined as

$$C_T = T_H / (1/2 \rho A_t R V_\infty^2) \quad (3)$$

where

T_H = hydraulic torque

R = turbine rotor radius.

Both the coefficient of performance and the torque coefficient are demonstrated through experiment to be functions of the hydrofoil Reynolds number (based on chord length) and tip speed ratio ([11], [25] and [64]). The tip speed ratio is the ratio of the rotor tangential velocity to that of the free stream

$$\lambda = \frac{\Omega_R R}{V_\infty} = \text{tip speed ratio} \quad (4)$$

where

Ω_R = angular velocity of the turbine rotor.

The Reynolds number dependency is due mainly to the sensitivity of hydrofoil lift and drag characteristics on Reynolds number (as demonstrated in [79]); Thus C_P and C_T can be assumed invariant with respect to Reynolds number for the purposes of control design (for a fixed turbine size) without introducing significant error. A representative plot of the coefficient of performance and torque coefficient is shown in Fig. 4.1.

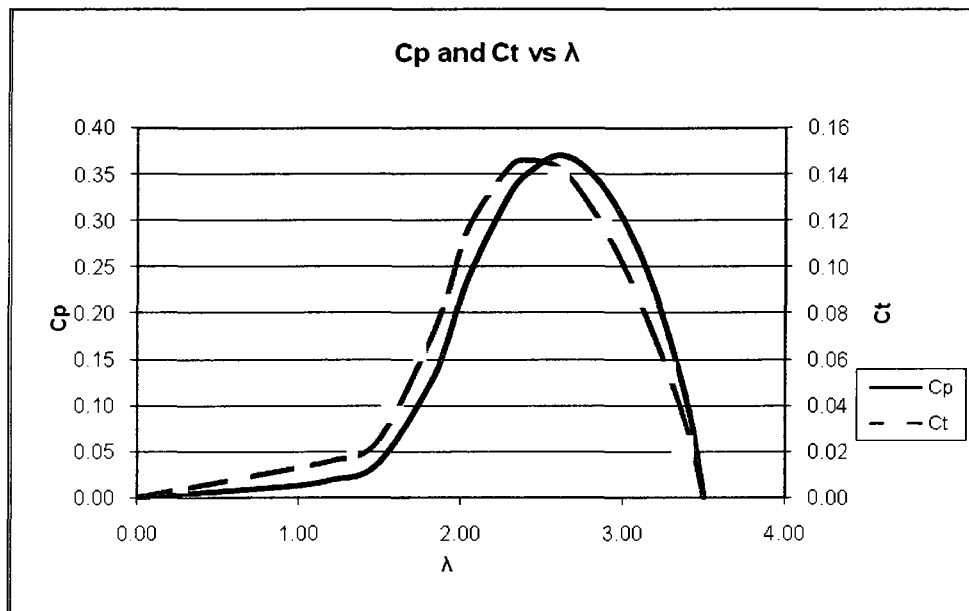


Figure 4.1: Coefficients of performance and torque versus tip speed ratio

It is important to note that the coefficient of performance and the torque coefficient are quantified through experiment by averaging over one or more rotor rotations at steady operating points. This effectively removes any dynamic flow interactions from the data. In fact there is significant pulsation in the hydraulic torque which could potentially have a destabilizing effect on any control system. This pulsation is highly dependent on turbine geometry and operating point. A representative plot is shown in Fig. 4.2. Also note that the peak global system (water to wire) efficiency is 31.5%, or in relation to the Betz limit, $31.5 / 59.3 \times 100 = 53.1\%$ overall efficiency (numbers attained from the manufacturer in [65]).

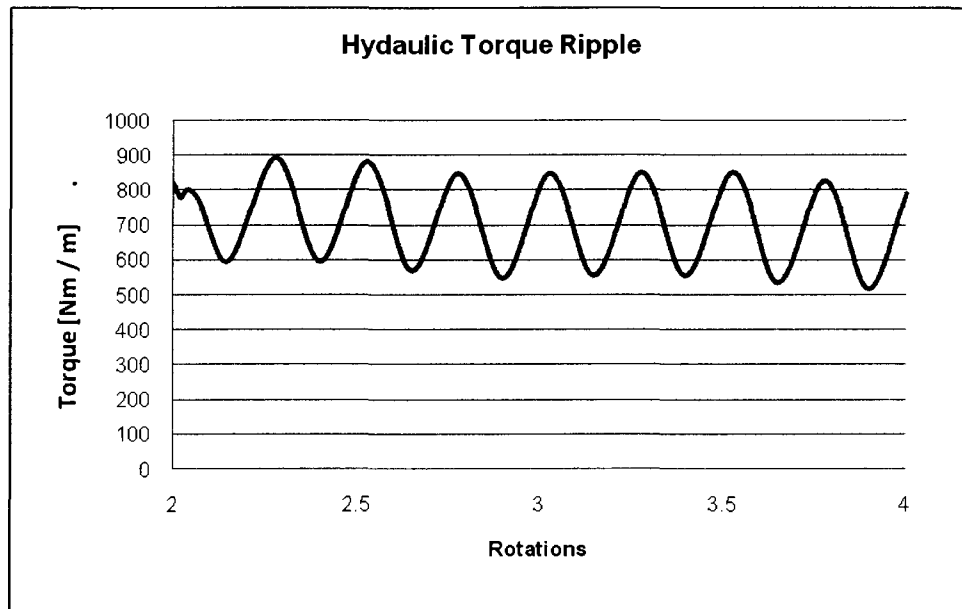


Figure 4.2: Hydraulic torque ripple example

4.3 Physical System Model

In the development of a physical system model, dynamics of the mooring and floatation systems are neglected and it is assumed that the turbine is fixed rigidly in space during operation. It is also assumed that a single scalar representation of the effective average flow velocity (whether as specified during simulation or based on velocity meter measurement) is valid due to the small rotor size. A rigid body model is employed due to the high torsional stiffness of drive system components required for rotor drag bending loads as well as the employed design methodology for infinite fatigue life (based on cyclic shaft loading). It is assumed that the generator and power electronics subsystem dynamics can be neglected since they are orders of magnitude faster than the turbine dynamics. Finally, since this control is for grid-tied distributed-generation applications, we can assume that the required electrical load is always available for control purposes (as opposed to grid isolated, or central power generation where this is not the case).

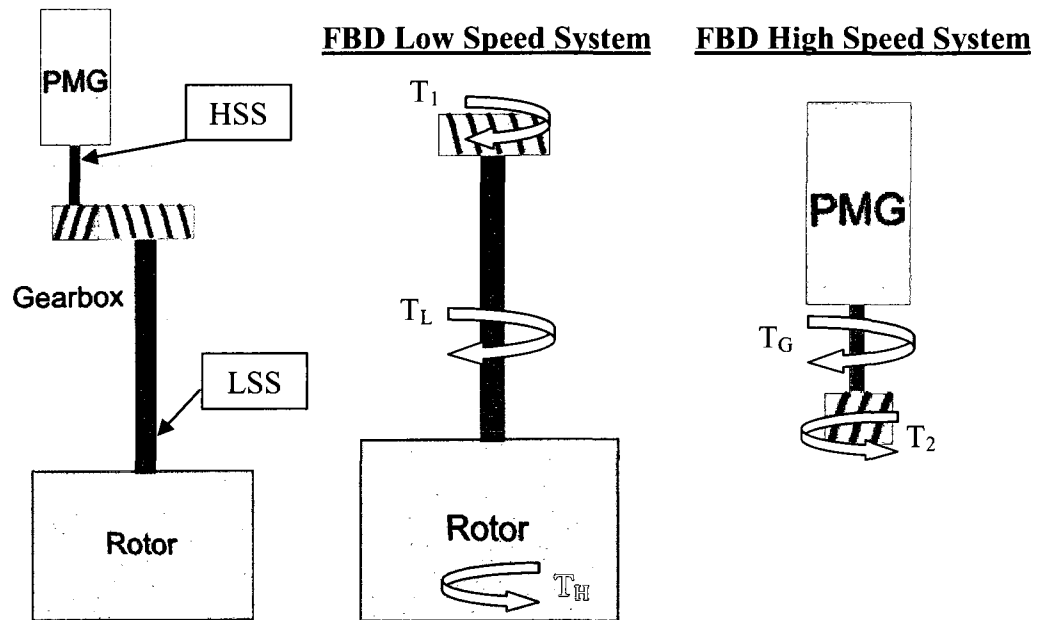


Figure 4.3: Generalized system (left), FBD low speed system (center), FBD high speed system (right)

A schematic diagram of the turbine system as well as free body diagrams (FBD) of the low speed and high speeds systems are shown at the left, center and right in Fig. 4.3 respectively. A hydraulic torque is imposed on the rotor by the water passing through it. This torque passes through the low speed shaft (LSS) to a step up gearbox. The reduced torque (and increased shaft speed) passes through the high speed shaft (HSS) to a permanent magnet generator (PMG) that supplies the reaction torque. From the FBD for the low speed system we can identify the loads and equation of motion as follows

$$J_{LS} \dot{\Omega}_R = T_H - \beta \Omega_R - T_1 \quad (5)$$

where

T_1 = torque at low speed side of gearbox

T_L = loss torque (drive bearings, gearbox, PMG losses) = $\beta \Omega_R$

β = loss proportionality constant

T_H = hydraulic torque

J_{LS} = rotating inertia of low speed system

Ω_R = speed of turbine rotor.

Correspondingly, from the FBD for the high speed system we can identify the loads and equation of motion as

$$J_{HS} \dot{\Omega}_G = T_2 - T_G \quad (6)$$

where

T_2 = Torque at high speed side of gearbox

T_G = Electromagnetic generator torque

J_{HS} = rotating inertia of high speed system

Ω_G = speed of generator.

Now, by combining the high speed and low speed systems the equation of motion for the overall system with respect to the low speed shaft is derived. Let

c = the gear ratio in the gearbox.

Then at the gearbox we have

$$T_1 = c T_2 \quad (7)$$

$$\Omega_G = c \Omega_R . \quad (8)$$

Solving Eq. 6 for T_2 , inserting this into Eq. 7 and finally inserting this result into Eq. 5, gives

$$J_{LS} \dot{\Omega}_R = T_H - \beta \Omega_R - c (T_G + J_{HS} \dot{\Omega}_G) . \quad (9)$$

Taking the time derivative of Eq. 8, inserting the result into Eq. 9 and rearranging we have

$$J_{LS} \dot{\Omega}_R + c^2 J_{HS} \dot{\Omega}_R = T_H - \beta \Omega_R - c T_G . \quad (10)$$

Define the equivalent polar moment of inertia for the entire system at the low speed shaft as

$$J = J_{LS} + c^2 J_{HS}$$

and substitute into Eq. 10 giving the governing equation of motion

$$J \dot{\Omega}_R = T_H - \beta \Omega_R - c T_G . \quad (11)$$

Finally, the torque of a permanent magnet generator is proportional to the stator current for resistive loads [99]

$$T_G = 1.5 n i_q \Phi$$

where n (the number of pole pairs) and Φ (the permanent magnet flux), are both constant.

The equation can be rewritten by combining all the constants into a single value K_G called the generator torque constant

$$T_G = K_G i_q . \quad (12)$$

Substituting Eq. 12 into Eq. 11 gives the final equation of motion with respect to the control input i_q

$$J \dot{\Omega}_R = T_H - \beta \Omega_R - c K_G i_q . \quad (13)$$

4.4 Linearization of the Equation of Motion

Eq. 13 is a first order dynamic system where i_q is the input variable to be controlled. The disturbance enters through the hydraulic torque term and is caused by flow disturbances as seen by solving Eq. 3 for T_H

$$T_H = \frac{1}{2} \rho A_t R V_\infty^2 C_T(\lambda). \quad (14)$$

The expression for hydraulic torque requires linearization. Note that the torque coefficient is a function of the tip speed ratio λ alone, and is thus completely specified by the turbine speed and water speed ($\bar{\Omega}_R, \bar{V}_\infty$). Here the symbol “ $\bar{}$ ” denotes the steady state value of a variable, and “ $\hat{}$ ” denotes deviation of a variable with respect to the steady state value of that variable. For instance

$$\hat{V} = V - \bar{V}.$$

Perform a multivariable Taylor Series expansion about an equilibrium point for the hydraulic torque (Eq. 14) and simplify (ignoring higher order terms) to get

$$\hat{T}_H = k_\omega \hat{\Omega}_R + k_V \hat{V}_\infty \quad (15)$$

where

$$k_\omega = \left. \frac{\partial T_H}{\partial \Omega_R} \right|_{(\bar{\Omega}_R, \bar{V}_\infty)} = f_\omega(\bar{\Omega}_R, \bar{V}_\infty) \quad (16)$$

$$k_V = \left. \frac{\partial T_H}{\partial V_\infty} \right|_{(\bar{\Omega}_R, \bar{V}_\infty)} = f_V(\bar{\Omega}_R, \bar{V}_\infty). \quad (17)$$

To find these derivatives, an expression for $C_T(\lambda)$ is required. A quadratic approximation of the form

$$C_T(\lambda) = a \lambda^2 + b \lambda + c \quad (18)$$

was found to fit the data well over the required portion of the operating range as shown in Fig. 4.4.

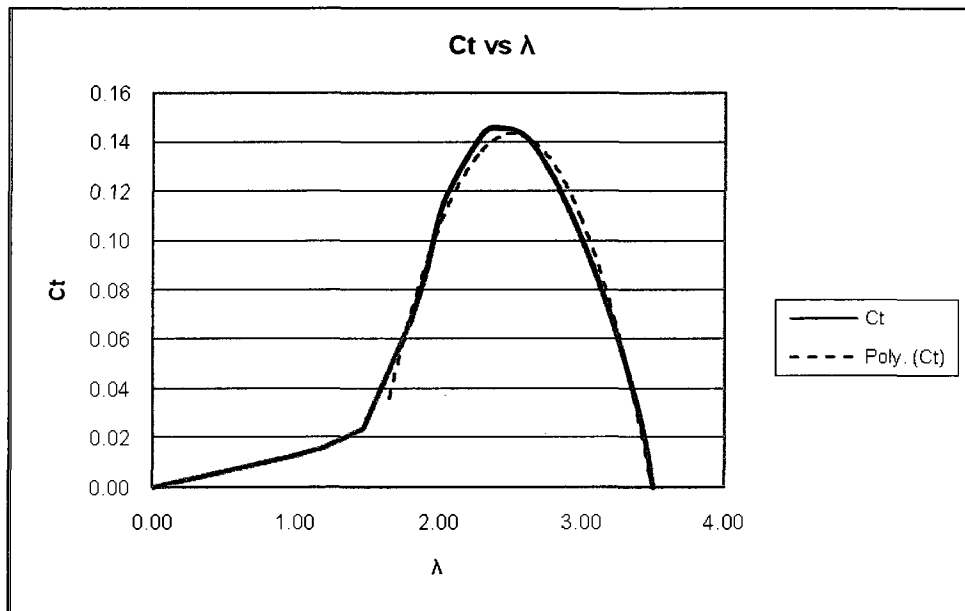


Figure 4.4: Comparison of quadratic approximation for C_t and test data

Substituting Eq. 18 into Eq. 14, the unknown derivatives k_ω and k_V can be found

$$k_\omega = \left. \frac{\partial T_H}{\partial \Omega_R} \right|_{(\bar{\Omega}_R, \bar{V}_\infty)} = \rho R^3 h a \left(\frac{b}{2 * a} \bar{V}_\infty + R \bar{\Omega}_R \right) \quad (19)$$

$$k_V = \left. \frac{\partial T_H}{\partial V_\infty} \right|_{(\bar{\Omega}_R, \bar{V}_\infty)} \quad (20)$$

$$= -\rho R^3 h a \left(R \bar{\Omega}_R + \frac{b}{2 * a} \bar{V}_\infty \left(1 + \frac{4 a c}{b^2} - \frac{4 a^2}{b^2} + \frac{1}{a} \right) \right)$$

where

h = height of the rotor.

Finally, substitute Eq. 15 into Eq. 13 denoting variable deviations around the equilibrium point to define the linearized equation of motion

$$J \hat{\dot{\Omega}}_R = k_\omega \hat{\Omega}_R + k_V \hat{V}_\infty - \beta \hat{\Omega}_R - c K_G \hat{i}_q \quad (21)$$

4.5 LPV model

The LPV general model form (outlined in [81]) is

$$\dot{x} = A_m(\theta) x + B_{m1}(\theta) w + B_{m2}(\theta) u \quad (22)$$

$$y = C_m x + D_m u. \quad (23)$$

Note that $A_m(\theta)$, $B_{m1}(\theta)$ and $B_{m2}(\theta)$ are time varying matrices parameterized by the vector of time varying parameters $\theta(t)$. Thus for any given trajectory of $\theta(t)$, the LPV system is a linear time varying system. Moreover, in the case of a constant θ , the LPV system is reduced to linear time invariant. The linearized dynamic system is now expressed as the LPV model

$$\hat{\dot{x}} = A_m(\theta) \hat{x} + B_{m1}(\theta) \hat{V}_\infty + B_{m2}(\theta) \hat{i}_q \quad (24)$$

$$\hat{y} = C_m \hat{x} + D_m \hat{i}_q.$$

The control variable is chosen as the load current and the feedback variable is chosen as the turbine speed. Thus, the state, input, output, disturbance, and parameter vector are

$$\hat{x} = \hat{\Omega}_R; \hat{u} = \hat{i}_q; \hat{y} = \hat{\Omega}_R, w = \hat{V}_\infty, \theta = [\overline{\Omega}_R, \overline{V}_\infty]^T.$$

It is important to remember that all these values with the exception of the parameter vector θ , are deviations of the variables with respect to some steady state operating point. For example, the disturbance has the physical interpretation of turbulence, not mean water speed.

In the present case, the plant is first order, reducing $A(\theta)$, $B_1(\theta)$, $B_2(\theta)$, C and D to scalar values. Thus, comparing Eq. 21 and Eq. 24 we get

$$A_m(\theta) = (k_\omega - \beta) / J$$

$$B_{m1}(\theta) = k_V / J$$

$$B_{m2} = -c * K_G / J \tag{25}$$

$$C_m = 1$$

$$D_m = 0 .$$

Chapter Five: Controller Design

5.1 Introduction

This chapter begins with a description of the general control problem considering plant nonlinearities and open loop stability which highlight the requirement for some form of nonlinear control. The control objectives are then outlined, followed by a discussion of the control strategy. Based on all of these considerations, H_∞ LPV control synthesis is carried out, explicitly incorporating the tradeoff between tight speed reference tracking and controller-induced drive-train load transients. A PI controller is also generated for comparative results produced during the numerical simulation and field testing portions of this work.

5.2 General Control Problem

The control problem is a challenging one due to the nonlinear and time varying plant over which only a portion of the operating range is open loop stable. A discussion of stability is presented first, followed by an outline of important nonlinearities and time varying portions of the plant that need consideration.

5.2.1 Open Loop Stability

Consider point *A* in Fig. 5.1 and Fig. 5.2, where the water velocity is 2.5 m/s, turbine speed is 81 rpm and power output is 2.9 kW. This point corresponds to the maximum power point for this water speed. Note that this point is not at the peak of the torque curve, but to the right side. It is also important to realize that for operation to remain at point *A*, a load torque must be applied to the turbine that is equal in magnitude

and opposite in direction to the hydraulic torque produced by the turbine rotor (in fact the same can be said of all points on all torque curves in Fig. 5.1).

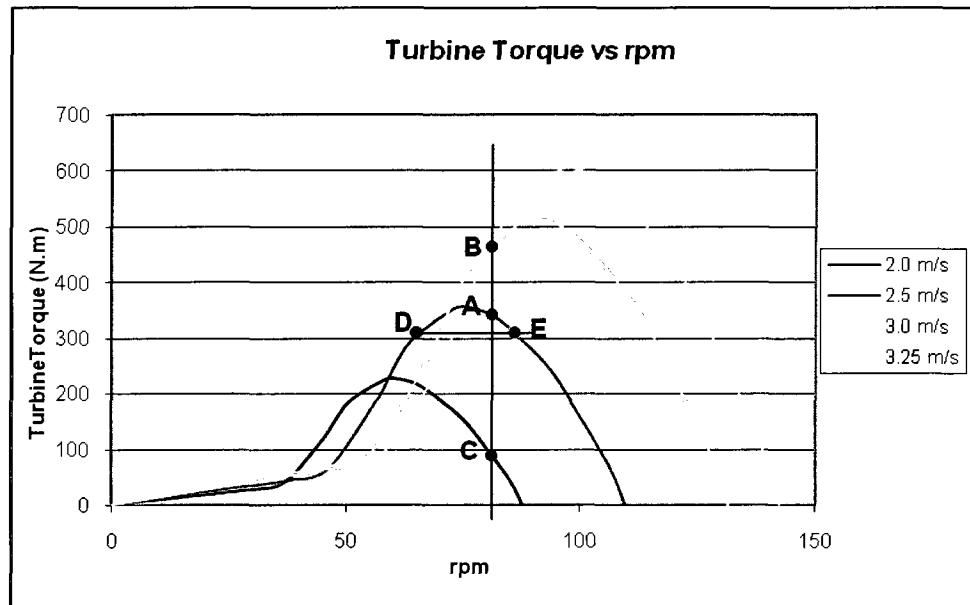


Figure 5.1: Turbine torque versus rpm for different free stream velocities

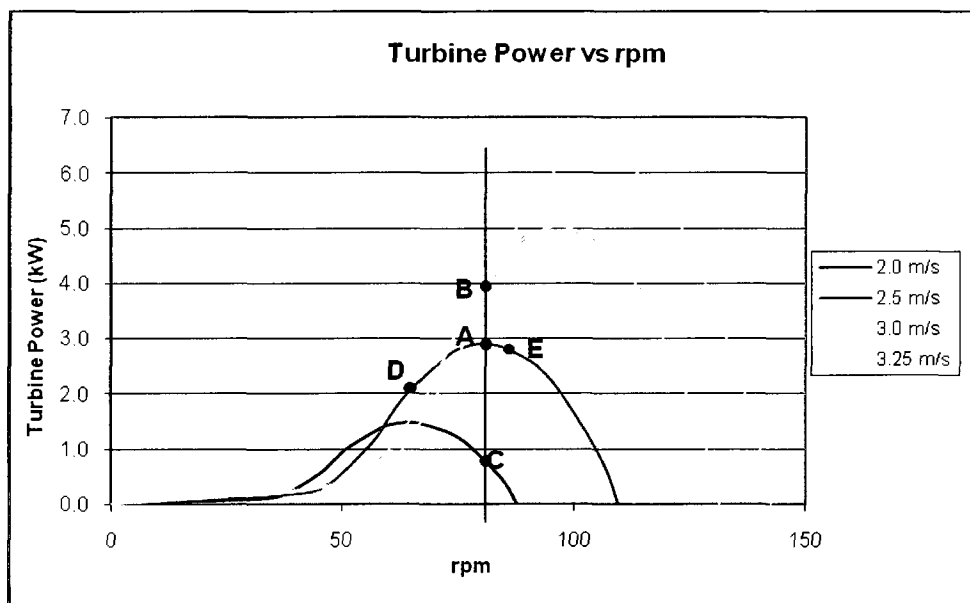


Figure 5.2: Turbine power versus rpm for different free stream velocities

If the load torque applied to the turbine were deviated so as to increase slightly, the turbine rpm would decrease causing an increase in turbine torque output and the system would find a new stable equilibrium point slightly to the left of point *A* (where the output and load torques match). Now, again starting from point *A*, if the load torque were deviated in such a way as to decrease slightly, the turbine would accelerate to a higher rpm value, thus decreasing the turbine output torque and finding a new equilibrium point right of point *A*. This represents stable operation.

To demonstrate unstable operation, we now consider point *D* which is to the left of the torque peak with similar deviations in the applied load torque. For a small increase in load torque, the turbine rpm again drops with a corresponding reduction in torque output causing the turbine to stall. Conversely if the load torque is reduced slightly, the turbine accelerates until a new equilibrium is reached at point *E* where the load and output torques again match. However, the operating point has effectively flipped to the right hand side of the curve with a corresponding large increase in rpm, again demonstrating unstable operation. Thus, the peak of the torque curve (and more generally the peak of the torque coefficient curve), defines the open loop stability boundary with the right hand portion of the curve corresponding to open-loop stable turbine operation. Note that the unstable portion of operation is also non-minimum phase. This is demonstrated by the inverse response characteristic in this region (i.e.: to increase the rpm in this region we must first reduce the load briefly then increase it to the required value for the new equilibrium point).

5.2.2 Nonlinearities

The main plant nonlinearities are twofold. The first is due to the quadratic dependency of hydraulic torque on flow velocity (as shown in Eq. 3 and demonstrated in Fig. 5.1). The second is due to the shape of the torque coefficient versus tip speed ratio curve (demonstrated in Fig. 4.4). Both of these nonlinearities become inconsequential if the plant operation can be restricted to a small range of water speeds and tip speed ratios, however, this is unrealistic in practice. The turbine is designed to operate between free stream velocities of 1.5 m/s and 3.25 m/s, covering a broad range of seasonal and daily flow variations found in a large number of rivers and tidal streams. As well, turbulence and operation under power regulation cause significant deviations in the tip speed ratio, even to open-loop unstable operation. For instance, to demonstrate the effect of turbulence, again consider operation at point *A* in Figures 5.1 and 5.2. If the free stream velocity suddenly increases from 2.5 m/s to 3.0 m/s, fast enough that the turbine rpm initially remains at its value of 81 rpm, then operation moves along a vertical line from point *A* to point *B*. This point is to the left of the corresponding peak torque of 510 N.m at 3.0 m/s and 90 rpm, and has therefore forced the plant to an unstable operating point. Note that operation under power regulation forces the plant to an open loop unstable operating point when the turbine rpm is lowered as flow velocities exceed 3.0 m/s to maintain the rated power output of 5 kW.

5.2.3 Time Varying Plant

There are several important time varying components of the plant which act to change the system performance characteristics, and whose effects are realized on

different time scales. The first is the effect of ambient temperature on drive system losses. As ambient temperature decreases, gearbox oil viscosity increases, effectively increasing the drive system losses. This effect can be realized on the time scale of a day; for instance daily high temperatures compared to cool evening temperature during the fall season. This causes the turbine performance curves to shift to a lower efficiency and a slightly lower tip speed ratio.

Another important time varying component is the turbine hydrofoil. These blades are subject to biofouling, corrosion and erosion. Biofouling is caused by marine organisms and algae growth. The effect is to change the lift and drag characteristics of the hydrofoil sections reducing their ability to generate thrust. For a stationary rotor this can occur in just a few weeks, whereas for rotating systems it can be delayed considerably. Corrosion is more of an issue in sea water, but can also be problematic in long term fresh water applications. Hydrofoil erosion due to suspended abrasives in the flow can cause similar changes to hydrofoil performance on the order of just two years in extreme circumstances (for instance rivers with very large sediment transport characteristics).

Finally, more traditional items such as bearing or gearbox wear also influence plant characteristics, but on much larger time scales such as 5 to 10 years.

In the present work where a turbine speed control system is to be developed, the time varying components of the plant are not treated directly other than to ensure reasonable robustness margins in the H_∞ LPV control design by maintaining a reasonably low worst-case-magnitude of the chosen input-output transfer function infinity-norm (denoted by the performance level γ). However, it must be noted that this synthesis technique was originally chosen in large part for the ease of incorporating more specific

information about this variability directly in the controller synthesis (for future work, when the information becomes available) to guarantee performance and stability.

Adaptive techniques such as intelligent memory found in [95] may be employed to modify the speed reference in conjunction with the H_∞ LPV controller, to ensure optimal energy extraction for the entire operating range.

5.3 Control Objectives

Control system objectives normally include implementation considerations such as starting and emergency shutdown, as well as performance considerations. The implementation considerations while important are not the focus of this research though some consideration of them will be required when field-testing the system. To develop control system objectives we should begin with consideration of the variable speed turbine system advantages ([65] and [68]), which are;

- Allows the turbine system to maximize energy capture for a wide range of operating conditions by varying the turbine rpm.
- Allows power regulation and smoothing
- Cavitation mitigation
- Alleviation of torque and force transients in both the turbine and mooring systems.
- Allows a method to induce desired system dynamics.
- Allows a method to decouple the generator and turbine from electrical grid dynamics.

Since the “energy” in our process is free (for instance, we do not need to fill it with gasoline or purchase coal for it), stating increased efficiency as an objective does not

add value unless it reduces the cost of electricity. However, validating that a certain method of increasing the efficiency lowers the cost of electricity is a research project in itself and is thus beyond the scope of this work. We will assume that maximizing the energy capture is a reasonable objective for the control system and forego the economic analysis at this time.

Power regulation can be accomplished by either increasing or reducing the turbine speed as flows increase past the rated speed (i.e.: as flows exceed the speed at which the rated power output is achieved, in this case 3.0 m/s). In both cases the overall extraction efficiency is reduced to allow the power output to be maintained at, or below the rated power limit. For instance, Fig. 5.3 displays the reduction in efficiency (from 37% to 20%) as the tip speed ratio is reduced (from 2.5 to 2.0) by reducing turbine rpm.

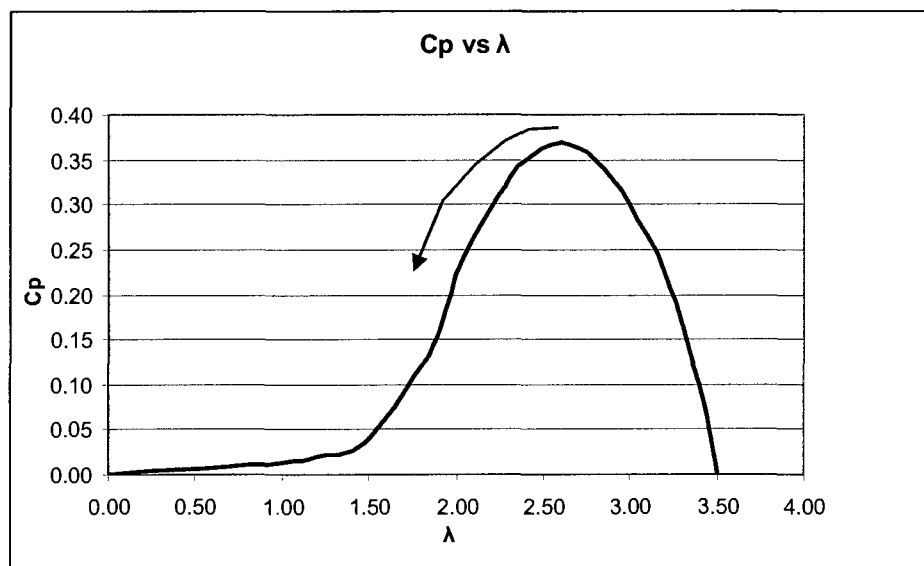


Figure 5.3: Power regulation by reducing turbine rpm to reduce system efficiency

Allowing an increase in turbine speed corresponds to increased centripetal forces on rotating components, increased hydrofoil normal forces and is limited by the open

loop time constant (since the generator and power electronics do not allow four-quadrant operation negating the possibility of motoring the turbine to a higher speed). Reducing the turbine speed reduces centripetal and hydrofoil normal forces and can be achieved much more quickly depending on control action, though at the expense of moving the operating point to the open loop unstable side of the performance curve where torque pulsation magnitudes are much larger.

Cavitation control can be accomplished in part by slowing the rotor to reduce the relative blade velocities and consequently hydrofoil peak suction pressures. As flow velocities go above rated speeds it is desirable to generate power as long as possible before shutting the system down due to high flow speeds (as opposed to shutting the turbine down at the cavitation limit). It must be noted that hydrofoil relative velocity magnitude decreases accomplished by reduction of turbine speed (even though the peak angle of attack is higher at low tip speed ratios) are more effective for cavitation reduction than increasing the turbine speed (and thus relative velocity magnitude) in an attempt to reduce the peak angle of attack.

Smoothing the power output has several advantages. First, due to the nature of vertical axis turbines, torque pulsations can be significant. Therefore, if the turbine speed were rigidly fixed at an rpm setpoint (for instance in a very smooth flow with little turbulence), the power output would fluctuate in proportion to the hydrodynamically induced torque pulsations. This has a tendency to destabilize turbine control as well as the electrical grid (especially for very large turbine systems). Since smoothing the power output for our particular turbine system corresponds in part to mitigating torque pulsations and thus load current, it is therefore related to the current control used for

turbine speed management (note that the exact relation between power smoothing and torque control is quite complex and depends on system rotating inertia, turbine torque production characteristic and generator voltage/rpm curve slope and is beyond the scope of this discussion). Second, these torque pulsations impact every component of the drive system. Reducing their magnitude would directly result in a much longer fatigue life of all components (especially on systems where *lean* design methods are employed to remove weight and reduce system cost). The third advantage is that energy due to torque transients caused by mooring system dynamics and turbulent flows can be smoothed through hydraulic energy/rotor kinetic energy exchanges giving a similar improvement in drive component fatigue life.

Finally, isolation of the turbine and electric generator systems from electrical grid dynamics is attained by the use of a variable speed generator and power electronics. This allows the generator and drive system to remain unaffected by destructive grid transients. Normally the use of synchronous generators for direct grid connection of such small energy sources results in premature and catastrophic failure of the generator or drive system thus precluding their use. Since this decoupling is attained simply through the use of the variable speed electrical system, it is not required in the control system objectives. Based on the preceding discussion, the control system objectives can be summarized as follows.

- Obj 1. Maximize energy capture
- Obj 2. Allow for power output smoothing.
- Obj 3. Allow for power regulation above the rated turbine speed.
- Obj 4. Reduce cavitation over wider range of flow velocities.

Obj 5. Alleviate torque and force transients in both the turbine and mooring systems.

Obj 6. Induce desired system dynamics and stability over the required operating range

Note that these objectives are not quantitative and may seem somewhat vague.

However, there is a fundamental tradeoff between some of these objectives (such as maximizing power output and reducing torque transients) and it is felt that a better idea of quantitative aspects where these tradeoffs exist are better explored through simulation and field testing to enable a better understanding (especially for this early work where no maximum load magnitude corresponding to required fatigue life is available).

5.4 Control strategy

The choice of control strategy is also very important. We will begin by outlining the four regions of operation for the turbine system (shown in Fig. 5.4). In Region 1 (from 0 to 1.5 m/s), the turbine is shutdown as operation is not economical when considering wear on components for the corresponding low power output. The cut in speed is the water speed at which the turbine begins operation and is shown at point *a* to be 1.5 m/s.

Region 2 operation (from 1.5 m/s to 2.9 m/s) is where the turbine is made to run at its maximum power point for optimal energy extraction (shown in Fig. 5.4 and Fig. 5.5). There are many possible strategies to achieve this (for instance, tracking the peak efficiency tip speed ratio, power tracking, etc).

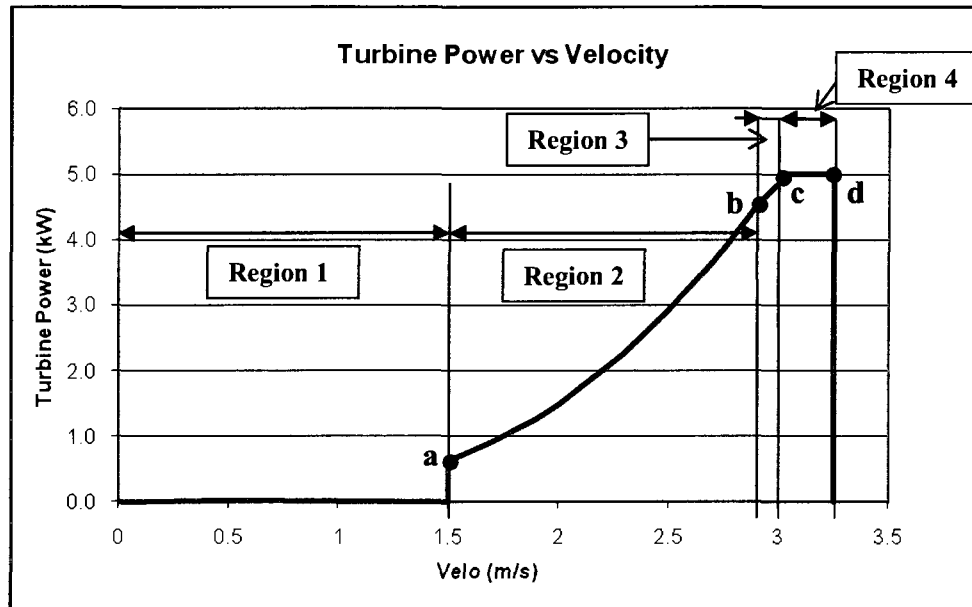


Figure 5.4: Four regions of turbine operation (power versus water velocity)

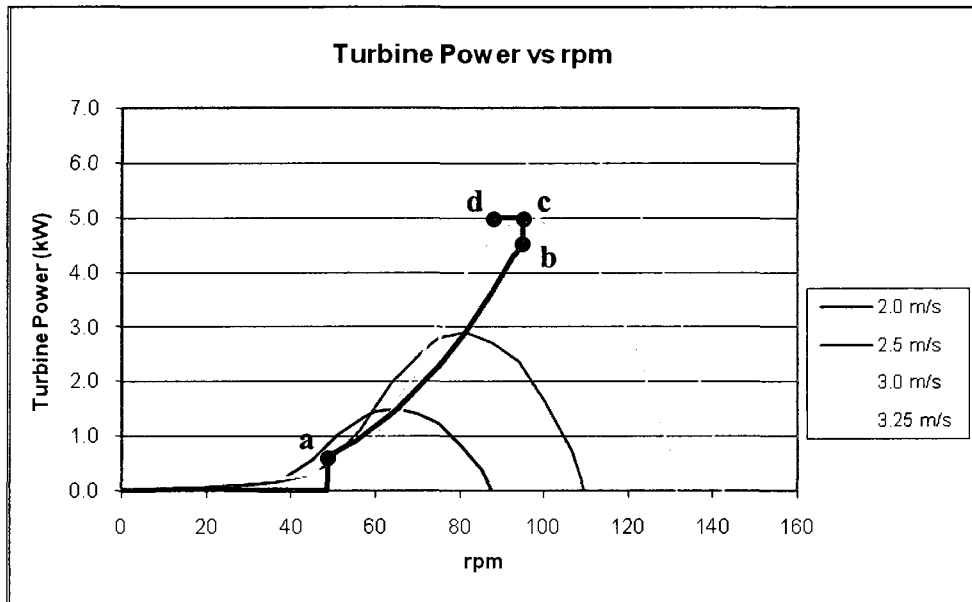


Figure 5.5: Control strategy example for turbine power versus rpm

A tradeoff exists between tight tracking of the peak power curve and increased drive train loads ([52], [53], [55] and [62]). In fact, tighter reference tracking is only achieved through stronger load torque action. Thus perfect tracking is not necessarily desired.

Since the turbulence characteristics for the test site (and river applications in general) are currently unknown, the method used in the present work is to track the maximum power point by maintaining turbine operation at the tip speed ratio corresponding to that of maximum efficiency (this is a constant value for any flow velocity).

In Region 3 (from 2.9 m/s to 3.0 m/s) the turbine is made to run at a constant speed. While some control strategies might eliminate this region (for example in [67] and [70]), the constant speed region significantly reduces overshoot during transitions between operation during maximum power (Region 2) and power regulation (Region 4). The curves in both Fig. 5.4 and Fig. 5.5 denote the locus of points for the idealized control strategy. Note that the flow velocity is a stochastic variable continuously trying to force operation off the control strategy locus.

In Region 4 (3.0 m/s to 3.25 m/s) the power output is limited to the rated power of the system. Power regulation is achieved by reducing the turbine rpm as flows increase past the rated flow speed. Note that *constant-power* regulation will be employed in the present work as flow velocities increase from point *c* to point *d* as shown in Fig. 5.4. There are advantages to reducing the power output in Region 4, such as with linear power reduction or constant torque operation, since torque pulsation magnitude increases at lower tip speed ratios', but this is at the expense of reduced output. Note that other methods of hydrodynamic power regulation such as centrifugally pumped lift spoiling [46], flaps or blade tilting mechanisms are not considered here due to reliability concerns with these forms of regulation in a marine environment.

At a flow velocity of 3.25 m/s the turbine is shutdown for protection purposes. This is called the cut out speed and is shown by point *d*.

5.5 Controller Synthesis

Gain scheduling techniques are widely popular in industry when dealing with significantly nonlinear or time varying plants. Two motivations for using these techniques are the ability to use powerful linear design tools and the intuitive nature of the design process. Traditional gain scheduling techniques commonly follow three steps.

1. Choose a set of operating points and scheduling variables followed by generation of an LTI model of the system behaviour for each point. This results in a family of models parameterized by the scheduling variables.
2. Design an LTI controller for each of the previously chosen operating points.
3. Formulate an algorithm to modify (through switching or interpolation) the controller according to the value of the scheduling variables.

The two main disadvantages to traditional techniques are that step 3 is not straightforward (and is rarely treated in literature) and stability and robustness are not guaranteed for the corresponding closed loop system over the operating range.

However, formulating gain scheduling problems in the framework of LPV systems removes these drawbacks by combining steps two and three into a single well defined design step and guaranteeing performance and stability properties for the closed loop system. Controller synthesis is cast into a convex optimization problem with linear matrix inequalities (LMI) for which several well developed numerical algorithms are available (details can be found in ([3], [4], [8], and [97])).

This section begins with a general introduction to robust gain scheduled control for LPV plants. Two controller designs are then presented. The first is the H_∞ LPV

controller which is the object of the current work. The second is a PI controller used for comparative testing of simulation and field testing results.

5.5.1 Introduction to Gain Scheduled Control for LPV Plants

In this section, a brief introduction to H_∞ LPV control is presented. To begin, we must derive an LPV description for a general nonlinear system

$$\begin{aligned}\dot{x}(t) &= f(x(t), w(t)) \\ y(t) &= h(x(t), w(t))\end{aligned}\tag{26}$$

where $x(t)$ is the state, and $w(t)$ is an external input. A vector of parameters $\theta(t) = [\theta_1, \dots, \theta_{n_\theta}]^T$ is then defined and used to parameterize the operating point. Each parameter contains information on the nonlinearities of the plant and is defined by a continuous function of time. The parameter vector $\theta(t)$ and its rate of variation $\dot{\theta}(t)$ are bounded as follows (from [13])

$$\begin{aligned}\theta(t) &\in \Theta, \forall t \geq 0 \\ |\dot{\theta}(t)| &< v_i, i = 1, \dots, n_\theta, \forall t \geq 0\end{aligned}\tag{27}$$

where Θ is a compact set.

The inequalities in Eq. 27 define a hypercube

$$\mathcal{V} = \{\dot{\theta}(t): |\dot{\theta}(t)| < v_i, i = 1, \dots, n_\theta, \forall t \geq 0\}$$

with vertices in

$$\mathcal{V}_v = \{[\theta_{d1}, \dots, \theta_{dn_\theta}]^T : \theta_{di} \in \{-v_i, v_i\}, i = 1, \dots, n_\theta, \forall t \geq 0.\}$$

Finding a state space LPV description involves linearizing the set of equations in Eq. 26 around an equilibrium operating point (the operating point is parameterized by the vector $\theta(t)$), so that after linearization we obtain the open loop plant

$$\begin{aligned}\dot{\mathbf{x}} &= \mathbf{A}(\theta(t)) \mathbf{x}(t) + \mathbf{B}(\theta(t)) \mathbf{w}(t) \\ \mathbf{y} &= \mathbf{C}(\theta(t)) \mathbf{x}(t) + \mathbf{D}(\theta(t)) \mathbf{w}(t) .\end{aligned}\tag{28}$$

The stability of an LPV system is established by finding a parameter dependent Lyapunov function which leads to the concept of parameter dependent quadratic (PDQ) stability (introduced in [88]).

Definition: PDQ Stability

Given the compact set Θ and hypercube \mathcal{V} , the continuous function

$\mathcal{A}(\theta)$ is PDQ stable if there exists a continuously differentiable

function $\mathcal{X}(\theta)$ such that $\mathcal{X}(\theta) > 0$ and

$$\mathcal{A}^T(\theta) \mathcal{X}(\theta) + \mathcal{X}(\theta) \mathcal{A}(\theta) + \dot{\mathcal{X}}(\theta) < 0$$

It is important to note that when there are no bounds on the parameter variation rate ($v_i \rightarrow \infty, i = 1, \dots, n_\theta$) the search for the Lyapunov function is restricted to a set of constant matrices ([13]) and PDQ stability simplifies to more familiar quadratic stability

$$\mathcal{A}^T(\theta) \mathcal{X} + \mathcal{X} \mathcal{A}(\theta) < 0 .$$

The assumption of unbounded parameter variation rates results in a more conservative controller, though this is noted to be insignificant in [14].

Performance of a closed loop LPV system can be specified in several ways though it is common to characterize it by the induced \mathcal{L}_2 -norm of a chosen set of input

output operators that represent the control objectives. This allows the performance in the control specification to follow closely that of H_∞ theory. For a given set of parameter trajectories the induced \mathcal{L}_2 -norm is defined as

$$\|T_{zw}\|_{i,2} = \triangleq \sup_{\|w_2\| \neq 0, w \in \mathcal{L}_2} \frac{\|z\|_2}{\|w\|_2} \quad (29)$$

where T_{zw} gives the forced response with zero initial condition to an input signal w (for the chosen variables). A bound $\gamma > 0$ placed on the input output operator such that $\|T_{zw}\|_{i,2} < \gamma$ for an exponentially stable LPV system is said to have performance level γ . Essentially for a constant parameter trajectory, induced \mathcal{L}_2 -norm performance simplifies to H_∞ performance [14]. Weighting functions are used to stress the importance of the selected inputs and outputs at the frequencies of interest during the minimization procedure. These are generally rational functions of the complex frequency s and must be proper (i.e.: bounded as $s \rightarrow \infty$). Thus, with the system linearized, the performance variables and weighting functions chosen, the standard LPV description of the open loop system can be written as the augmented plant,

$$\begin{aligned} \dot{\hat{x}} &= A(\theta) \hat{x}(t) + B_1(\theta) \hat{w}(t) + B_2(\theta) \hat{u}(t) \\ \hat{z} &= C_1(\theta) \hat{x} + D_{11}(\theta) \hat{w} + D_{12}(\theta) \hat{u} \\ \hat{y} &= C_2(\theta) \hat{x} + D_{21}(\theta) \hat{w} + D_{22}(\theta) \hat{u} \end{aligned} \quad (30)$$

where

$$A(\theta) = \left. \frac{\partial f}{\partial x} \right|_{(op)} \quad B_1(\theta) = \left. \frac{\partial f}{\partial w} \right|_{(op)} \quad B_2(\theta) = \left. \frac{\partial f}{\partial u} \right|_{(op)}$$

$$\begin{aligned}
 C_1(\theta) &= \left. \frac{\partial g}{\partial x} \right|_{(op)} & D_{11}(\theta) &= \left. \frac{\partial g}{\partial w} \right|_{(op)} & D_{12}(\theta) &= \left. \frac{\partial g}{\partial u} \right|_{(op)} \\
 C_2(\theta) &= \left. \frac{\partial h}{\partial x} \right|_{(op)} & D_{21}(\theta) &= \left. \frac{\partial h}{\partial w} \right|_{(op)} & D_{22}(\theta) &= \left. \frac{\partial h}{\partial u} \right|_{(op)}
 \end{aligned}$$

and x is the state, w is the disturbance, u is the input, z is the performance output, and y is the measured variable. Note that these derivatives are evaluated at the operating points (indicated by the notation op). An assumption implicit in this LPV model derivation is that the equilibrium point does not change. Therefore, only if the parameters vary slowly enough is the model valid.

The augmented plant is shown in Fig. 5.6 where $G(\theta)$ is the plant, $W_e(s)$ and $W_u(s)$ are the error and control weighting functions respectively and \tilde{e} and \tilde{u} are the performance output variables. The general problem where only these two weighting functions are employed is known as the Mixed Robust Stability and Performance Problem ([34] and [99]) in H_∞ control.

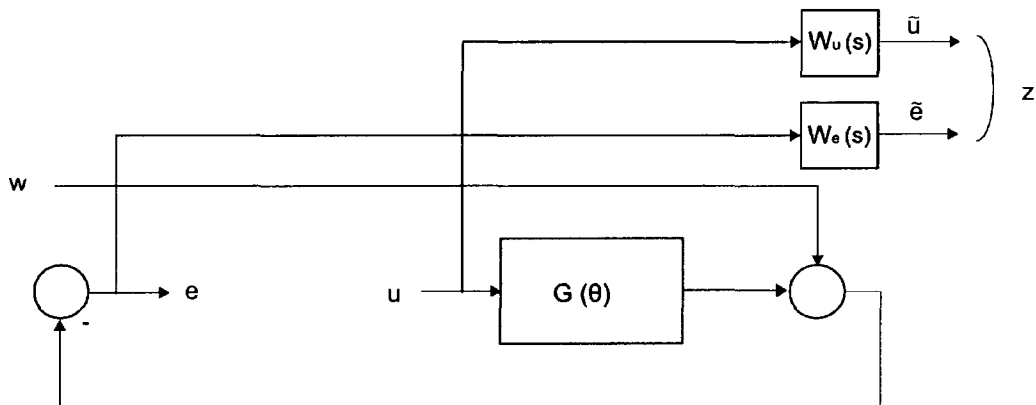


Figure 5.6: General augmented LPV plant

There are a few subtleties when solving the *general* convex optimization problem with the LMI constraints. First, D_{22} is assumed to be zero and the pairs $A(\theta), B_2(\theta)$ and

$A(\theta), C_2(\theta)$ must be parametrically dependent stabilizable and parametrically dependent detectable respectively. Second, the general optimization problem involves finding a solution for an infinite number of constraints (one for each $(\theta, \dot{\theta})$ pair in the parameter trajectory space) and infinite number of decisions variables. This can be overcome by the use of gridding techniques employed over the compact set Θ (by iteratively defining a grid, solving the optimization problem and verifying feasibility at each point in the grid and if infeasible, define a denser grid and reiterate). This must be carried out online and can involve considerable computation time and effort. However, in the special case that the plant matrices are affine in the parameters, Θ is a convex polytope, B_2, C_2, D_{12} , and D_{21} are parameter independent, and constant Lyapunov matrices are used, the solution and implementation becomes more practical. In this case both the set of unknowns and the set of LMI's become finite dimensional. As well, it is sufficient to check the LMI's at the vertices of the polytope. The general procedure follows

1. First the vertex controllers (control matrices at each vertex in the convex polytope Θ_v) are solved offline and stored (instead of online iteratively for every grid point with each grid point control matrix requiring storage).
2. The parameter vector is measured in real time and the convex decomposition of $\theta(t)$ calculated

$$\theta(t) = \sum \alpha_i \theta_{vi}(t) \quad (31)$$

where θ_{vi} are the vertices of Θ_v , $\alpha_i > 0$, and $\sum \alpha_i = 1$.

3. Finally the controller matrices for each control period are calculated from a linear combination of the constant vertex controller matrices

$$\begin{aligned}
A_c(\theta) &= \sum \alpha_i(\theta) A_{ci} & B_c(\theta) &= \sum \alpha_i(\theta) B_{ci} \\
C_c(\theta) &= \sum \alpha_i(\theta) C_{ci} & D_c(\theta) &= \sum \alpha_i(\theta) D_{ci}
\end{aligned} \tag{32}$$

where the A_{ci} , B_{ci} , C_{ci} , and D_{ci} are the vertex controller matrices.

Note the requirements that B_2 , C_2 , D_{12} , and D_{21} be parameter independent are not too restrictive in practice since parameter dependent B_2 and D_{21} matrices can be made constant by pre-filtering the control input u ; and parameter dependent C_2 and D_{12} matrices can be made constant by post-filtering the measured variable y . The requirement that the Lyapunov matrices be constant adds some conservatism to the controller, but this is noted to be insignificant in [14].

For a more detailed exposition of the theory for gain scheduled LPV systems, several works are available that summarize the background and synthesis procedures. For the expert in robust control a very concise exposition of the important concepts is available in *Appendix B* of [12]. More thorough expositions are available in [18], [35] and [47].

5.5.2 H_∞ LPV Controller Synthesis

In this section, the H_∞ LPV control synthesis for the 5kW vertical axis hydrokinetic turbine is presented. The control variable has been chosen as the load current and the feedback variable as the turbine speed. The vector of parameters is chosen as $\theta = [\overline{\Omega}_R, \overline{V}_\infty]$ which completely specify the operating point. The general interconnected system is shown in Fig. 5.7 where $P(\theta)$ is the augmented plant.

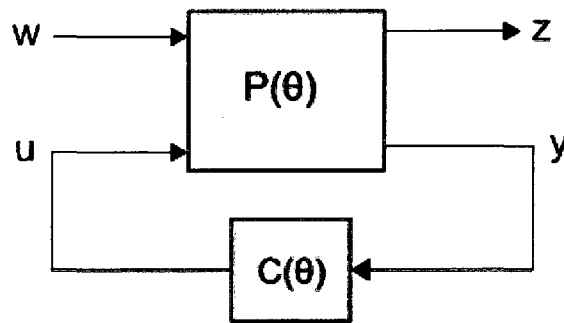


Figure 5.7: General interconnected system

Given the linearized LPV description of the plant in Sec. 4.5 (Eq. 23 and Eq. 24), the next step in the design process is to define the so-called input (w), output (z) pairs or performance variables that represent the control objectives.

Obj. 1 (maximize energy capture) is carried out by tight tracking of the maximum power point curve shown from points a to b in Fig. 5.4. Control objectives Obj. 3 (provide power regulation) and Obj. 4 (reduce cavitation) are carried out through choice of the control strategy by reducing the turbine rpm as flows exceed the rated flow velocity of 3.0 m/s. For Obj. 3, this corresponds to reducing the tip speed ratio in Fig. 5.3 to a point that reduces the system efficiency enough that only the rated 5 kW of power is produced. For Obj. 4, the effects of cavitation are reduced as turbine speeds are decrease since the hydrofoil relative water velocity magnitude (square root of the sum of the squares blade tangential velocity and water velocity magnitudes) and therefore peak suction pressures are reduced.

Obj. 2 (power output smoothing) and Obj. 6 (induce desired system dynamics) are related to Obj. 5 (reduce load transients) as discussed previously since the load current is the control variable. In the present work where a first order model of the plant is assumed, the load torque (or generator torque $T_G = K_G i_q$) is an approximation of the

turbine shaft torque. Thus ensuring smooth changes in the control variable i_q corresponds to fulfilment of these three objectives. Therefore, the disturbance w in Fig. 5.7 is chosen as the turbine speed reference and the performance variables are the weighted error \tilde{e} and the weighted control \tilde{u} . A two port diagram of the augmented plant in the interconnected system (showing the problem setup) is shown in Fig. 5.8.

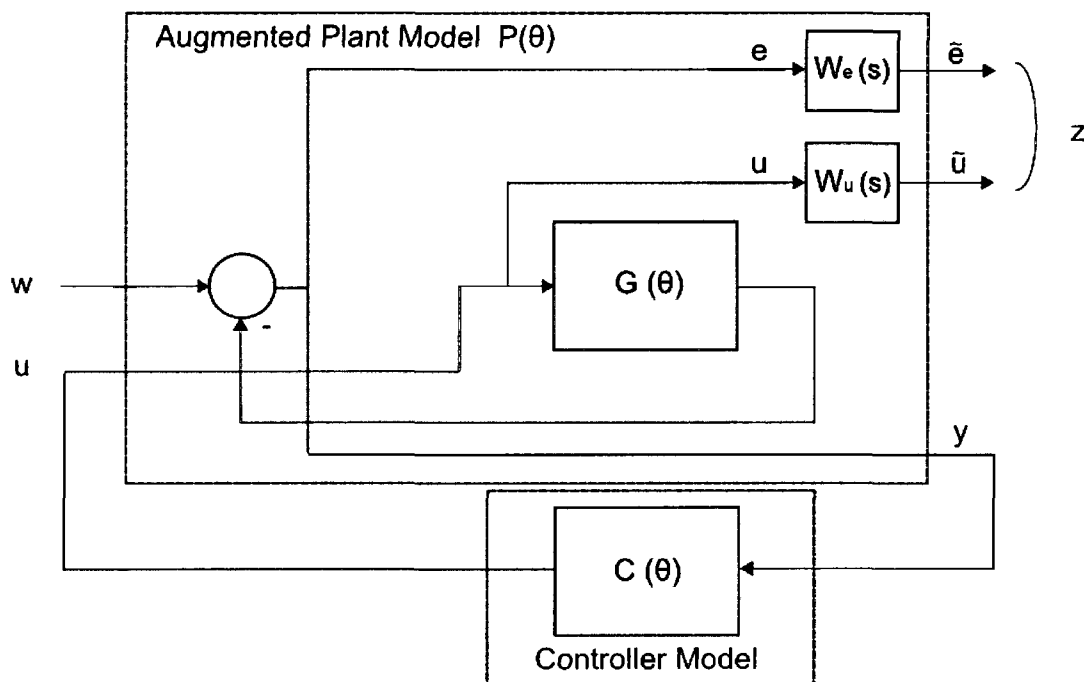


Figure 5.8: Two port diagram with weighting functions

A comparison of Fig. 5.7 and Fig. 5.8 demonstrates how the general control problem is transformed to fit the hydrokinetic turbine and prescribed performance objectives. It is important to note that this is used for the controller synthesis only, to facilitate the minimization procedure described in Sec. 5.5.1.

The weighting functions (also called tuning functions) are now specified to define the tradeoff between tight reference tracking and torque pulsation magnitude. $W_e(s)$ is the

sensitivity (or error) weight. Good control design should result in a sensitivity function satisfying both band width ω_b and peak sensitivity M_s requirements represented as (from [103] and [104]),

$$W_e = G_{we} \left(\frac{\frac{s}{\sqrt[k]{M_s}} + \omega_b}{s + \omega_b \sqrt[k]{\varepsilon}} \right)^k \quad (33)$$

where ε is maximum steady state error to a step input, G_{we} is a gain factor and k is the order of the filter (higher for steeper roll off). The magnitude of the sensitivity function is desired to be small at low frequencies where the magnitudes of the reference and disturbance are large (thus $W_e(s)$ amplifies low frequency components of the reference during the optimization to give good low frequency tracking performance). A similar reasoning is employed for the *control sensitivity* function to roll off as quickly as possible beyond the desired control bandwidth to reduce the effects of noise. Thus the control sensitivity (or control) weighting function $W_u(s)$ is

$$W_u = \left(\frac{s + \frac{\omega_{bc}}{\sqrt[k]{M_u}}}{\sqrt[m]{\varepsilon} s + \omega_{bc}} \right)^m \quad (34)$$

where M_u is the peak control sensitivity, ω_{bc} is the controller bandwidth and m is the filter order (higher for steeper roll off). Iterative testing to find appropriate values for these weighting functions was carried out resulting in a very good tradeoff between reference tracking and torque transients. The values used for the final controller are

$$M_s = 1 \quad k = 1 \quad \varepsilon = .008 \quad \omega_b = 12 \quad G_{we} = 10$$

$$M_u = 1 \quad m = 2 \quad \varepsilon = 1 \quad \omega_{bc} = 30$$

The frequency response for the error and control weighting functions used in the present work are given in Fig. 5.9.

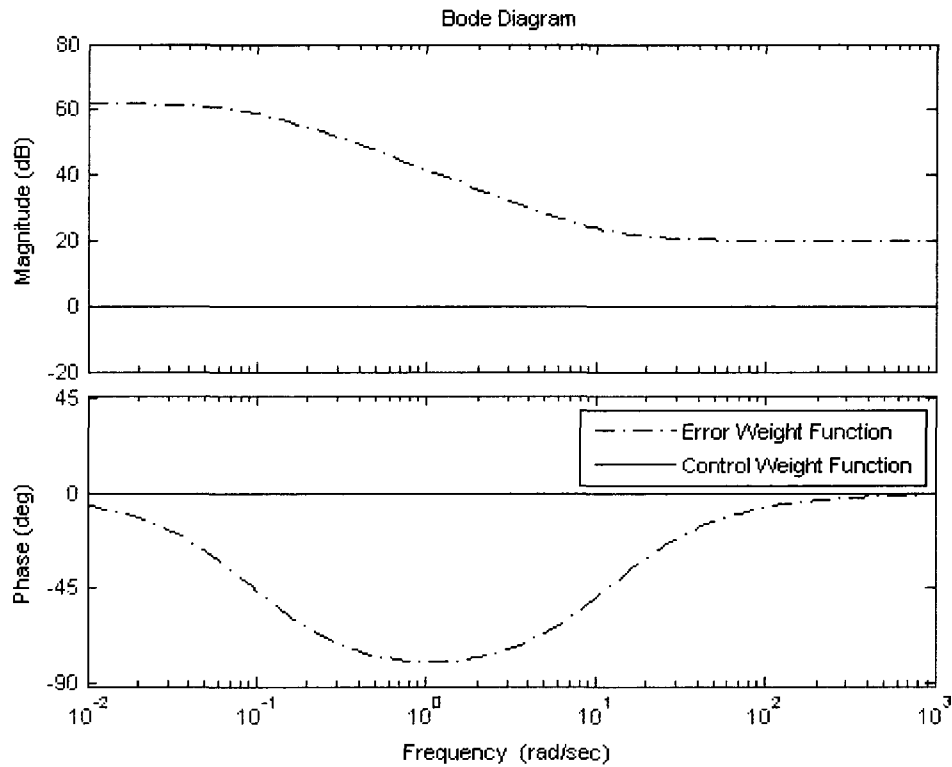


Figure 5.9: Frequency response for error and control weighting functions

With the input and performance variables chosen, and the weighting functions specified, the equations for the augmented plant can be written in standard form (as in Eq. 30). Let the state space representation of $W_e(s)$ and $W_u(s)$ be denoted by $(A_{we}, B_{we}, C_{we}, D_{we})$ and $(A_{wu}, B_{wu}, C_{wu}, D_{wu})$ respectively, with the state space representation of the plant given in Eq. 22 and Eq. 23. The augmented-plant state-space description can be written

$$P(\theta) = \begin{bmatrix} A & B_1 & B_2 \\ C_1 & D_{11} & D_{12} \\ C_1 & D_{21} & D_{22} \end{bmatrix} = \begin{bmatrix} A_m & 0 & 0 & 0 & 0 & B_m \\ B_{we} C_m & A_{we} & 0 & 0 & B_{we} & -B_{we} D_m \\ 0 & 0 & A_{wu} & 0 & 0 & B_{wu} \\ -D_{we} C_m & C_{we} & 0 & 0 & D_{we} & -D_{we} D_m \\ \hline 0 & 0 & C_{wu} & 0 & 0 & D_{wu} \\ \hline -C_m & 0 & 0 & 0 & I & -D_m \end{bmatrix} \quad (35)$$

Note,

$$D_{22} = -D_m = 0$$

$B_2 = [0 \ B_{we} \ 0 \ D_{we}]$, and does not depend on θ

$C_2 = [-C_m \ 0 \ 0 \ 0]$, and does not depend on θ

$D_{12} = D_{wu}$, and does not depend on θ

$D_{21} = I$, and does not depend on θ .

Finally, the region Θ in which the parameters vary must be specified. Since the parameters $\theta_1 = \overline{\Omega_R}$, $\theta_2 = \overline{V_\infty}$ completely specify the operating point, the locus of possible operating points is determined by the control strategy shown by the broken line in Fig. 5.10. A convex region (shown with solid line) that is large enough to account for operating point deviations during turbulent flow variations, and includes the control strategy is specified by three vertices v_1 , v_2 , and v_3 . It is interesting to note that the control strategy can be changed without the need to redesign the controller as long as it lies inside the polytope.

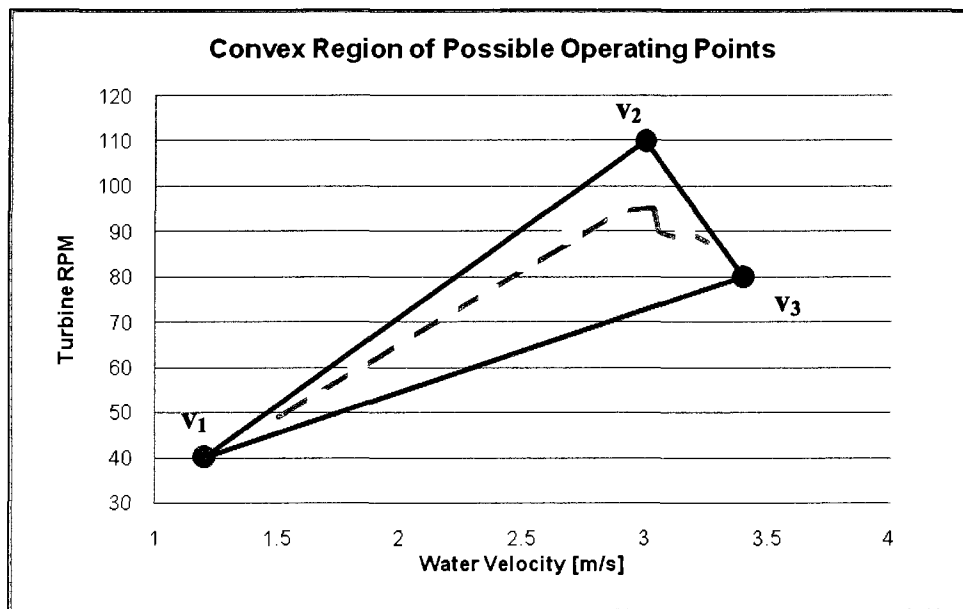


Figure 5.10: Convex region of possible operating points

MATLAB was used to solve for the controller using built in functions from the Robust Control Toolbox [33]. An m-file was generated to carry out the control synthesis and Simulink models were generated for iterative testing to tune the control system. The Simulink model is included in Appendix G.

A turbine speed reference signal generator is implemented for simulation as well as field testing. The signal generator automatically calculates the turbine speed reference based on a measurement of the water speed. For Region 2 operation, the tip speed ratio corresponding to maximum extraction efficiency is constant and known from the turbine manufacturers' performance information (in Fig. 4.1). Thus the turbine rpm corresponding to optimal power output can be calculated based on a flow speed measurement using Eq. 4. For Region 4 operation the water speed measurement is used in conjunction with the known C_p characteristic as well as Eq. 2 and Eq. 4 to calculate the rpm at which rated power is delivered. This method of reference generation is known as

tip speed ratio control. The closed loop implementation of the control system is shown in Fig. 5.11.

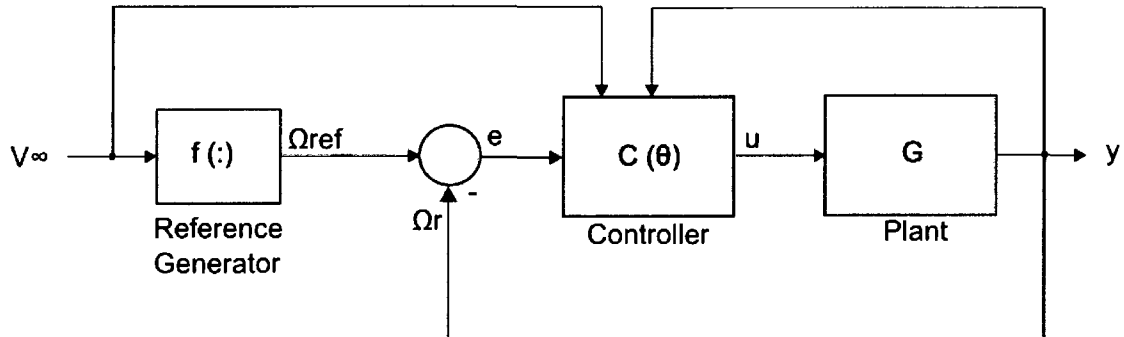


Figure 5.11: Closed loop implementation of the H_∞ LPV controller

Fifteen random parameter sets were generated with values corresponding to stable and unstable open loop operation, covering the entire range of operating points. The parameters are frozen at these values and the step response of the closed loop plant shown in Fig. 5.12. Each of the fifteen step response plots in Fig. 5.12 lay so closely on top of each other that distinction between individual plots is difficult. This demonstrates that the performance and stability for the closed loop system is consistent throughout the entire range of operation. The controller was generated with $\gamma = 1.4$, level of performance.

The fifteen parameter sets chosen for the step response are shown as black points in Fig. 5.13. For comparative purposes fifteen step responses of a fixed point controller (a controller whose structure is fixed), for the same fifteen parameter sets is presented in Fig. 5.14. The closed loop poles for the fixed point controlled system are the same as the H_∞ LPV controlled system at the operating point of 2.25 m/s and 69.1 rpm (i.e.: this is the design point of the fixed point controller).

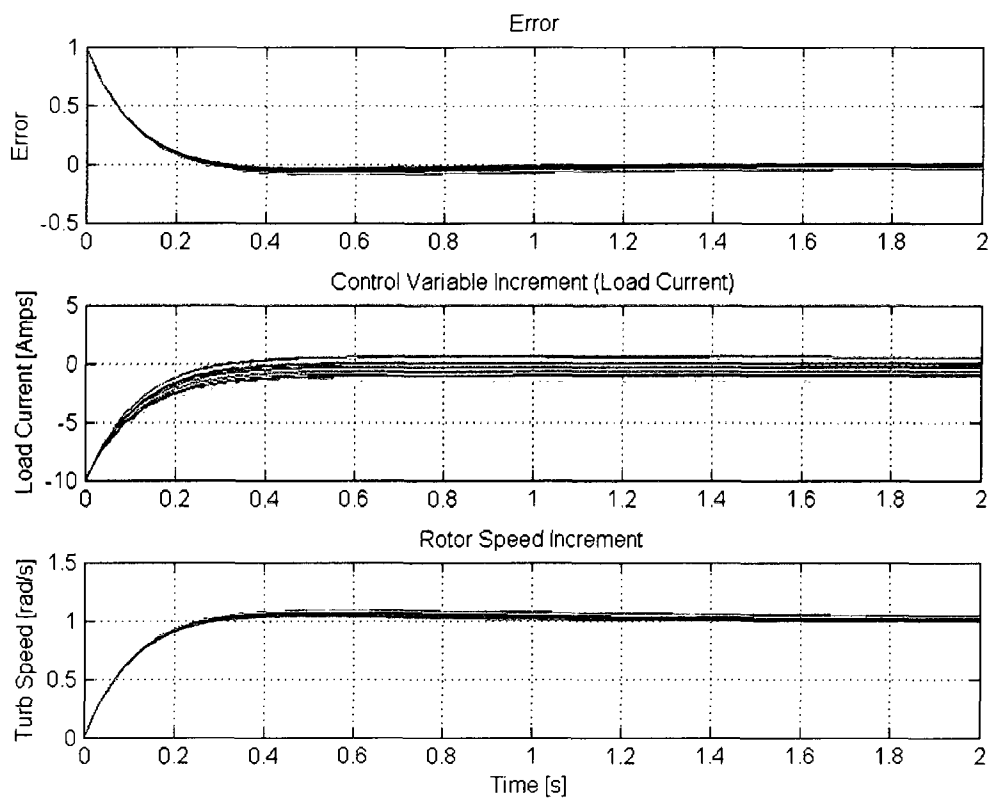


Figure 5.12: H_∞ LPV, 15 step responses for 15 frozen parameter sets

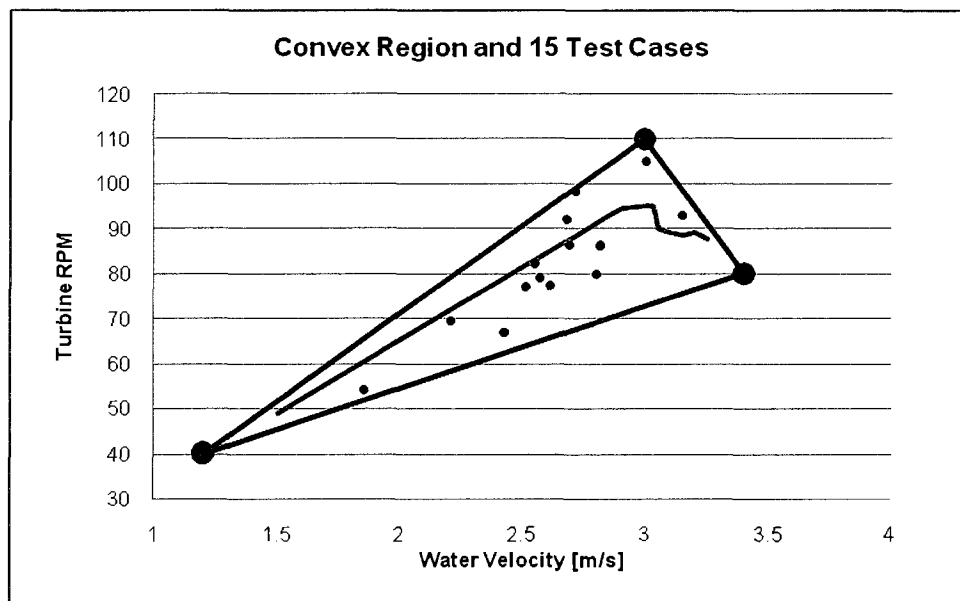


Figure 5.13: Fifteen parameter sets $\theta = [\bar{\Omega}_R, \bar{V}_\infty]$ chosen for step response

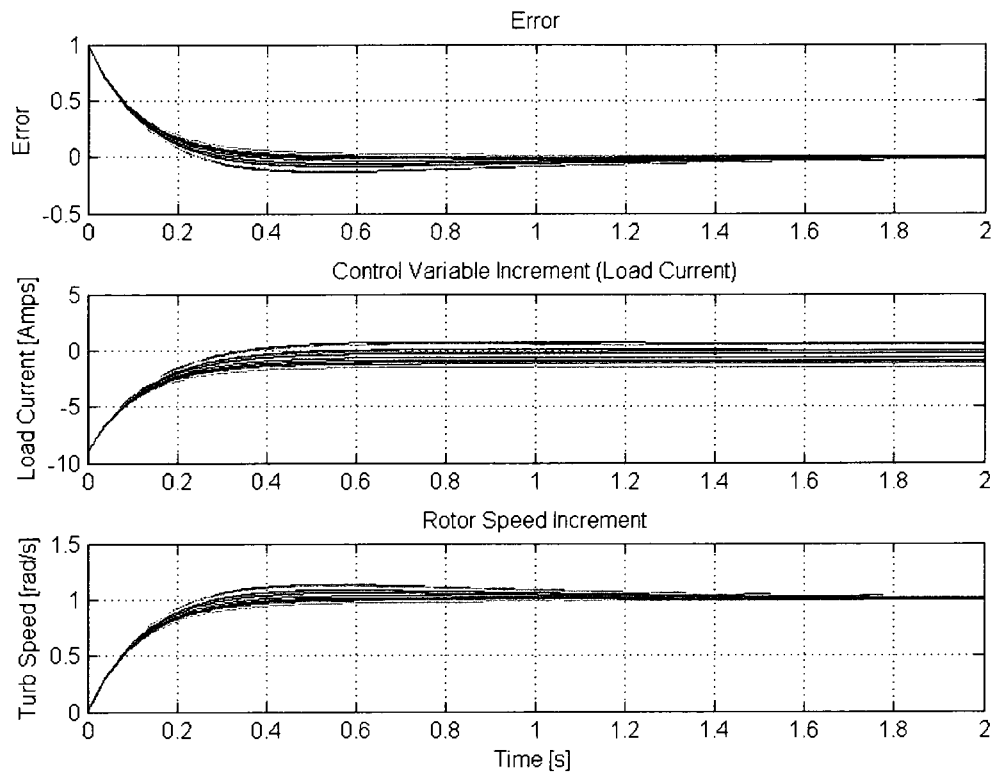


Figure 5.14: Fixed point control, 15 step responses for 15 frozen parameter sets

The error and turbine speed response is much more consistent for the gain scheduled controller. The steady state load current is very similar for both the gain scheduled and fixed point controlled systems since this is dictated by the operating point and turbine characteristics, not the type of control.

The closed loop system Bode plot for the operating point of 2.25 m/s and 69.1 rpm is shown in Fig. 5.15. This is the same for the gain scheduled and fixed point control and serves as an example of the frequency response of the closed loop system.

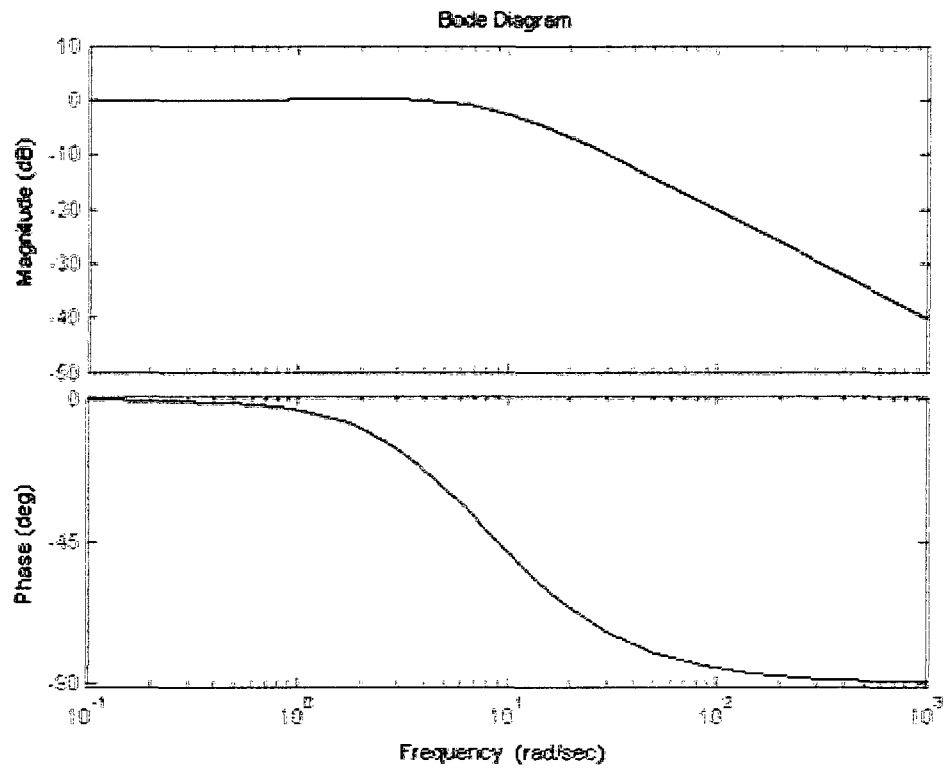


Figure 5.15: H_∞ LPV closed loop magnitude and phase plots for $\theta = [69.1, 2.25]$

To demonstrate the response to time varying parameters, MATLAB was used to generate the continuous time parameter trajectory shown in Fig. 5.16. The parameters traced the trajectory shown inside the polytope over a 20 second period. The step response is shown in Fig. 5.17 and is smooth given the large parameter changes.

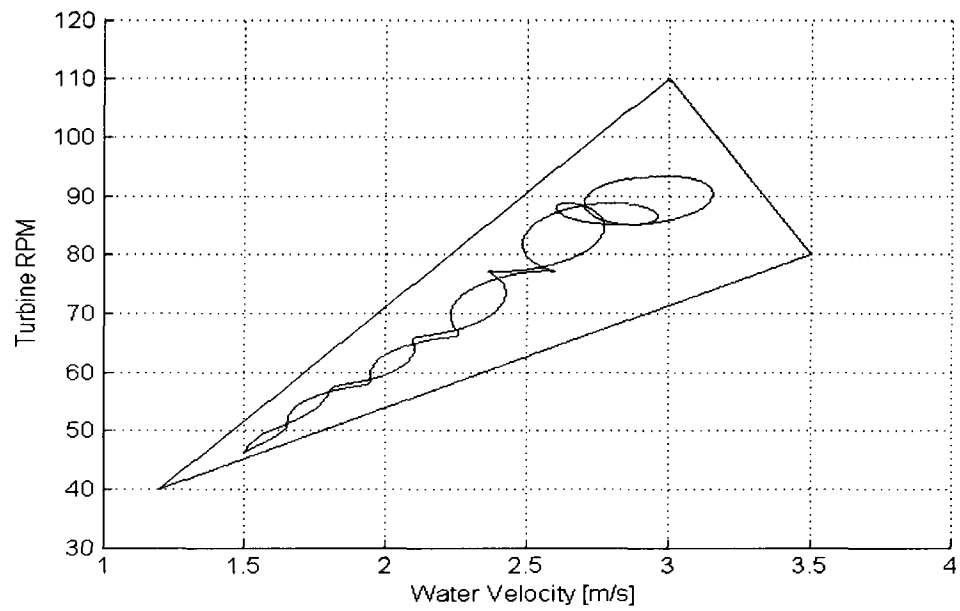


Figure 5.16: Twenty second time varying parameter trajectory shown inside polytope

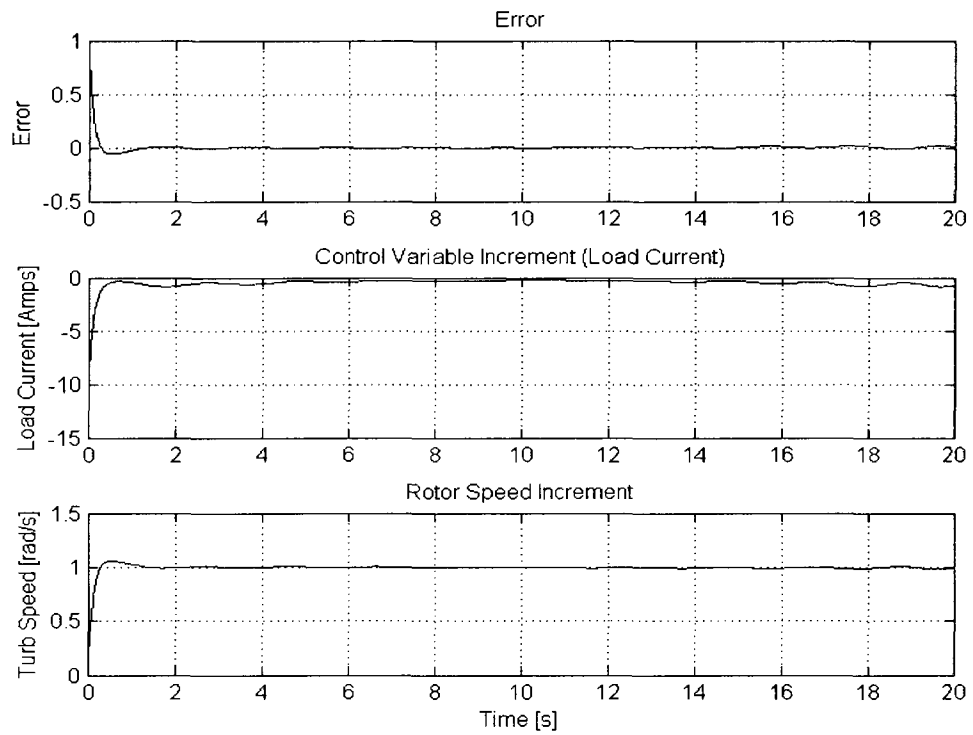


Figure 5.17: H_∞ LPV step response for time varying parameters

5.5.3 PI Controller Synthesis

A PID controller was synthesized for comparative purposes during simulation and field testing. As it turned out, the derivative gain was not required and the derivative term dropped from the controller. Note that this corresponds well to the fact that PI control is still widely used in the wind industry (not PID).

It was designed for a single operating point and does not take into account variations in the plant characteristics with changing values of the operating point. This is a turbine speed controller where the load current is the control variable and the turbine speed is the feedback variable. The controller was tuned at the test site manually for fast response and tight tracking of the control strategy without consideration of torsional transients. This is mainly to demonstrate the effects of control where load transients are not considered in the synthesis (and/or tuning procedures) such as all the methods listed in Sec. 2.4.1 and many in Sec. 2.4.2. Therefore the control gains are quite high and control action is aggressive. For this work, the proportional gain was chosen as 100 and the integral gain as 10, which gives tight reference tracking as well as relatively small steady state error at an operating point corresponding to peak extraction efficiency around a flow velocity of 2.25 m/s and turbine speed of 69 rpm.

5.5.4 Simulation Results

Simulation results are presented here to compare the response of the closed loop PI and H_{∞} LPV controlled plants. While reasonable comparisons can be made for Region 2 operation (maximum power tracking), the PI controlled system was not expected to perform well in Region 4 since the system parameters are significantly different than the

original design point. However, since the model is first order (and thus more forgiving than the actual plant) and the PI gains are very high, tracking performance turns out to be reasonable.

The step response for both systems is presented first, followed by system response to a flow velocity signal taken Oct 9, 2008 in the field. The automatic reference generator is employed to track the maximum power point as this flow signal changes to give the *tracking* response for both closed loop systems. Finally, operation under power regulation using the automatic reference generator is simulated and discussed.

5.5.4.1 Step Response (Region 2)

The step response is presented for both controllers at 2.25 m/s water velocity with a step increase in turbine rpm from 70 rpm to 75 rpm. The PI and H_∞ LPV results are shown in Figures 5.18 and 5.19 respectively.

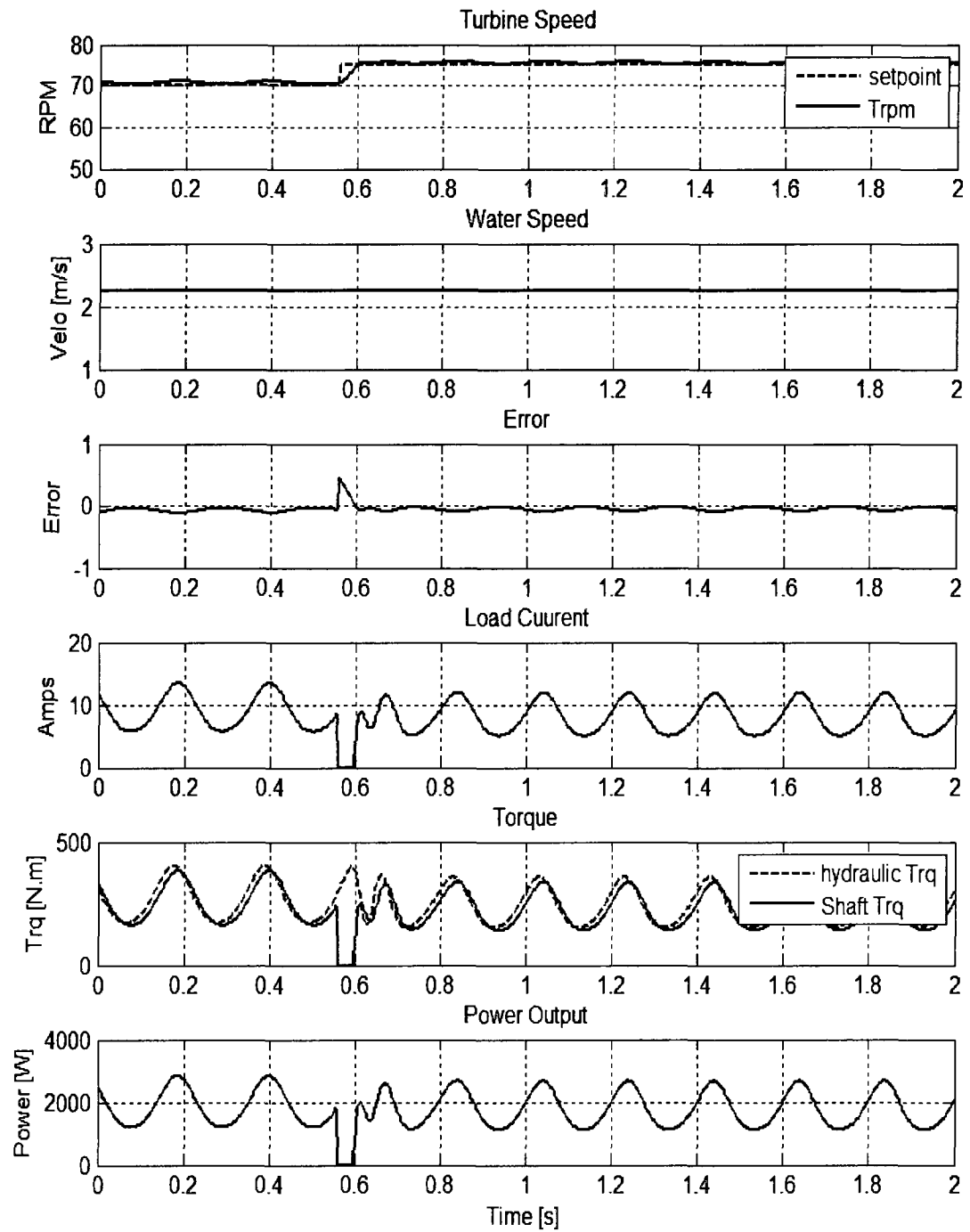


Figure 5.18: Simulation PI controller step response

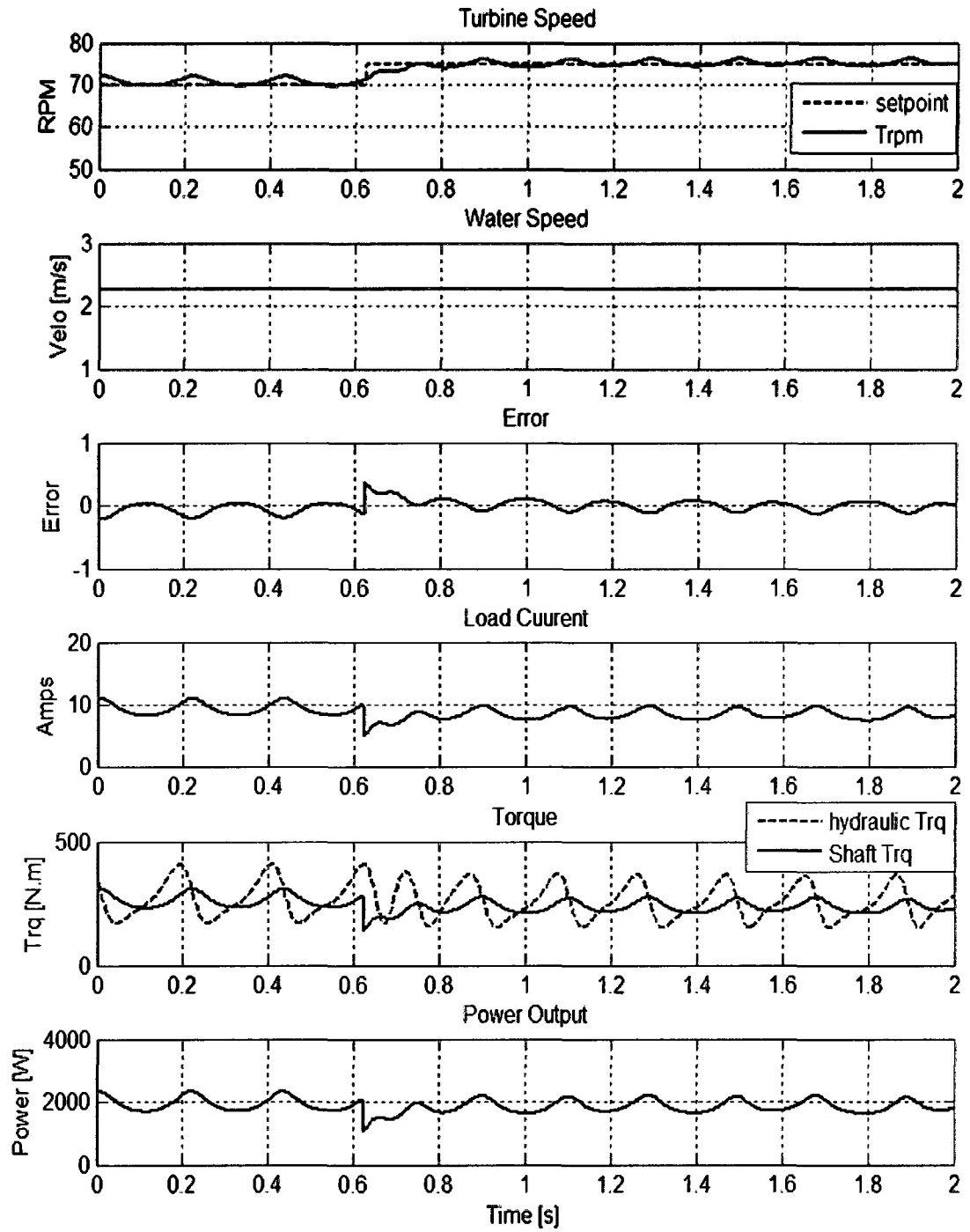


Figure 5.19: Simulation H_{∞} LPV step response

We can see that the PI control action is much more aggressive with shaft torque oscillations between 180 N.m and 400 N.m (before the step) compared to the gain scheduled controller of 215 N.m to 300 N.m (also before the step). The standard deviation of the shaft torque signal for the PI controller is 75.61 N.m compared to 28.13 N.m for the gain scheduled controller demonstrating superior mitigation of cyclic torque disturbances. The power output is also much smoother for the gain scheduled controller, though the tracking error has a slightly higher oscillation magnitude. This demonstrates the important tradeoff between reference tracking and controller induced torque transients on which turbine component fatigue life depends so strongly. It is also noted that tighter tracking of the PI controller corresponds to reduced cyclic rpm pulsations (seen by comparing the turbine rpm traces) caused by the pulsating hydraulic torque of the rotor. Conversely, the H_∞ LPV controller allows higher turbine rpm oscillations to minimize torsional transients. A comparison of the standard deviation of the error for the PI controller (0.053) with the gain scheduled controller (0.091) shows that while the oscillations are higher, tracking is quite good.

5.5.4.2 Tracking Response (Region 2)

For the tracking response comparison, a velocity curve taken from a field test trial October 9, 2008 is used as input to the simulation using each controller with the automatic reference generator. This allows a reasonable comparison between simulation data and field test data in exploring controller performance. Results for the PI controller are displayed in Fig. 5.20 and for the H_∞ LPV controller in Fig. 5.21. It should be noted that the turbulence levels experienced by the test turbine are much higher than that due to

river turbulence levels alone since it was tested in the wake of the larger 25kW turbine platform (about 50 ft directly in front of the 5 kW test system).

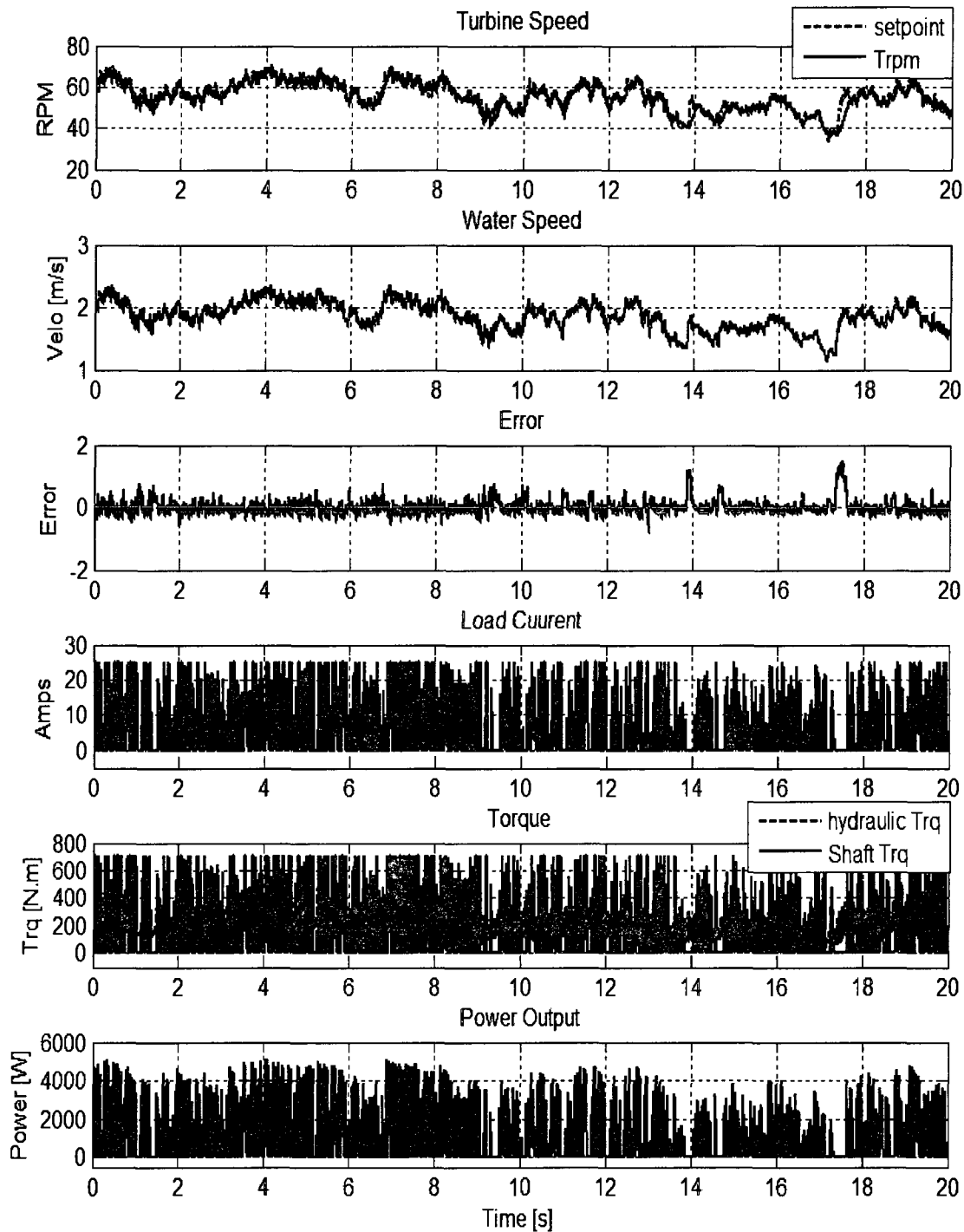


Figure 5.20: Simulation PI tracking response results

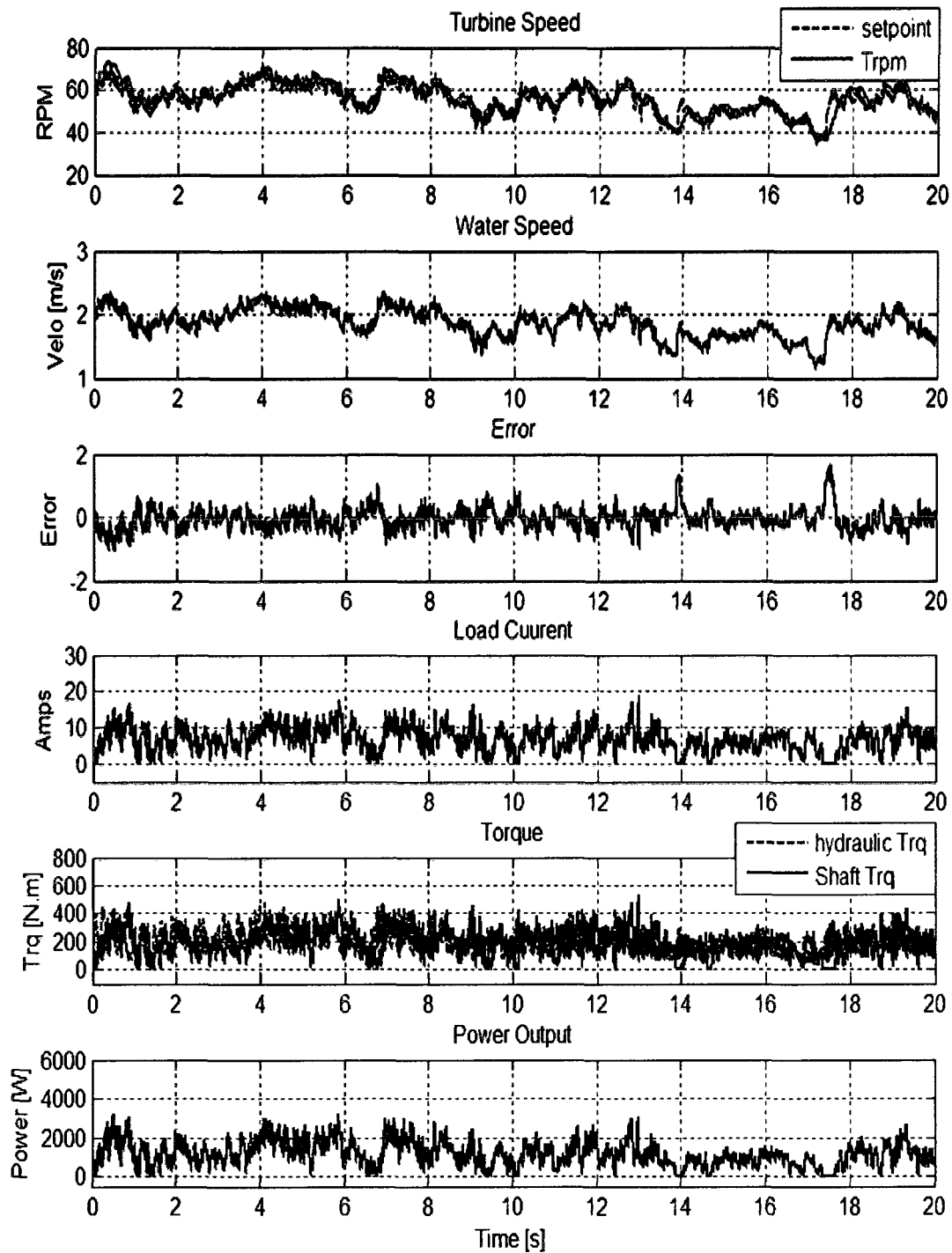


Figure 5.21: Simulation H_{∞} LPV tracking response results

Again the tight tracking and large torque transients associated with the PI controller are readily apparent. This is due to the high gain values used for the PI controller since it was tuned for tight tracking without consideration of load transients. Note that the shaft torque amplitude is significantly higher than the hydraulic torque amplitude. The standard deviation of the shaft torque signal for the PI controller is 237.75 N.m compared to 81.95 N.m for the gain scheduled controller. Also note that the standard deviation of the hydraulic torque input signals for both control tests is 96.9 N.m showing that the gain scheduled controller reduces shaft torque peaks below that of the input. Though the error amplitude is slightly smaller for the PI controller, the turbine life would be significantly reduced with such large and ongoing torque transients. The standard deviation of the error for the PI controller is 0.24 compared to 0.34 for the gain scheduled controller again demonstrating excellent error tracking characteristics for both sets of tests.

5.5.4.3 Power Regulation (Region 4)

Simulations for operation under power regulation are achieved by using a velocity trace taken from a field trial that is scaled to pass above 3.0 m/s forcing the operating point into the power regulation region. The automatic reference generator is used to track the flow velocity to ensure the mean output power does not exceed the rated output.

Power regulation simulation results are presented for the PI controlled system in Fig. 5.22. Torsional oscillations and output power fluctuations are again very large due to the high control gains employed. A notable amount of overshoot is also present in the rpm trace. This was not seen in other test results since in this operating range the fixed PI control structure (originally designed for an operating point around 2.25 m/s and 69 rpm)

is not ideally tuned. This demonstrates the significance of the plant nonlinearities and the need for modification of the control structure as operational parameters change.

Tracking results for the H_∞ LPV controlled system are presented in Fig. 5.23. We can see that the shaft torque transients are considerably smaller than the hydraulic torque input. A comparison of the standard deviation of the shaft torque for the PI and gain scheduled controllers at 266.78 N.m and 164.09 N.m respectively, shows superior transient mitigation characteristics of the gain scheduled controlled system. Also note that the peak power oscillates between 4000 W and 6000 W. It must be noted that during simulations with perfectly smooth flow, the power output oscillation with the H_∞ LPV controller at the rated output for a water velocity of 3.0 m/s is 4100 W to 5900 W, thus power regulation is considered good for a test flow (and rpm reference signal) with such high frequency content. Comparing the standard deviation of the error for the PI controller at 0.30 and gain scheduled controller at 0.31 it can be seen that good tracking performance is maintained for the gain scheduled controller.

It should also be noted that this water speed measurement should be run through a low pass filter (for control purposes) since it is supposed to be a measure of the average flow velocity, without the turbulent component. This would smooth the turbine rpm reference signal, and thus increase closed loop performance in all regions of operation.

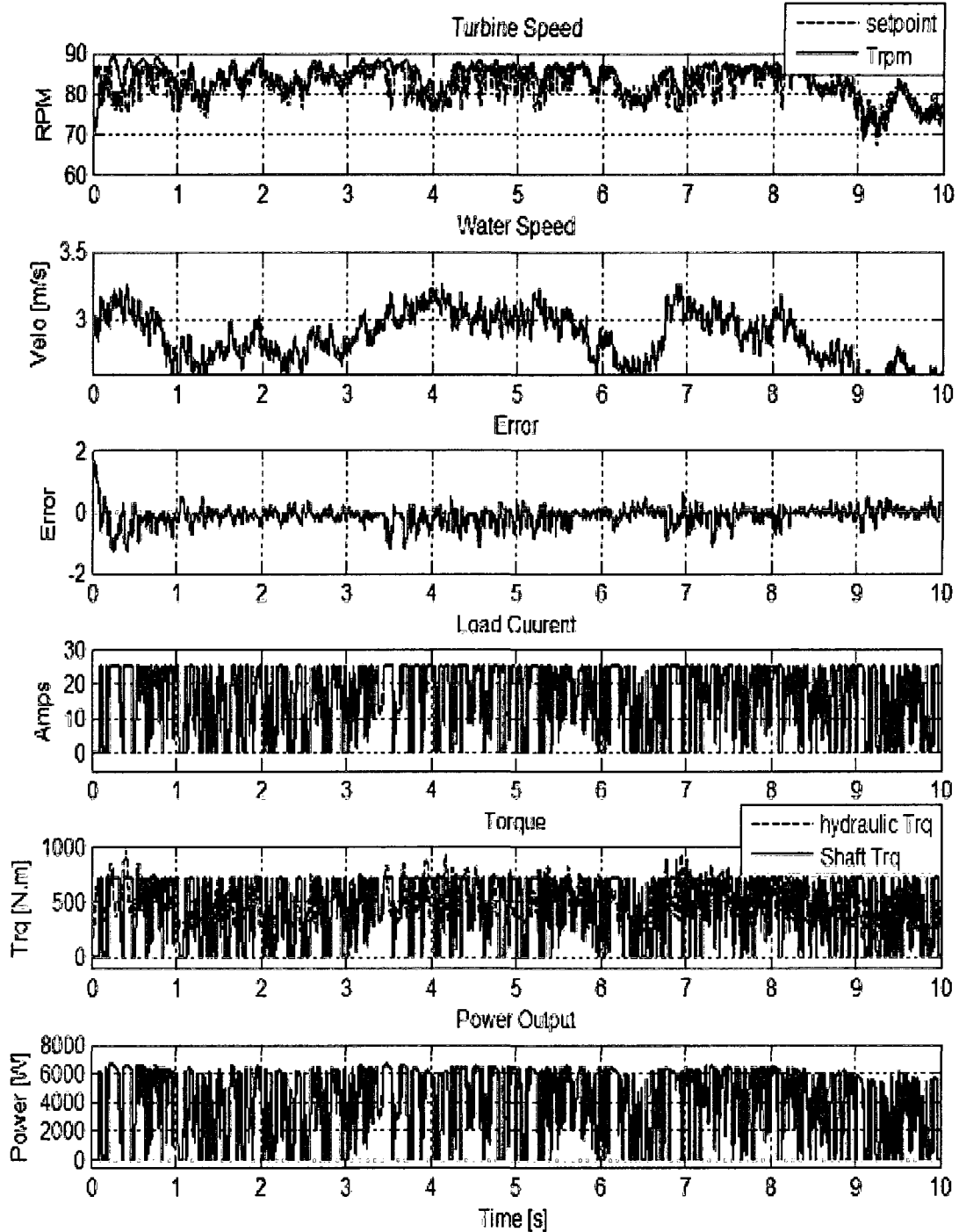


Figure 5.22: PI tracking response under power regulation

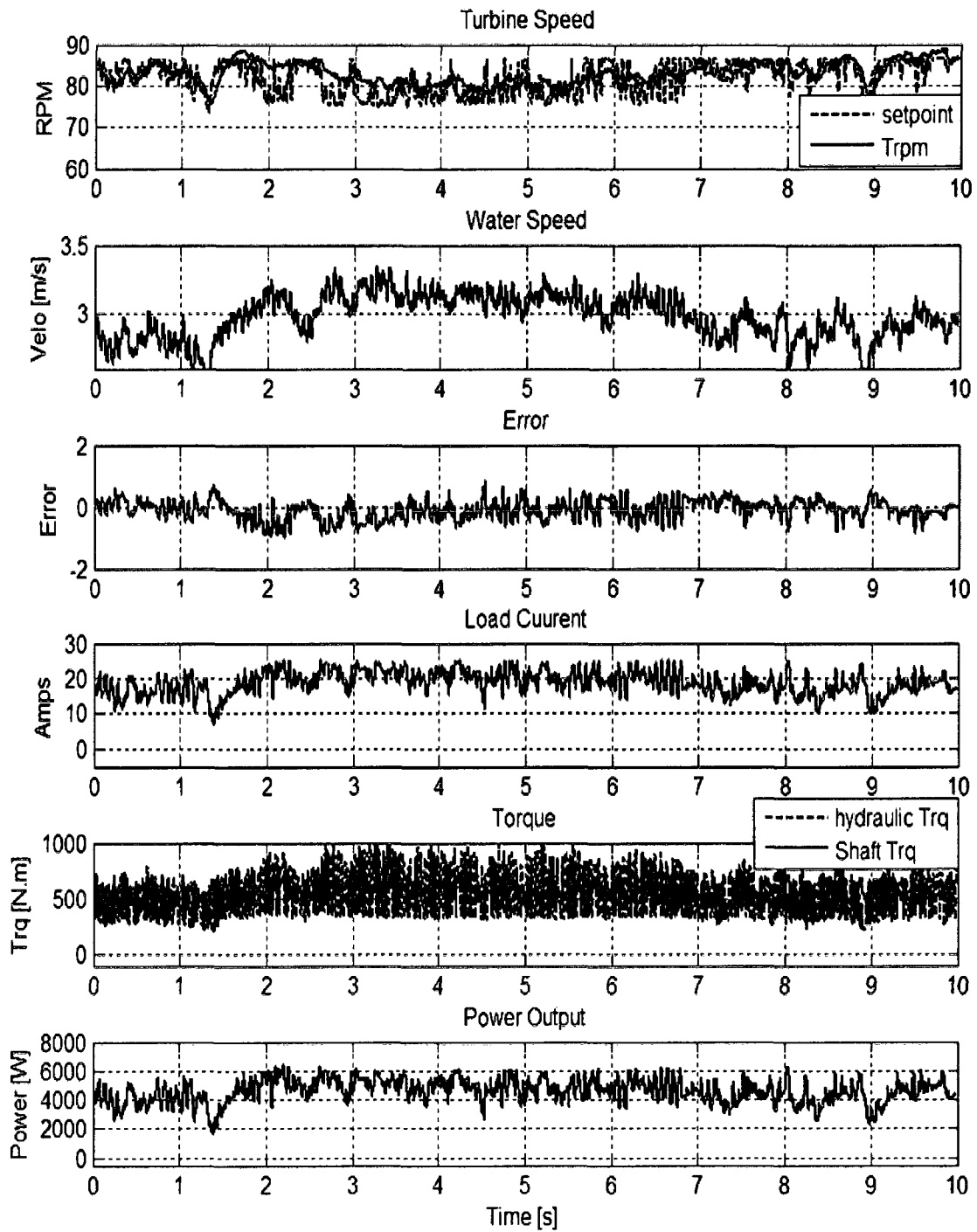


Figure 5.23: H_{∞} LPV tracking response under power regulation

Chapter Six: Implementation

6.1 Introduction

In this section the installation of the control hardware as well as turbine deployment are discussed along with the various issues encountered. Initially one work week (5 days) for testing seemed a reasonable time frame to complete the required testing, though the various implementation issues reduced this to a single day. In the end a sufficient amount of good data was acquired though only for two of the six controller versions developed (one PI, and one of the five H_{∞} LPV controllers developed).

6.2 Turbine Installation

Initially the 5kW turbine system was already moored in place behind the 25kW system test platform at the site as shown in Fig. 6.1. It was decided that the log boom would not be deployed since it was felt that such short duration testing did not warrant the work to install it.



Figure 6.1: Turbine initially deployed behind larger 25kW test platform

However, an attempt to start the turbine failed since the rotor would not turn. The problem was traced to debris in the rotor. Two large logs were removed from the rotor and the system was then free to rotate (one of which is shown in Fig. 6.2). These were the only logs reported on this system in the year it was deployed at this test site and it was noted that the non-standard method of mooring this system to the test platform resulted in the anchor lines acting as a funnel for debris.



Figure 6.2: Log removal

Pre-cut $\frac{3}{4}$ inch plywood sheet was screwed to the top of the aluminum frame to serve as a work platform. The turbine system was then started but seemed sluggish even with no load and a low pitched grinding noise was audible. The system was removed from the water and the problem traced to water ingress through the top of the generator due to a missing cover resulting in failure of the generator bearings, gearbox NEMA flange bearings and drive system bearings. Since the generator cover is bolted in place the most likely cause was neglect to reinstall the cover by previous users.

The turbine was completely disassembled and the gearbox and bearings replaced. Pictures of the repair are shown in Fig. 6.3. The rebuilt system was redeployed behind the 25kW test platform.

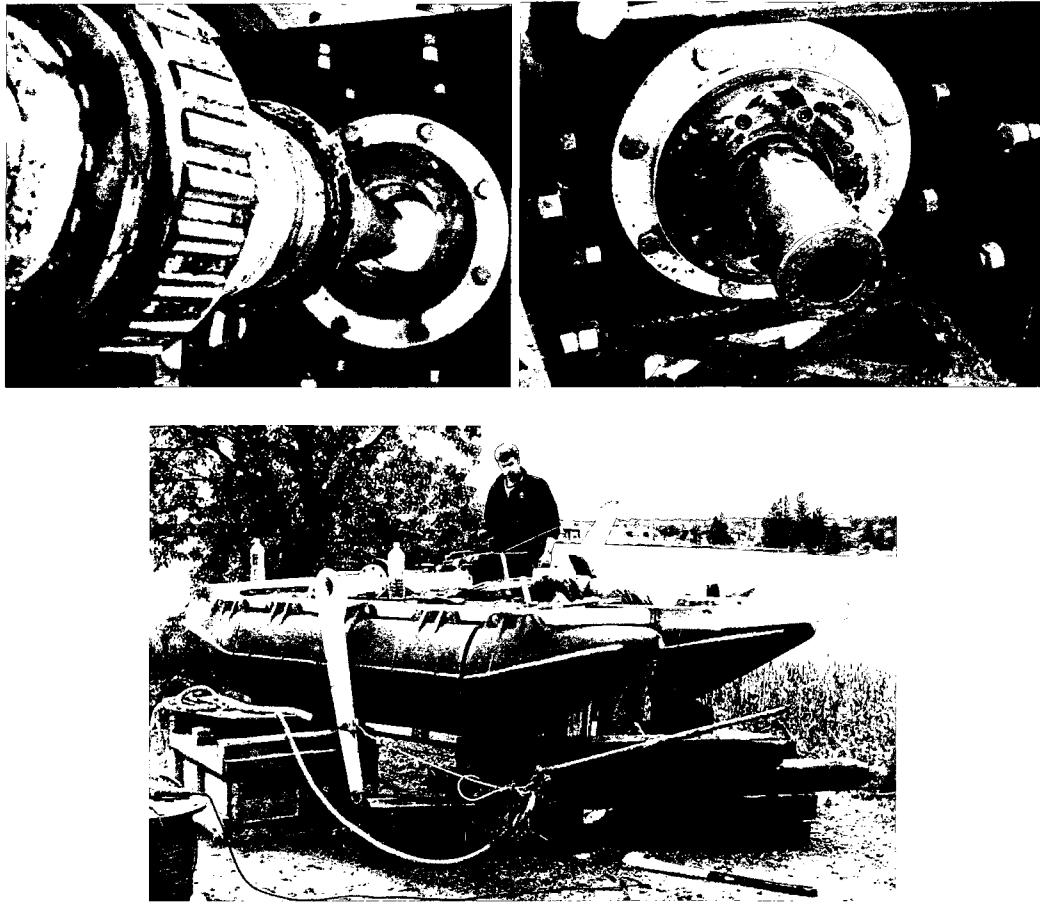


Figure 6.3: Rebuild of turbine drive system

The generator power cable was run along the winch line that attached the larger 25kW turbine platform to the small 5kW floating platform. There was no convenient place to run the instrumentation cabling to the test platform away from the generator power cable. Therefore it was decided that individually twisted pair and individually shielded cable would be used to run the turbine rpm and water velocity signals from the small platform to the larger one along the generator power cable. No noise issues were

noted though this is definitely not the preferred method of cabling due to the potential for signal noise problems. It was also decided that instead of running an AC power source to the 5kW floating platform to release the fail safe brake, a mechanical brake bypass would be employed instead.

The water speed sensor was attached to its mount and the cabling strapped in place. The turbine was started and allowed to freewheel. The response now seemed normal and the noise gone. The system was now ready for installation of the control hardware and subsequent testing.

6.3 Control Hardware Installation

The control hardware was initially assembled at the NECI prototyping facility in South Calgary prior to shipment to the test site. All systems were thoroughly tested by connecting the entire system together (all loads, inductors, sensors, controller and laptop computer) and using appropriate equipment to generate the velocity and rpm signals. For instance, the metal lathe and rpm sensor were used to generate the turbine speed signal and a small fan driving the velocity sensor was used to generate the water speed signal. Then by moving the rpm reference point slightly above or below the lathe speed, control action would vary the application of the resistors. With the system verified to be functioning as required, it was shipped to the test site.

6.3.1 Hardware Enclosures

The system required some form of an enclosure to protect it from the elements since the hardware was required to sit on the deck of the large test platform (unprotected) just upstream of the 5kW turbine system. The load resistors were mounted to a wooden

pallet and a plywood box was built around it. This would protect the resistors from the elements as well as serve as a shipping enclosure. Thin gauge sheet metal was screwed to the bottom of the pallet prior to resistor installation to serve as a heat shield so the wood would not be damaged during operation. Air holes were cut through the bottom of the pallet (and heat shield) with a plasma cutter, to facilitate convective cooling when the lid was propped open (as shown in Fig. 6.4).

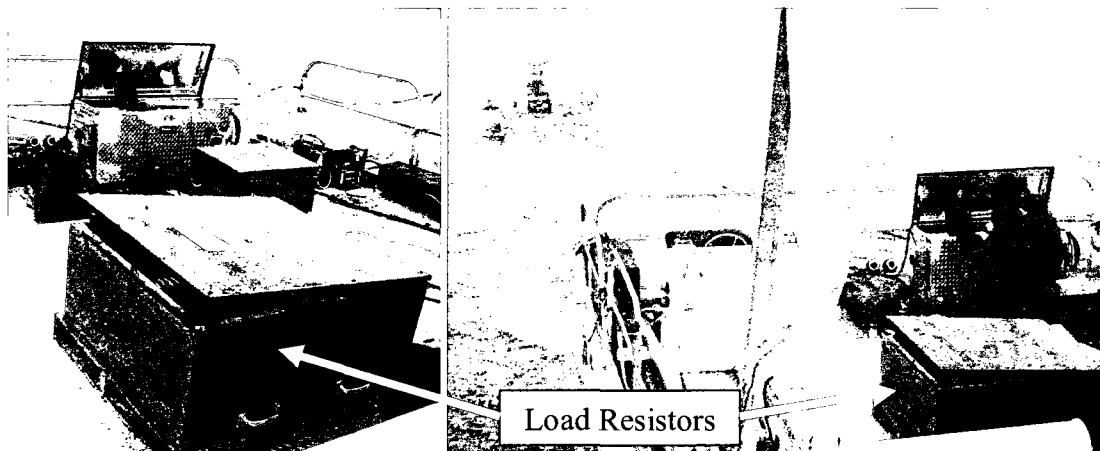


Figure 6.4: Weather proof control testing hardware on test platform

The remaining control equipment (real time controller, inductor, 3 phase rectifier and filter) underwent similar treatment with a slightly smaller box. Cat6 ethernet cable was used to connect the laptop computer to the control hardware box as shown in Fig. 6.5. The laptop was put beneath the lid of a small metal instrumentation enclosure on the back of the large test platform for when it started raining and snowing.

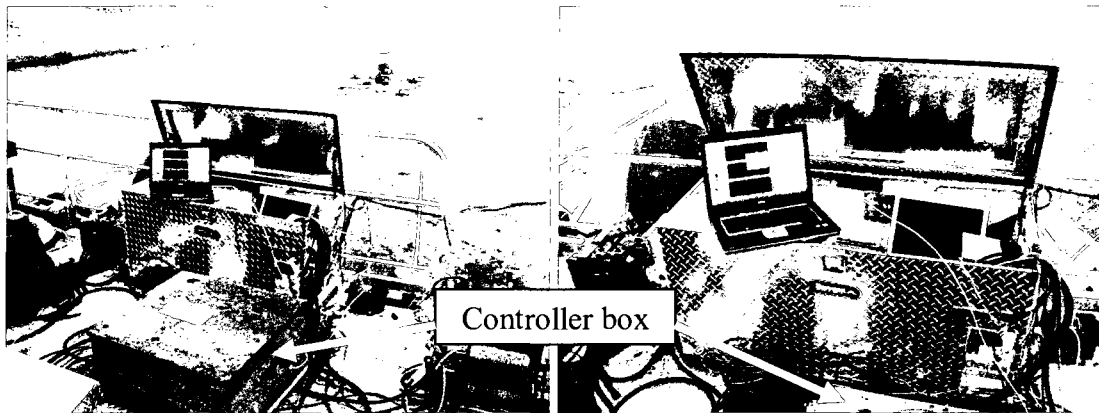


Figure 6.5: Laptop placement in metal instrumentation enclosure

6.3.2 Supervisory Control Levels

Control complexity for implementation was kept to a minimum. Control levels for automatic turbine start up and shut down were not employed. Start up was facilitated by manually bypassing the fail safe brake and using a cordless screw driver to drive a hex lug installed on the very top of the generator. Stalling of the turbine was prevented by self load limiting. As the turbine speed dropped below 22 rpm the generator voltage dropped quickly enough that full application of the load bank was not enough to stall the turbine (due to significantly reduced generator efficiency at such low rpm). Effectively at this speed the electric load drops much more quickly than hydraulic power when reducing turbine speed, due to the sharp generator performance characteristic at this rpm level. Thus even with full electrical load, the turbine speed could not drop below 18 rpm for the range of water speeds tested. This is demonstrated with test data in Fig. 6.6 where the setpoint turbine speed is dropped to 3 rpm in an attempt to stall the turbine.

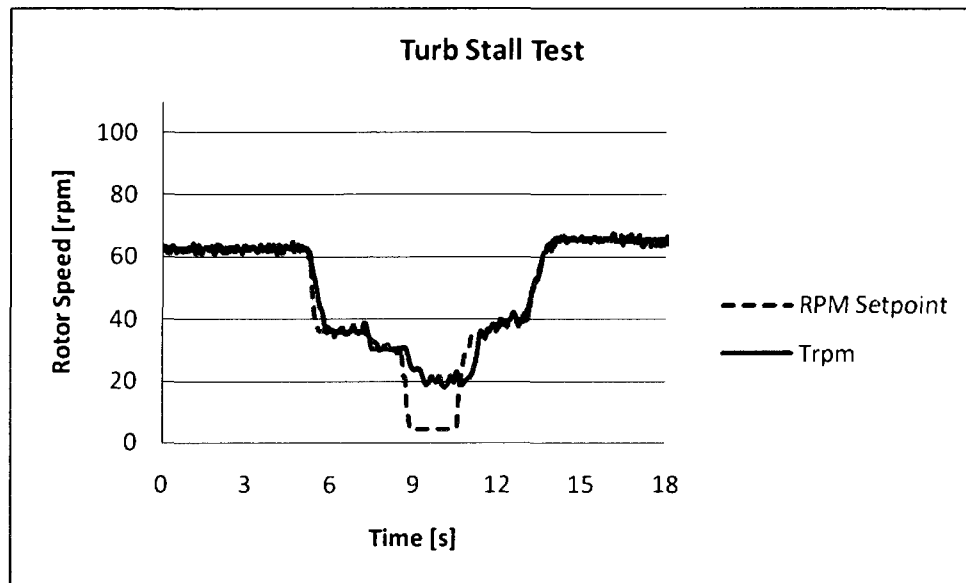


Figure 6.6: Turbine Stall Test

Monitoring functions were also not employed for such short duration testing (for instance generator temperature, excessive water speed and turbine rpm, etc.). Water speeds at this location are consistently below the rated maximum, negating the requirement for this type of supervision.

6.4 Problems Encountered During Field Testing

A number of problems at the test site significantly delayed and almost prevented field testing of the control system. A fixed time constraint was the removal of all equipment before winter arrived at the test site. Thus it was very important the work be finished by November to allow the remainder of the scheduled site tests (for other parties) to be completed.

A series of delays in shipment of the test hardware, software development, and (as previously mentioned) the overhaul of the drive system left a single work week (5 days) for testing. Though this essentially delayed field testing to the last possible moment, it

left ample time to acquire data and fine tune the controller. Essentially two of the days were required for setup, with the remaining three open for testing. In fact five different H_∞ LPV controllers (all with different weighting functions ranging from very tight control and very loose control for low torsional oscillations) were prepared for field testing. However, due to the series of problems outlined below, only the PI controller and a single H_∞ LPV controller (the best from simulations) were tested.

6.4.1 Coupling Failure

In the haste to put the turbine system back together during its overhaul, and get it redeployed at the site, one of the couplings (damaged from the water ingress) was borrowed from an old prototype that had been decommissioned. Its long lead time precluded ordering, and none were in stock at the manufacturer. It was not known at the time that a very subtle difference in the coupling allowed the flexible insert to fall out of place effectively disengaging the generator from the gearbox. With the turbine redeployed at the site, it was started and initial system checks (involving verification of general system functionality and measurement of generator voltage at no load rpm) were completed. The turbine brake was then applied and the coupling failed. This resulted in consumption of one day just to get the system shutdown and the problem diagnosed. The flexible insert was destroyed. A new flexible insert was transported by plane, overnight to Winnipeg and driven by car to the test site. A make shift spacer was fabricated from scrap material found at the site, and used to prevent the new flexible insert from falling out of place. The turbine was reassembled and the system checks re-performed. Another $\frac{3}{4}$ of a day had been spent, leaving only $1 \frac{1}{4}$ days left for testing.

6.4.2 Test Platform Problems

During the system checks the water velocity signal was noted to be missing. The turbine platform was again accessed with the Zodiac and the flow speed sensor rotated out of the water for inspection. No problem could be found. All cables and connections were checked without notable issues. The real time controller was reset and the problem was resolved.

The system was finally ready for testing. However, it was noted that the zero offset and amplifier sensitivity had changed slightly. The values were readjusted and testing commenced. Open loop testing was performed without event. Test runs with the H_{∞} LPV controller also proceeded without incident. However, the temperature dropped significantly in the evening and the relative humidity increased to 100% (noted by visible fog and light rain). Testing was terminated for the day. The final day was slated for completion of PI controller testing and more gain scheduled controller testing (if time permitted). The system checks were again performed first thing in the morning and the controller zero-offset and sensitivity readjusted. Testing proceeded with tuning of the PI controller as well as initial test runs to acquire comparative data. Toward the end of the testing the entire system became unstable with the turbine going into its characteristic slow roll due to excessive electrical load. Even previous controllers that performed very well did not work. Open loop testing revealed that the amplifier sensitivity became very large (very sensitive to small input voltage changes). The amplifier was retuned and worked for a brief time before suffering the same issue. Testing was terminated. It is speculated this issue was an effect of the high relative humidity.

One final quirk that was experienced was due to the amplifier high voltage limit. For freewheel turbine speeds witnessed at this site, it was noted that the generator voltage was past the upper limit for the amplifier. This meant that some tests required a small waiting period for turbulent flow fluctuations to reduce the turbine speed (and thus generator voltage) so that the amplifier inhibitor would allow connection of the amplifier to the generator. This problem was anticipated and it was planned to apply a small stationary constant load briefly to the generator to allow connection of the amplifier (at which point it would be removed). However, it was decided that the small wait time for each test did not warrant the extra effort of connecting this circuit (especially with such high turbulence levels).

With test runs performed for both the PI and H_∞ LPV controller as well as the fact that time had run out, everything was repacked and shipped home.

Chapter Seven: Field Test Results

7.1 Introduction

Field testing results are presented in this chapter. In the first section results for the H_∞ LPV controller tests are displayed and discussed. These are followed by test results for the PI controller. It must be noted that the turbulence levels in the flow are much higher than normal river turbulence levels experienced at this site due to the fact that the test turbine was moored in the wake of the larger 25 kW turbine test platform. Thus it is very likely that tracking performance would be better in a normal application due to the lower level of flow disturbances.

7.2 H_∞ LPV Controller Test Results

Part of a typical test run is shown in Figures 7.1, 7.2, and 7.3. The turbine speed reference is set above the freewheel speed (at 93 rpm) and the turbine is started and allowed to freewheel. The speed setpoint is then reduced to 71 rpm at 26 seconds and the controller begins to load the turbine. At 31 seconds the turbine automatic reference generator (for maximum power tracking) is engaged for tracking of water speed changes.

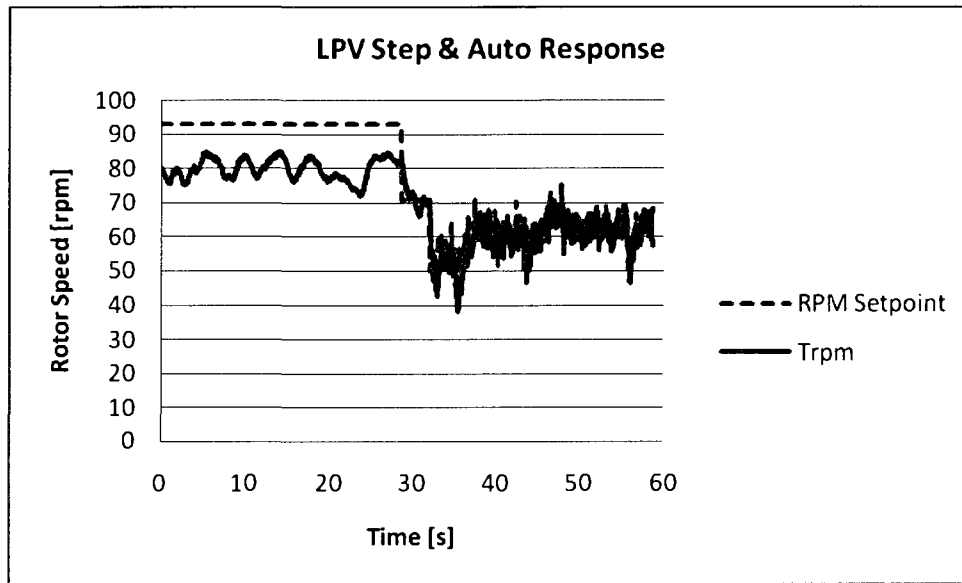


Figure 7.1: H_{∞} LPV Step and auto response rpm versus time

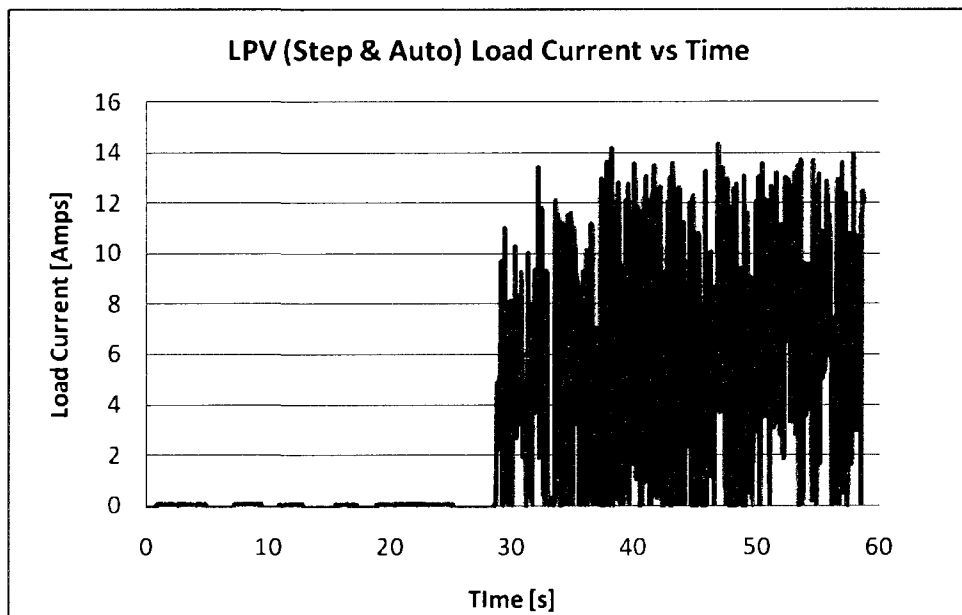


Figure 7.2: H_{∞} LPV Step and auto response load current versus time

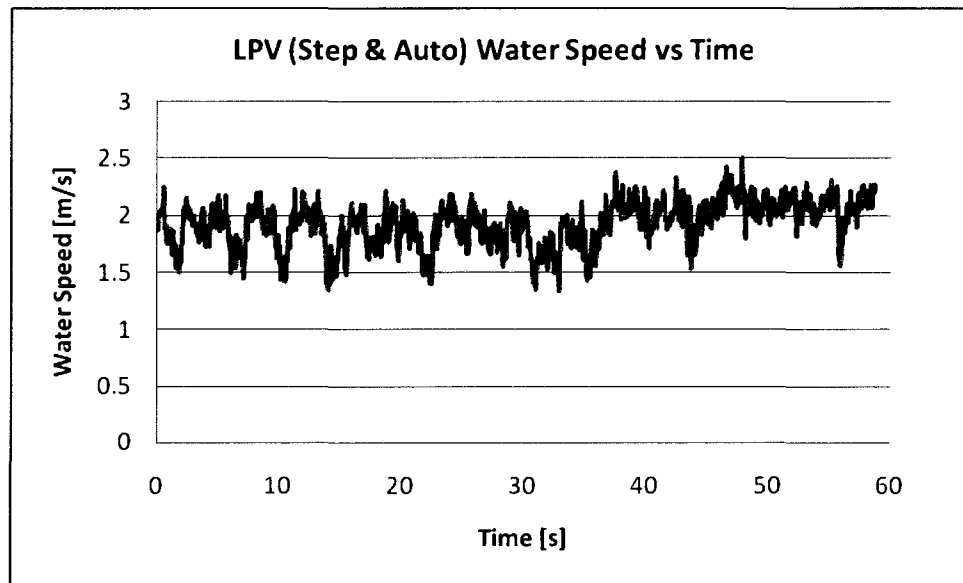


Figure 7.3: H_{∞} LPV Step and auto response flow speed versus time

It is apparent that the water speed signal contains a high content of turbulence information causing a very noisy rpm set-point signal. This is due to the previously unknown response characteristics of the flow velocity meter which are much better than anticipated. Future testing should filter this water speed signal when used for reference point generation using the *tip speed ratio* method, so that only changes in the mean water speed are tracked.

The step response over a ten second time window is presented in Figures 7.4, 7.5 and 7.6.

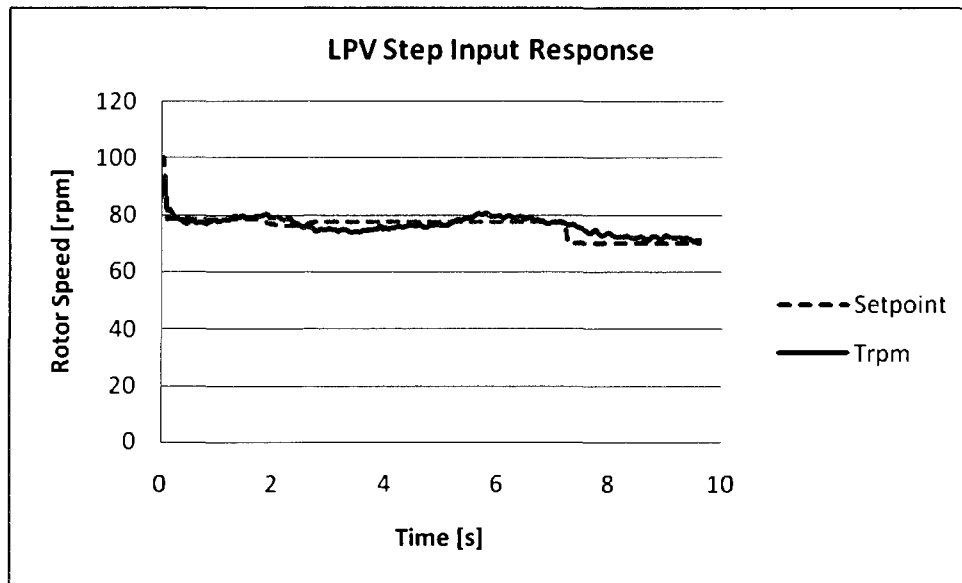


Figure 7.4: H_{∞} LPV Step response rpm versus time

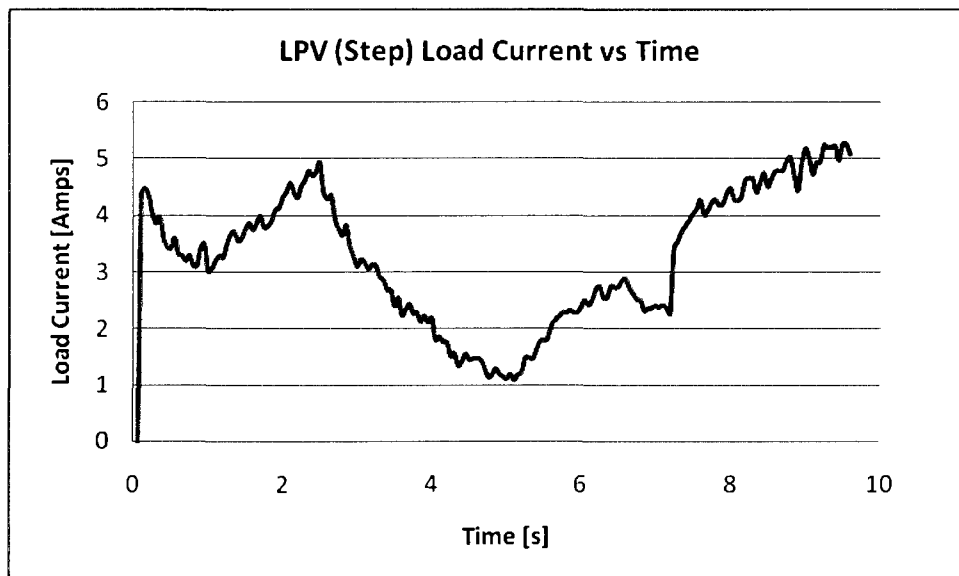


Figure 7.5: H_{∞} LPV Step response load current versus time

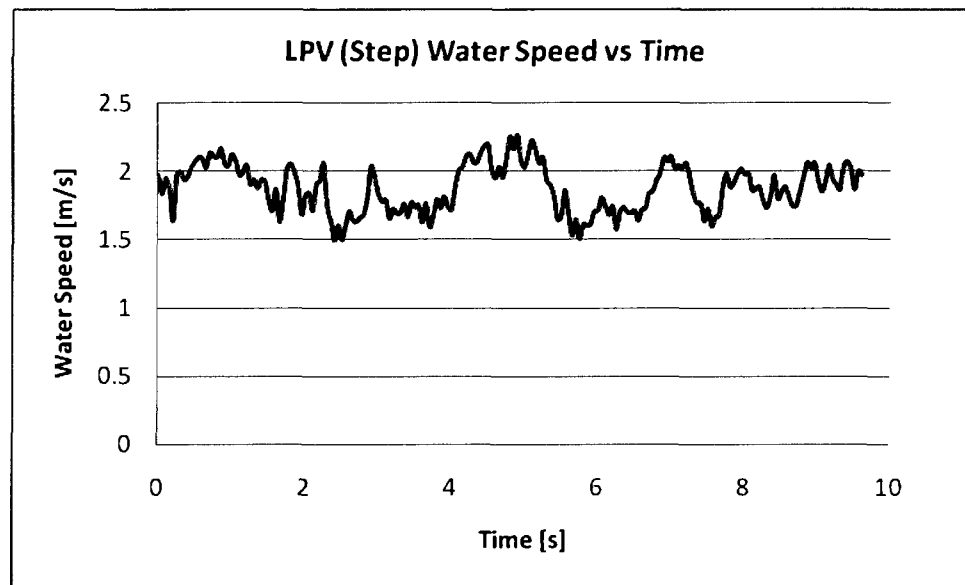


Figure 7.6: H_{∞} LPV Step response flow speed versus time

The step response is quite good considering a flow surge occurs at the same moment the set-point is reduced from 79 to 75 rpm. The load current curve is directly proportional to the drive shaft torque (related through the generator torque constant) and serves as an indication of the turbine shaft torque. This is very smooth compared to the constant rpm section in Fig. 7.11 for the PI controller. The disturbance rejection characteristics due to flow surges as high as 2.25 m/s and recessions as low as 1.5 m/s are also demonstrated between zero and six seconds. Finally, we can also compare the standard deviation of load current and error for the gain scheduled controller versus the PI controller at similar turbine rpm (70 rpm) and flow speeds (1.6 m/s to 2.1 m/s). The standard deviation of the error and load current for the gain scheduled controller from 7.5 s to 10.0 s are 1.52 and 0.48 Amps respectively. We can compare this to the standard deviation of the error (1.10) and load current (5.45 Amps) for the PI controller step response in Figures 7.10, 7.11 and 7.12 between 46 and 48 seconds. Though the flow

velocity is not the same for both tests in these time frames (due to the stochastic nature of this variable), the trend for smaller load transients while maintaining reasonable tracking performance is demonstrated for the gain scheduled controller.

The auto tracking response over a ten second time window is shown in Figures 7.7, 7.8 and 7.9. The excessive fluctuation of the set-point signal can be seen and is again due to the turbulence content of the flow speed signal. However tracking is quite good with a standard deviation for the error of 3.39. While the load current transients (and therefore drive train torque transients) are notable, they are markedly reduced compared to the PI controller in Fig. 7.13 for a similar test run with standard deviations of 4.60 Amps and 6.55 Amps for the gain scheduled and PI controllers respectively. The error standard deviation for the PI controller of 2.05 is similar to that of the gain scheduled controller of 3.39.

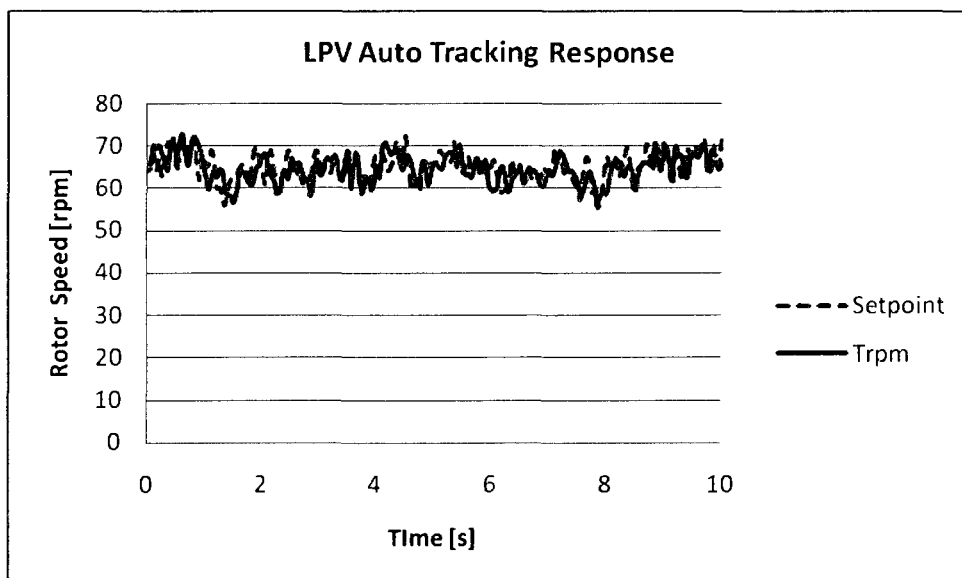


Figure 7.7: H_{∞} LPV Auto tracking response rpm versus time

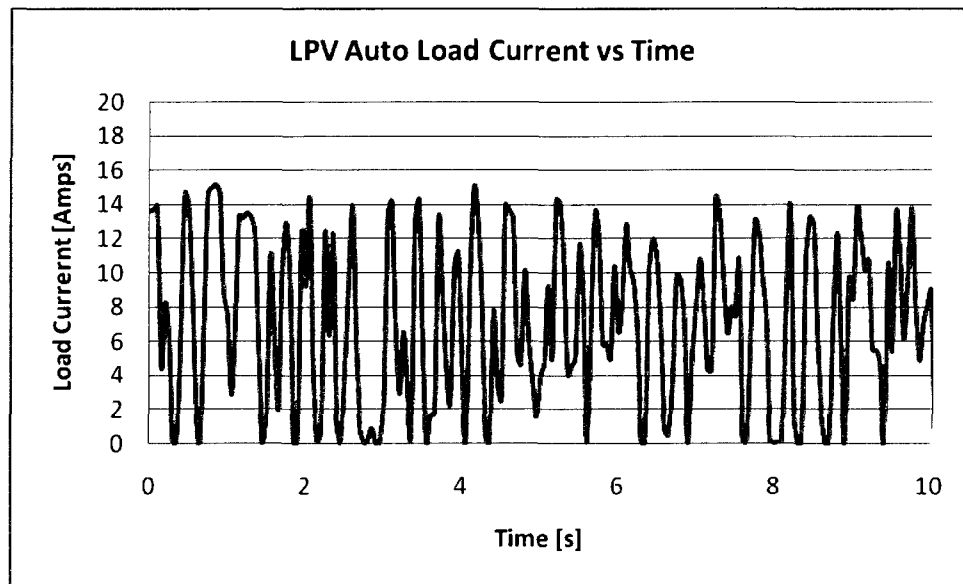


Figure 7.8: H_∞ LPV Auto tracking response load current versus time

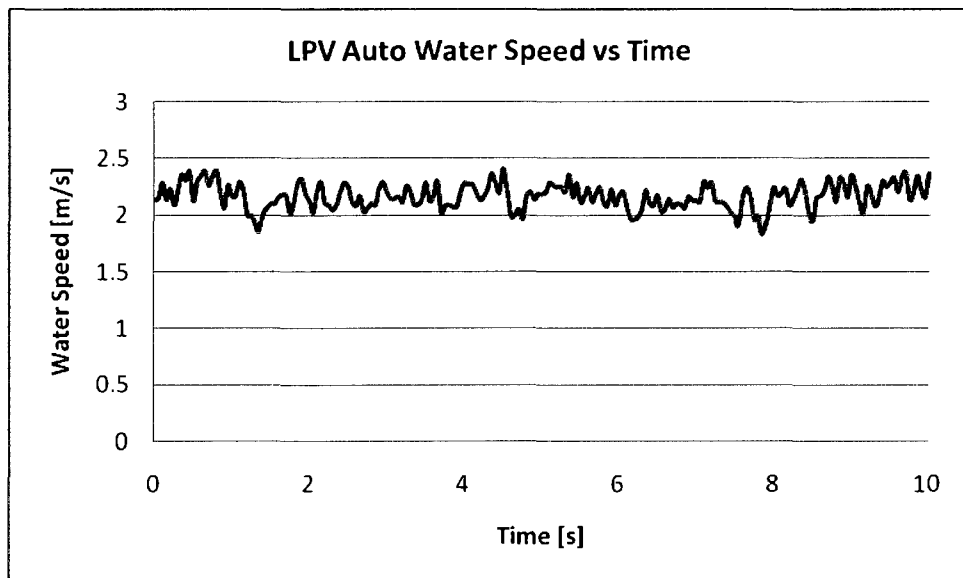


Figure 7.9: H_∞ LPV Auto tracking response flow speed versus time

7.3 PI Controller Test Results

The test results for PI controller response to a step input in turbine speed set-point are shown in Figures 7.10, 7.11 and 7.12.

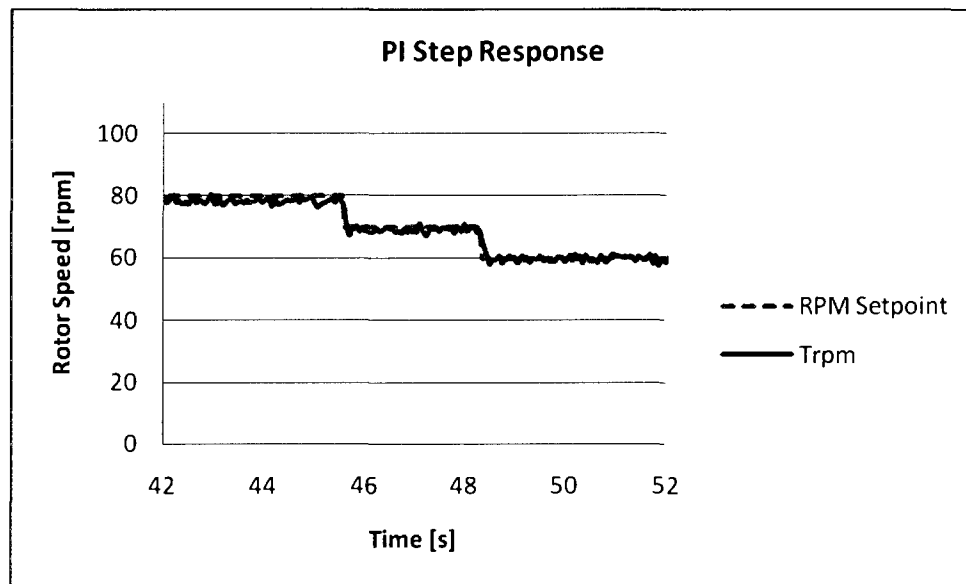


Figure 7.10: PI Step response rpm versus time

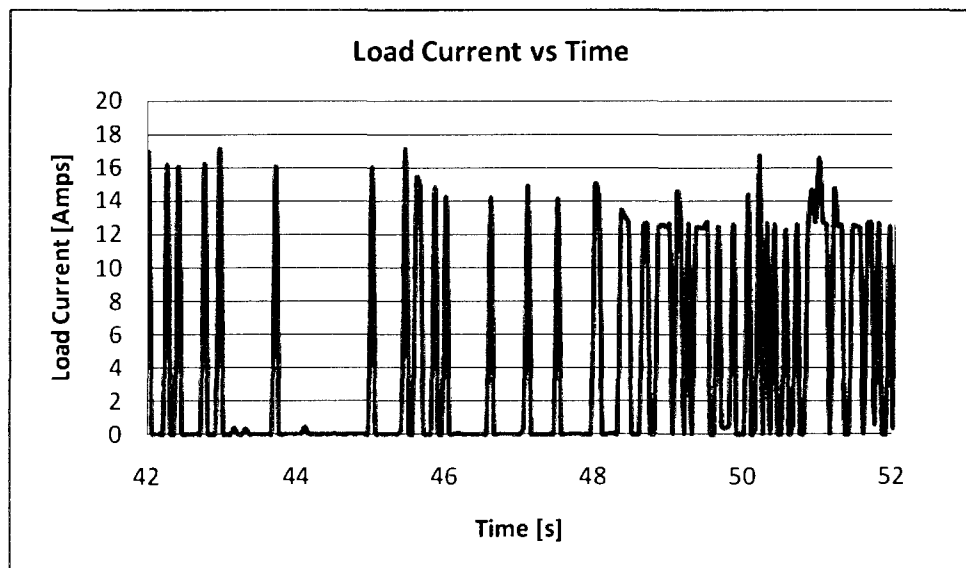


Figure 7.11: PI Step response load current versus time

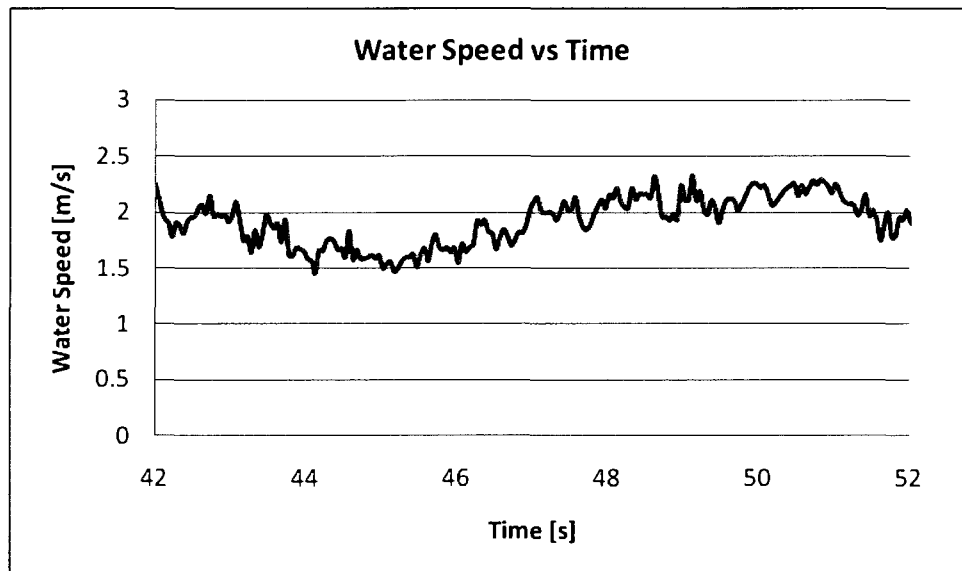


Figure 7.12: PI Step response water speed versus time

Speed tracking is excellent. However, the sharp load changes required to maintain a constant speed are tremendous, and get worse when making set-point changes. This is especially notable between 50 and 52 seconds where the flow speed is the highest. A comparison of Fig. 7.5 with Fig. 7.11 highlights the comparatively smooth load changes of the H_{∞} LPV controller for a constant rpm set-point.

The PI controller response using the automatic reference generator for a ten second time window is shown in Figures 7.13, 7.14 and 7.15.

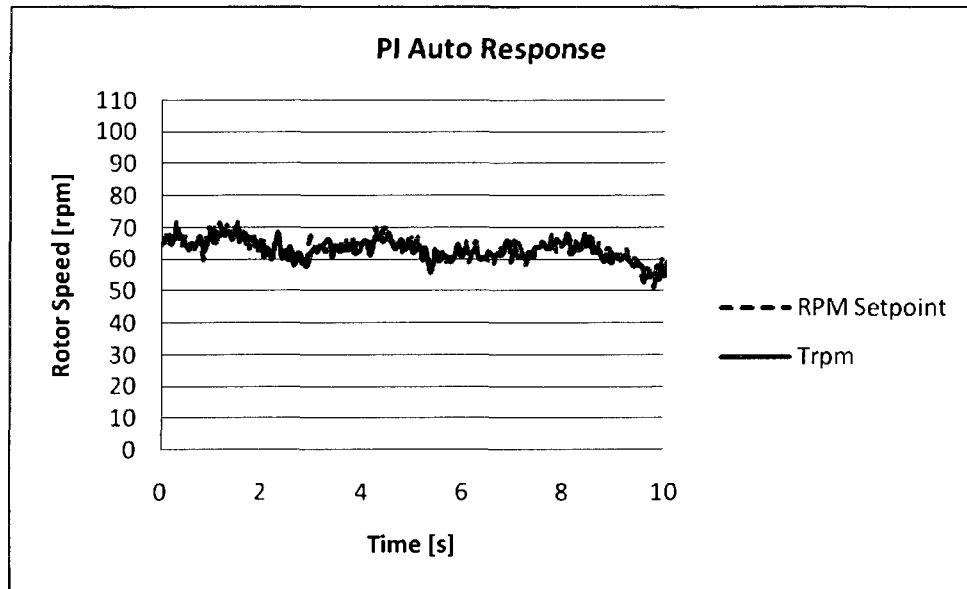


Figure 7.13: PI Auto tracking response rpm versus time

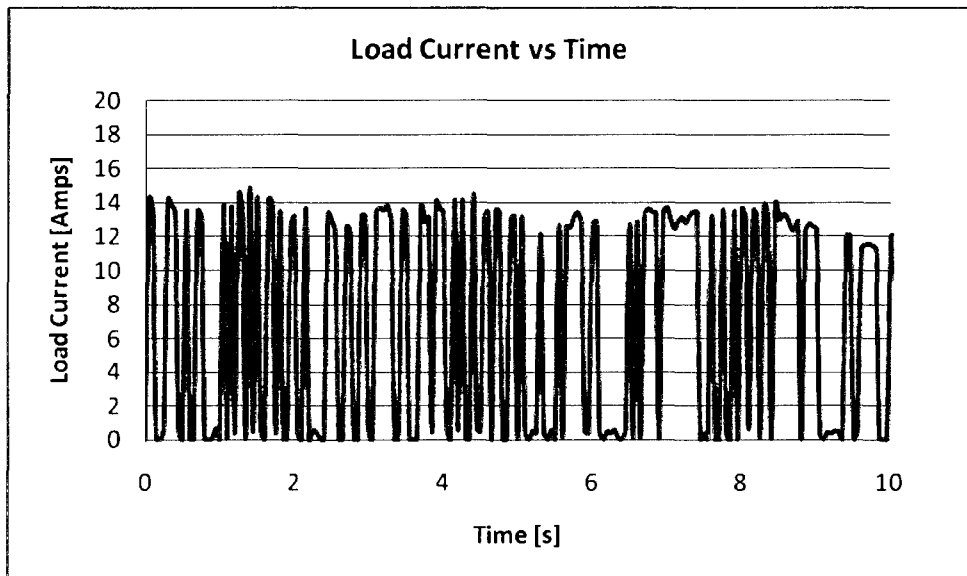


Figure 7.14: PI Auto tracking response load current versus time

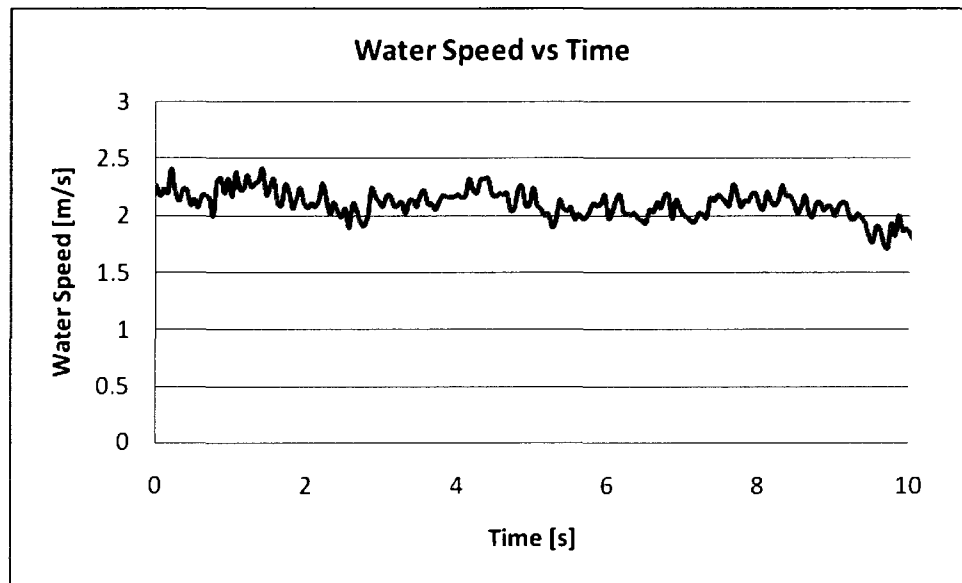


Figure 7.15: PI Auto tracking response flow speed versus time

Tighter speed tracking is demonstrated, though at the expense of large load transients. The flow turbulence is significantly lower for this test than that for the H_{∞} LPV controller in Fig. 7.9 and still has considerably larger load fluctuations. This would indeed significantly reduce the fatigue life of turbine drive components.

Chapter Eight: Summary and Recommendations

8.1 Introduction

This chapter outlines a summary of the work carried out for this research project which is the first iteration of a hydrokinetic turbine speed control system. Important results for qualitative controller performance as well as implementation considerations are outlined. Recommendations for future work for hydrokinetic turbine speed control are presented.

8.2 Summary of Work

A literature search for hydrokinetic turbine speed control revealed that very little work has been published in this area. Of the four papers located only one ([88]) discusses turbine speed control (in particular outlining a preliminary fixed point PID strategy). Due to the vacuum of published work on this subject, an additional search was carried out to identify the state-of-the-art of speed control for the closely related (and far better developed) system of wind turbines. This revealed that there are two broad classes of control for turbine speed or load. The first uses nonlinear system models, generally using search algorithms or perturbation techniques to continuously seek the optimal energy extraction operating point (examples include fuzzy logic, sliding mode control, and derivative techniques). While they generally have the advantage of requiring little detailed plant information, they do not incorporate explicit methods of accounting for uncertainty, and do not consider mechanical loading transients to minimize component fatigue. The second uses linear system models, and range from traditional PID to more advanced methods of robust control and adaptive techniques. While they require more

complex methods of dealing with nonlinearities, they have the advantage of being more intuitive and flexible with better defined performance and stability characteristics.

Regarding wind turbines, there exists a significant technology disconnect between academia/research and industry (mainly due to the non-intuitive, heavily mathematical approaches taken), making identification of state-of-the-art somewhat difficult. However, it is clear that the most popular methods of torque control in industry are deficient. It is also clear that a key consideration motivating much control system research (in the effort to reduce cost of electricity) is mitigation of component fatigue loading. Thus an intuitive, well developed control procedure, with guaranteed stability and performance characteristics, that explicitly incorporates fatigue loading considerations and maintains the highest possibility of industry acceptance is required. Gain scheduled control meets all of these requirements if formulated in the framework of linear parameter varying systems. Since traditional gain scheduling techniques are widely used in industry, and there are already examples of H_∞ LPV control used in test platforms at industrial research facilities, this advanced technique was chosen for the current work.

A mathematical model of the plant was developed (using information from the test-turbine manufacturer), a control strategy outlined, and a MATLAB software program to synthesize a controller generated. At the time of the controller design no data was available for simulation model validation. Due to the expense of testing as well as time constraints, none was available until final testing of the controller. Control objectives were outlined and a general strategy chosen. Simulink was used for simulations in which the weighting functions (for the defined performance variables) were tuned to allow the required amount compliance between tracking performance and induced load transients.

A PI controller was also synthesized for comparative purposes of simulation and field test results.

A rapid prototyping test platform was required for control algorithm testing. A CompactRIO ruggedized industrial controller and software interface to link with MATLAB and Simulink was acquired from National Instruments. This allowed direct conversion of Simulink code to executable code that was run on the CompactRIO control hardware. A PWM amplifier that allowed manipulation of the control variable (load current) was also acquired and connected to stand alone loads of high power resistors (two 15kW resistors). The final component in the test platform was the 5kW hydrokinetic turbine supplied by New Energy Corporation Inc. All this equipment was setup at a hydrokinetic turbine test site in Pointe du Bois, Manitoba, Canada.

Controller field testing was completed, validating the control system approach and highlighting some unique implementation requirements.

8.3 Summary of Results

The H_∞ LPV controller performed very well demonstrating an excellent tradeoff between reference tracking and induced load transients. The system maintained stability and performance over a large range of operating conditions. Compared to the PI controller the H_∞ LPV system demonstrated much smoother load transitions while maintaining good tracking performance.

The automatic turbine speed reference generator utilized for test purposes produced a very noisy signal due to the underestimated flow-velocity sensor response characteristics (not published with the specification material for the sensor). Thus it was

not filtered during testing which would have produced a much smoother reference signal. This reference generator uses known information about the turbine system to produce an rpm that corresponds to the constant tip speed ratio at which maximum power output for any given flow is attained (in Region 2 operation); and a speed reference that corresponds to the rated power output for Region 4 operation. This noisy turbine speed reference caused excessive control action not normally required to track smoother mean water speed changes (as opposed to the turbulent variations that occur at much higher frequencies).

Testing with the 5kW turbine in the wake of a larger 25kW turbine (located 50 feet directly upstream) also contributed to larger and more frequent control actions due to enhanced turbulence characteristics of the flow. While this is a more challenging test of the control system due to the enhanced disturbance characteristics, it may not be realistic in terms of what is actually seen in normal applications. The H_∞ LPV controller performed very well in this field testing but would likely be tuned for more aggressive reference tracking if expected flow disturbances were known to be significantly reduced (while maintaining some maximum allowable load transient magnitude and frequency).

8.4 Recommendations for Future Work

The following recommendations for future work are based on field testing experience and considerations of time varying components of the plant. Note that while quantification of maximum load transient magnitude and frequency is certainly noteworthy it is not included here due to the considerable effort and time this would take at such an early stage of control system development.

8.4.1 Quantify Range of Turbulence Levels

Further studies into turbine speed controller design should begin with a study to quantify the range of expected turbulence levels and frequencies in real installation sites. This is a very important design variable that can be taken into account in the design process. This directly affects the required control response characteristics for a given reference tracking specification and modifies the allowable trade-off for load transient response (potentially allowing much better closed loop response characteristics than demonstrated in the present work).

8.4.2 Generate, Verify and Validate a Higher Order Model

The system model used for simulations in the present work was first order; based on equilibrium performance information; and not validated with test data. Preliminary open loop field tests verified that the model was reasonable, but a more sophisticated higher order model for simulation based testing that incorporates the effects of drive system spring constants, damping characteristics, dynamic flow effects and mooring system dynamics, is most definitely required.

8.4.3 Revise Control Problem Setup

The H_∞ LPV control synthesis procedure allows explicit incorporation of model uncertainty. This powerful ability allows foreknowledge of structured and unstructured uncertainty to be included directly in the synthesis procedure. Though this information about the plant was not available at the time of this work, it can be attained at a relatively small price with some additional testing and analysis.

A design iteration to include flow disturbances in the cost function should also be carried out. This should allow for rejection of both random turbulent flow disturbances as well as the near sinusoidal hydraulic torque pulsations which occur at the blade passing frequency (due to the way in which the angle of attack varies with angular position of the rotor). Explicit incorporation of these transfer matrices in the cost function to minimize the effect of these disturbances could significantly reduce power oscillations in the system output as well as smooth load transients.

8.4.4 Reduce Required Instrumentation

The feedback variable in the H_∞ LPV control scheme is the turbine rotational speed. In this work, the electric generator rpm is taken as an estimate of the rotor speed. Due to the special requirements of hydrokinetic turbine system components, it may be convenient to place the control hardware close to the power conversion hardware. For instance, if the field testing in this research project utilized a grid tied load, the power conversion hardware would need to be placed as close as possible to the grid connection point to minimize voltage drops on the fixed voltage output of the power converter. For the Pointe du Bois test site, this would have been approximately 130 m from the generator. This is a long way to run instrumentation signals for turbine and flow speed measurements (other turbine sites could be much worse). Though the technology to run these signals exists in the form of current loops or wireless information transfer, the added cost of cabling and other hardware may add significant cost and reliability issues. Locating the control hardware with the Power conversion equipment would also reduce the enclosure requirements of the control hardware (and have allowed testing to be

carried out indoors instead of the cold rain for this particular project). To facilitate this, two methods have been identified (and others may exist). First, a small circuit could be constructed to generate the turbine speed information from the frequency of the generator output (as noted from [72]) at the conversion hardware (this frequency is directly proportional to the turbine rpm through the gearbox ratio and generator pole count). Second, a new technology exists that would transfer the rpm signal over the generator output line, but would require coder/decoder hardware/software that may be prohibitively expensive (thus option 1 may be better suited to this application).

The second signal required for the controller is the flow speed information. While this is not used in the feedback scheme, the real-time measurement is required for scheduling of the controller. To facilitate placement of the control hardware as already outlined, a flow speed estimator should be developed to remove the need for a sensor. Some work on this topic has been noted in [15] and [28]. Note that two significant implementation problems associated with flow measurement would also be solved. First, a point measurement of the complex, three-dimensional, time varying flow field passing through the rotor is an extremely poor representation of the flow variable in this problem. Second, a robust flow velocity measuring device for water does not yet exist off-the-shelf. It takes a small amount of debris to damage the sensor or change its sensitivity characteristics (such as a small weed stuck to the measurement element) rendering it useless and resulting in unexpected turbine operation.

8.4.5 Revise Turbine Speed Reference Generator

The turbine speed reference generator used for maximum power tracking and constant power output in the present work, produced an excessively noisy signal. This was due to the superior response characteristics of the flow velocity meter and unfiltered signal used to generate the rpm reference signal. If a similar reference generator is to be used for future testing, the velocity signal should be passed through a low pass filter to remove the high frequency turbulence components.

Other methods to generate this reference may be superior to the constant tip speed ratio method such as using a real power measurement instead of the generator speed measurement (*Voltage*Current*, taken off the DC buss of the converter, easily employed through the use of current transformers) and knowledge of the ideal power curve (attained from performance data). This should be investigated more thoroughly and is an excellent project for future development work.

An adaptive reference generator accounting for temporal variations in the plant such as biofouling of hydrofoils, ambient temperature changes, etc (as previously discussed), would also be extremely beneficial. Some starting points for these methods are identified in [38] and [95], and would serve as an excellent jump off point for further development work.

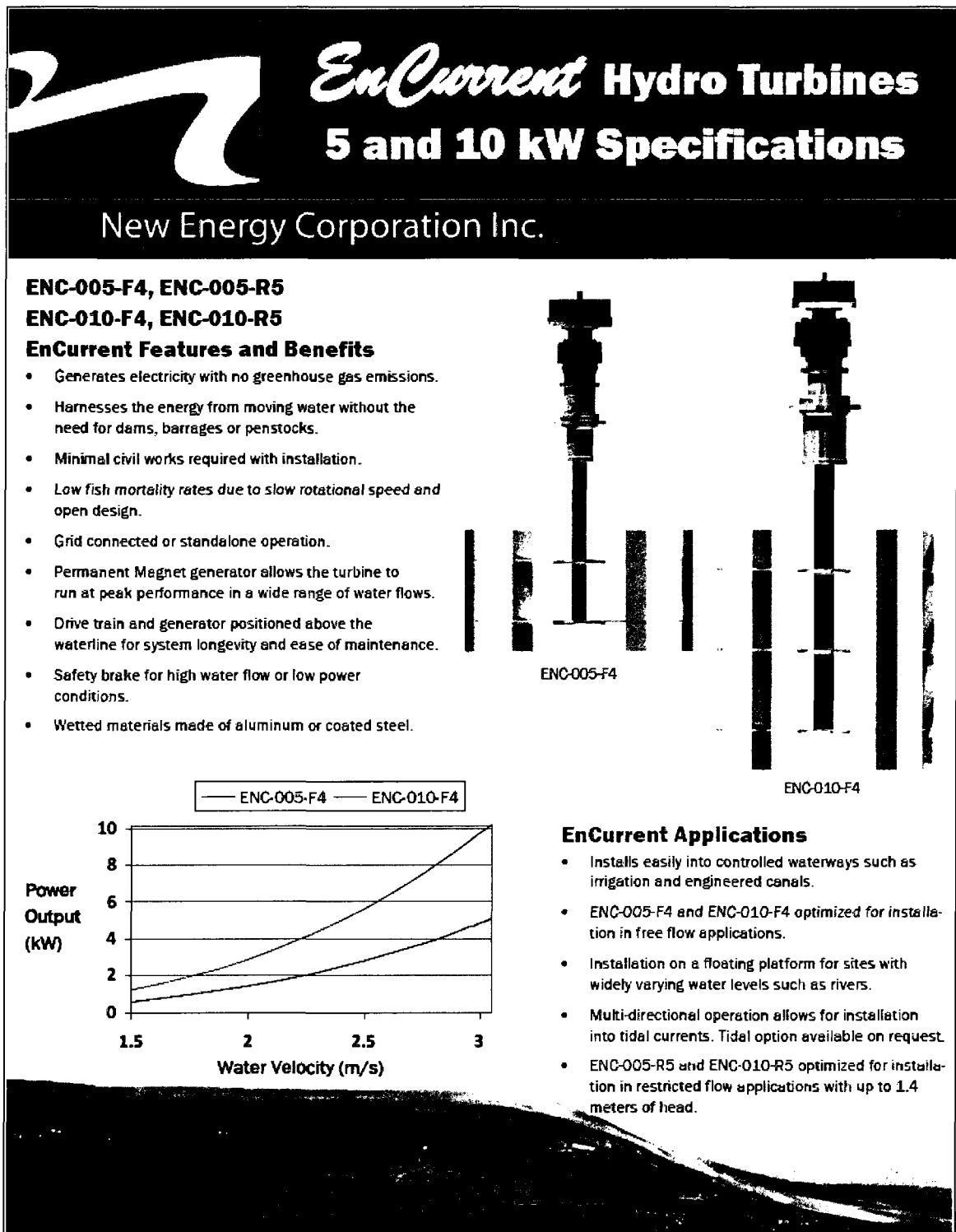
Finally, it has been demonstrated in [61] that increasing the tip speed ratio at which power is extracted increases the overall energy capture during operation in turbulent flows. This is more prominent for systems with asymmetrical power coefficient curves and radical drop of efficiency as the tip speed ratio is reduced (when experiencing turbulent deviations in the tip speed ratio value). A method to incorporate this into the

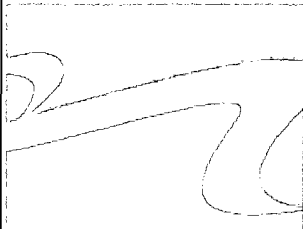
reference generator could significantly increase the average energy extraction for this type of hydrokinetic turbine, thus reducing the cost of electricity in turbulent locations.

8.4.6 Field Testing for Power Regulation

The range of flow velocities at the Pointe du Bois test site did not allow testing of the power regulation functionality built into this control system. Future work should test and make modifications as required. If more time had been allowed for testing (or if fewer problems had been encountered) it was planned to carry out power regulation testing with the existing test platform by using a lower programmed *rated power*, corresponding to a value just below that supported by the range of flows at the test site. However it would be more beneficial if a site with flows exceeding that corresponding to the rated power (3 m/s) could be located.

APPENDIX A: TEST TURBINE SPECIFICATION





Sustainable Hydropower

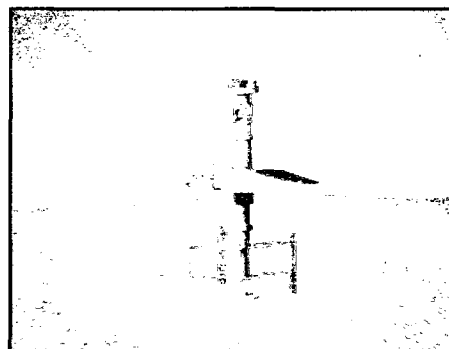
New Energy Corporation Inc.

Characteristic	ENC-005-F4	ENC-005-R5	ENC-010-F4	ENC-010-R5
Maximum Power Output	5 kW	5 kW	10 kW	10 kW
Water Velocity at Max Power	3 m/s	3 m/s*	3 m/s	3 m/s*
Rotor speed at Max Power	90 RPM	74 RPM	90 RPM	74 RPM
Overall System Mass	340 kg	360 kg	640 kg	670 kg
Overall System Height	2.25 m	2.25 m	3.14 m	3.14 m
Rotor Diameter	1.52 m	1.52 m	1.52 m	1.52 m
Rotor Height	0.76 m	0.76 m	1.52 m	1.52 m
Number of Blades	4	5	4	5
Distance from top of rotor to:				
Center of Bottom Bearing	0.467 m	0.467 m	0.467 m	0.467 m
Mounting Surface	0.654 m	0.654 m	0.751 m	0.751 m
Gearbox Ratio	13.5:1	13.5:1	19.85:1	23.97:1
Generator Output	0-198 V	0-165 V	0-287 V	0-285 V

* For the ENC-005-R5 and ENC-010-R5 the water velocity is based on the ambient water velocity and head differential.

Inverters

- For standalone applications, the 5 kW Turbines use one (1) off-grid inverter. The 10 kW Turbines use one (1) off-grid inverter and one (1) grid-tie inverter.
- For grid-tie applications the 5 kW Turbines use one (1) grid-tie inverter. The 10 kW Turbines use two (2) grid-tie inverters.
- Country and region specific inverters are available for adherence to local electrical codes. For more information on your area, contact sales at New Energy Corporation Inc.



<http://www.newenergycorp.ca>

New Energy Corporation Inc.

e sales@newenergycorp.ca

t 403.260.5248

Suite 473, 3353-31st Street NW

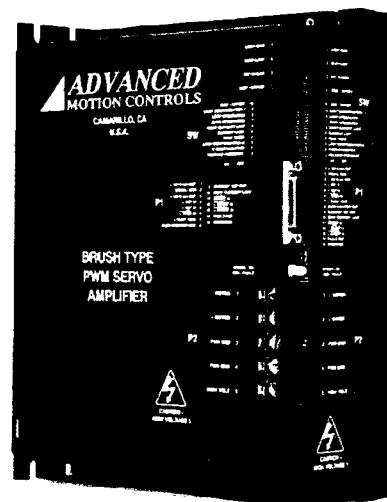
Calgary, AB, Canada, T2L 2K7

APPENDIX B: PWM AMPLIFIER SPECIFICATION

SERIES 100A SERVO AMPLIFIERS MODELS: 100A25, 100A40

FEATURES:

- Surface-mount technology
- Small size, low cost, ease of use
- Optical isolation, see block diagram
- DIP switch selectable: current, voltage, velocity, IR compensation, analog position loop
- Four quadrant regenerative operation
- Agency Approval:



BLOCK DIAGRAM:

POWER STAGE SPECIFICATIONS	MODELS	
	100A25	100A40
DC SUPPLY VOLTAGE	60 - 250 V	60 - 400 V
PEAK CURRENT (2 sec. max., internally limited)	+ 100 A	+ 100 A
MAXIMUM CONTINUOUS CURRENT (internally limited)	± 50 A	± 50 A
MINIMUM LOAD INDUCTANCE*	300 µH	600 µH
SWITCHING FREQUENCY	14.5 kHz ± 15%	
HEATSINK (BASE) TEMPERATURE RANGE	0 °C to +65 °C; disables if > 65 °C	
POWER DISSIPATION AT CONTINUOUS CURRENT	625 W	1000 W
OVER-VOLTAGE SHUT-DOWN (self-reset)	260 V	420 V
BANDWIDTH (load dependent)	2.5 kHz	

MECHANICAL SPECIFICATIONS	
POWER CONNECTOR: P2	Screw terminals
SIGNAL CONNECTOR: P1	P1 is a 15 pin female low density D-sub connector
SIZE	9.25 x 7.21 x 3.64 inches 235.0 x 183.2 x 92.4 mm
WEIGHT	7.5 lb. 3.41 kg

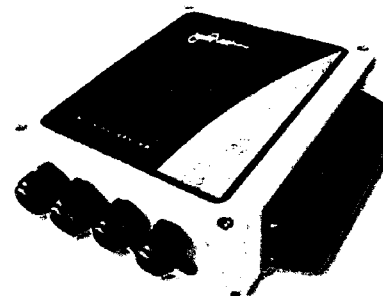
APPENDIX C: THREE PHASE RECIFIER AND FILTER SPECIFICATION

GENERAL SPECIFICATIONS PVI-WIND-INTERFACE

Wind Interface Box

The Power-One Aurora Wind Interface Box represents an application of the successful Aurora inverter to small wind applications. The compact wind interface box is designed for a grid-connected application. The Aurora inverter can be configured to an OEM's specific MPPT power curve.

The model PVI-Windbox is used in combination with the Aurora Wind Inverter.



Wind Interface Box

AURORA[®] Wind Interface Features

- Conversion efficiency at rating: 99.4%
- 3-Phase input from PMG
- High output power at full rating 7200W
- Fused wind input
- Automatic brake function above 530 Vdc
- External brake resistor options

Description	Parameter
Input Voltage Range (no damage)	0 to 400 VAC
Operating Input Voltage range from PMG (permanent Magnet Generator)	40-400Vac / 0-600Hz
Max. Operating Input Current	16.6A RMS
Input Overcurrent (fuse protected)	20A RMS
Max. Output Power (400 VAC PFC>0.7)	7200W
Output Voltage Range (operating)	50-600 Vdc
Automatic Brake Function	>530 Vdc
Efficiency (>400 VAC, PFC>0.7)	99.4%
DC Output Voltage Range	0-600 Vdc
Max. Current in the Brake Resistor	30 A
Operating Ambient Temperature	-25°C to +55°C
Enclosure Type	NEMA 4X
Relative Humidity	0-100% condensing
Audible Noise	<40 dBA
Size (height x width x depth)	29 x 26 x 9.5 (mm)

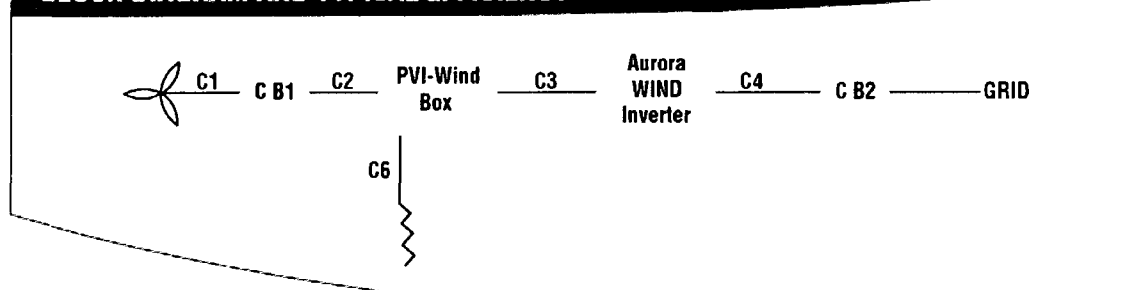
MODEL SUMMARY

Model Number	Power
PVI-7200-WIND-INTERFACE	7200W
PVI-4000-WIND-INTERFACE	4000W
PVI-2500-WIND-INTERFACE	2500W

STANDARDS AND CODES

The WIND-INTERFACE BOX comply with standards set for grid-tied operation, safety and electromagnetic compatibility including: UL1741 and CSA C22.2 No.107.1-01

BLOCK DIAGRAM AND TYPICAL EFFICIENCY



APPENDIX D: ELECTRICAL LOAD SPECIFICATION

Avtron Edgewound Resistors

Avtron Dynamic Braking Resistor Ratings:

Rating: 25 Amps (15kW) Continuous

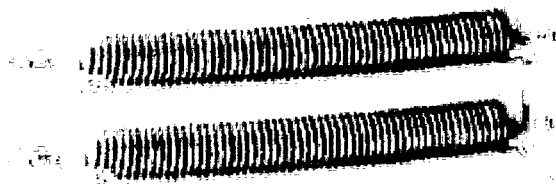
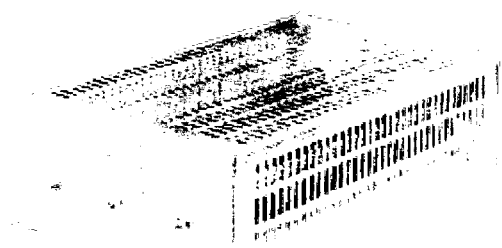
Resistance: 24 Ohms (+5,-5%)

Resistor Type: Avtron Edgewound Resistors (Type AER)

Enclosure Type: NEMA 1, indoor, screened

Dimensions (Approximate): 26.5"L x 16"W x 10"H **Weight:** 60 pounds

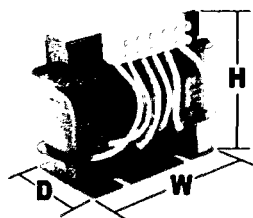
Avtron Part Number: 9 AER7-26-30S



RL Line/Load Reactors

MTE
AN RL POWER ELECTRONICS COMPANY

MTE
CORPORATION



RLC
REACTOR

RL-01801
RL-01801

MTE Line Reactors

ITEM # RL-01801

MFG # RL-01801

Series GUARD-AC

REACTOR, 18A, 0.8mH 18 AMPS/0.8 mH

APPENDIX E: CONTROL HARDWARE

CompactRIO High-Performance Real-Time Controllers

NI cRIO-9012, NI cRIO-9014 *NEW!*

- Small and rugged embedded real-time controllers
- Execution target for NI LabVIEW Real-Time applications
- Reliable and deterministic operation for stand-alone control, monitoring, and logging
- 400 MHz Freescale MPC5700 real-time processor
- -40 to 70 °C operating temperature range

Operating System

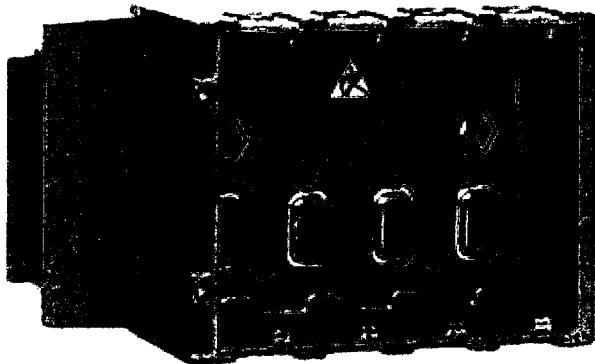
- LabVIEW Real-Time (VxWorks)

Driver Software

- NI-RIO for reconfigurable embedded systems



Product	DRAM Memory (MB)	Internal Nonvolatile Storage (MB)	10/100BaseT/TX Ethernet Port	RS232 Serial Port	USB Port	LEDs	DIP Switches	Power Supply Input Range	Power Consumption	Backup Power Input	Remote Panel Web Server	FTP Server
cRIO-9012	64	128	✓	✓	✓	4	5	9 to 26 VDC	6 W max	✓	✓	✓

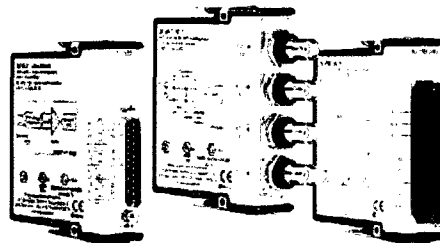


Type of Chassis	Reconfigurable Embedded System	R Series Expansion System
Standard real-time	cRIO-9101 4-slot 1 M gate RIO chassis	PXI-7831R or PXI-7811R, and

C Series Analog Input Modules

NI 9201, NI 921x, NI 9221, NI 923x

- Signal conditioning for high voltage (± 60 V), thermocouples, RTDs, accelerometers, microphones, strain gages, current inputs
- Advanced features such as smart TEDS sensor capability, antialiasing filters, open-thermocouple detection
- ± 80 mV, ± 10 V, or ± 60 V analog input ranges
- 12-, 16-, or 24-bit (delta-sigma) resolution
- Up to 800 kS/s multiplexed or up to 100 kS/s simultaneous-sampling analog-to-digital converter (ADC)
- Up to 32 channels per module
- Up to 2,300 V_{rms} isolation (withstand), up to 250 V_{rms} isolation (continuous)
- NIST-traceable calibration certificate for guaranteed accuracy



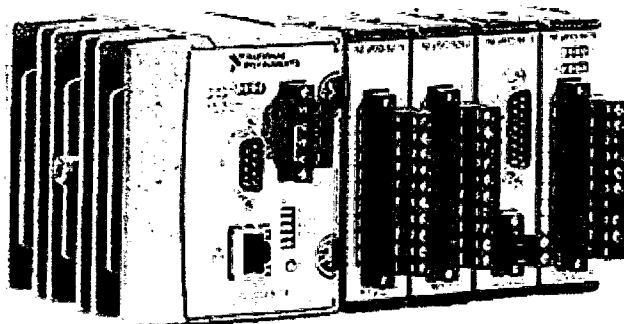
Model	CompactRIO	NI CompactDAQ	Signal Type	Channels	Resolution (bits)	Max Sampling Rate (S/s)	Signal Input Ranges	Simultaneous Sampling	Antialiasing Filters	Isolation	Connector Options
NI 9215	✓	✓	Voltage	4	16	100 k/ch	± 10 V	✓	-	✓	Screw Terminal, BNC

C Series Analog Output Modules

Product	Compatibility		Signal Type	Channels	Resolution (bits)	Max Update Rate (S/s)	Range	Current Drive	Simultaneous Updating	Isolation	Connector Options
	CompactRIO	NI CompactDAQ									
NI 9263	✓	✓	Voltage	4	16	100 k/ch	± 10 V	1 mA/ch	✓	✓	Screw Terminal

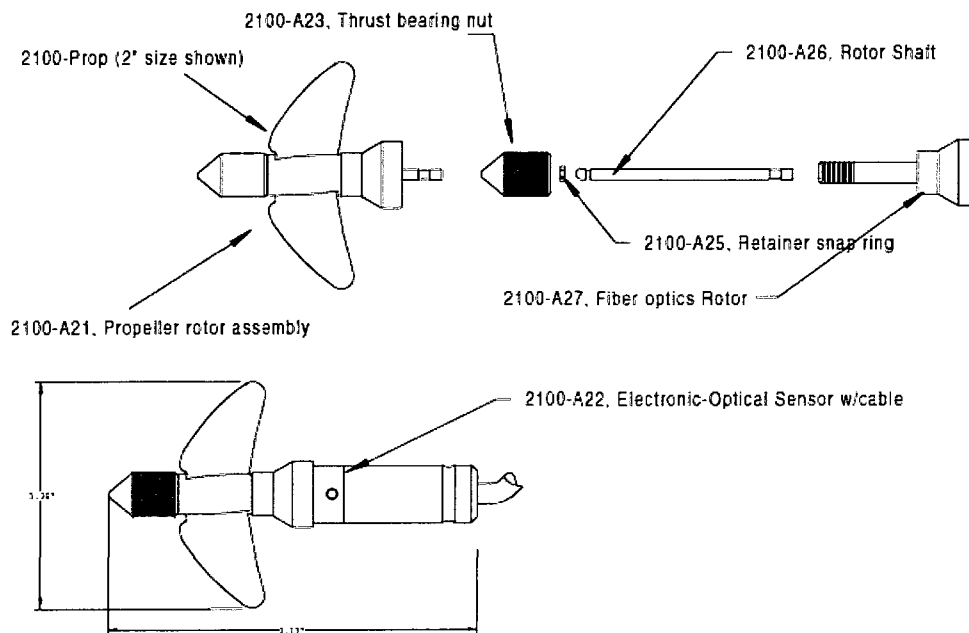
C Series Digital Input and Counter/Timer Modules

Product	CompactRIO	NI CompactDAQ	Logic	Channels	Source/Sink	I/O Delay Time	Signal Levels	Isolation	Connector Options
NI 9411	✓	✓	Differential or 5V/TTL	6	-	500 ns	± 5 to ± 24 V	✓	D-Sub



APPENDIX F: INSTRUMENTATION SPECIFICATION

Swoffer Instruments Model 2100 Current meter



MODEL 2100 CURRENT METER SPECIFICATIONS *

VELOCITY RANGE	0.1 to 25 Feet Per Second (0.03 to 7.5 Meters Per Second)
DISPLAY	4 digit, Liquid Crystal Digital, 0.7" digits
RESOLUTION	To hundredths, both feet and meters.
ACCURACY	Can be held to within 1% with periodic <u>user-required</u> calibration tests and adjustments.
DISPLAY AVERAGING	Three selectable averaging times: 5, 20 and 90 seconds-FPS mode. 1.5, 6 and 30 seconds-MPS mode.
OPERATING TEMPERATURE	LCD Min. -14° F (-25.6°C) Max. 180°F (82°C) @ 15% humidity Max. 120°F (49°C) @ 95% humidity Sensor Min. 0° F (-17.8°C) Max. 300° F (149°C)
SENSOR TYPE	PHOTO-FIBER-OPTIC two-conductor electrical with all electronics permanently encapsulated in epoxy resin.

Magnetic Sensors Corp Hall Sensor

REVISIONS			
LTR	DESCRIPTION	DATE	APPROVD
-	PRELIMINARY RELEASE	4.19.86	D.P.
-	PRODUCTION RELEASE	1.2.87	S.C.
A	REVISED PER ECO 1859	11.19.02	

SCHEMATIC

GEAR PITCH vs AIRGAP

SENSOR

TARGET GEAR

SCOPE

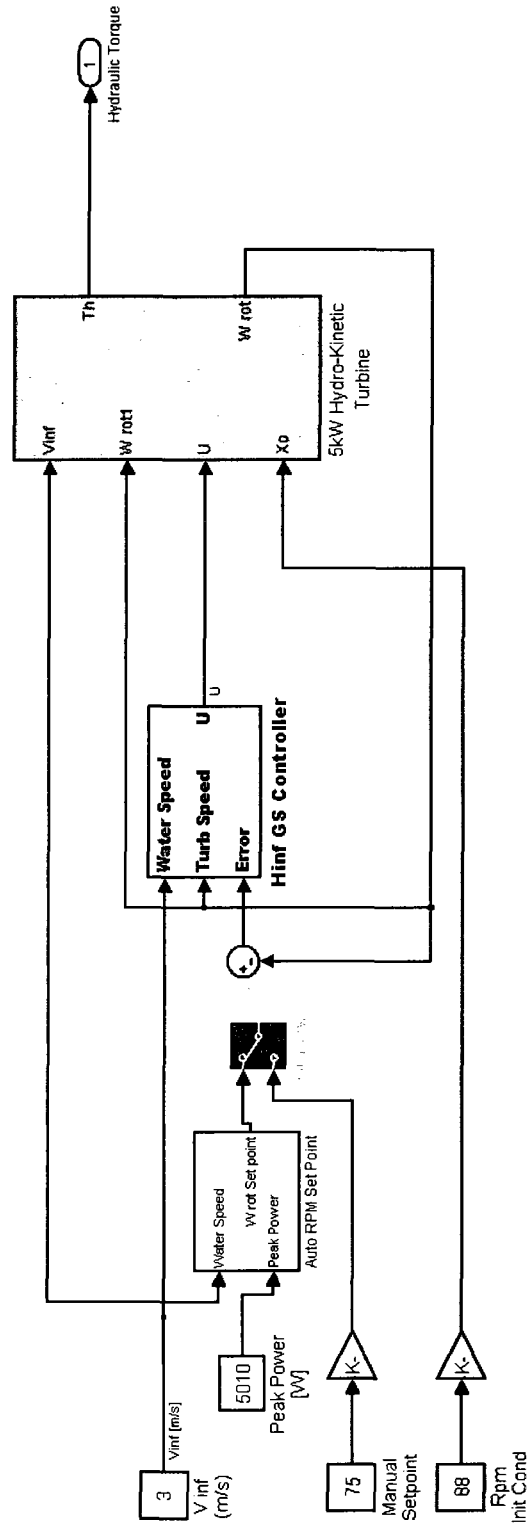
SPECIFICATIONS:

- INPUT VOLTAGE: Vcc: +4.5 TO 24 VDC.
- INPUT CURRENT: Icc: 10 mA TYP, 20 mA MAX.
- OUTPUT: OUTPUT IS AN OPEN COLLECTOR NPN WITH INTERNAL 4.7K OHM PULL UP.
- OUTPUT CURRENT: 20 mA MAX, SINKING.
- TARGET WHEEL: 10 PITCH, FERROUS, .150 x .150 TOOTH.
- SPEED RANGE: 0-10,000 R.P.M. (FOR ≤ 46.00)
- AIRGAP: SEE GRAPH, INSPECT AT .110.
- OPERATING TEMPERATURE: -20°C TO 140°C.
- VIBRATION: 15G, 10-2000 Hz
- HUMIDITY, STEADY STATE: 85% RH WITH CONDENSATION.
- DIELECTRIC STRENGTH: 150 VRMS

12 THE PROBE ROTATIONAL MARK MUST POINT IN THE PLANE OF THE GEAR. GEAR ROTATION CAUSING TEETH TO ADVANCE TOWARD THE REFERENCE MARK TO BE REFERRED TO AS THE FORWARD DIRECTION OF ROTATION.

MAGNETIC SENSORS CORPORATION 1355 AL HANSON STREET MARIETTA, GA 30066	
HALL EFFECT ZERO SPEED SENSOR	
SCALE CODE	ORDERING NO.
B	0LVP6
SCALE: NONE	SK10468
SHEET 1	OF 1

APPENDIX G: SIMULINK CODE



References

- [1] Abo-Khalil A.G., D-C Lee, and J-K Seok, "Variable speed wind power generation system based on fuzzy logic control for maximum output power tracking", *Proceedings of 2004 IEEE 35th Annual Power Electronics Specialists Conference*, 2004, vol 3, pp 2039-2043.
- [2] "Amesbury Tidal Energy Project (ATEP): Integration of the Gorlov Helical Turbine into an Optimized Hardware/Software System Platform, Final Report", *Prepared by Verdant Power and GCK Technology Inc. Rev 07.26.2005 for the Massachusetts Technology Collaborative*, 2005.
- [3] Apkarian, P., and R. Adams, "Advanced gain-scheduling techniques for uncertain systems", *IEEE Transactions on Control Systems Technology* 1998, 6(1), 21-32.
- [4] Apkarian, P., P. Gahinet, and G. Becker, "Self-scheduled H_∞ control of linear parameter-varying systems: a design example", *Automatica*, 1995, 31(9), 1251-1261.
- [5] Åström, K. J., B. Wittenmark, *Adaptive control, 2nd edn.* Addison-Wesley, 1995, ISBN: 0201558661.
- [6] Batten, W.M.J., A.S. Bahaj, A.F. Molland, and J.R. Chaplin, "Hydrodynamics of marine current turbines", *Renewable Energy*, Feb. 2006, 249-56.
- [7] Batten, W.M.J., A.S. Bahaj, A.F. Molland, and J.R. Chaplin, "Experimentally validated numerical method for the hydrodynamic design of horizontal axis tidal turbines", *Ocean Engineering*, May 2007, p 1013-1020.
- [8] Becker, G., and A. Packard, "Robust performance of linear parametrically varying systems using parametrically-dependent linear feedback", *System and Control Letters*, 1994, p 205-215.

- [9] Bedard, R., M. Previsic, O. Siddiqui, G. Hagerman, and M. Robinson, "Survey and Characterization: Tidal In Stream Energy Conversion (TISEC) Devices", *Technical Report : EPRI-TP-004 NA prepared for the Electric Power Research Institute*, 2005.
- [10] Beltran, B., T. Ahmed-Ali, M. El Hachemi Benbouzid, "Sliding mode power control of variable-speed wind energy conversion systems", *IEEE Transactions on Energy Conversion*, June 2008, p 551-558.
- [11] Betz, A., *Introduction to the Theory of Flow Machines*, London: Pergomon Press, 1966.
- [12] Bianchi, F. D., H. De Battista, and R. J. Mantz, *Wind turbine control systems: principles, modelling and gain scheduling design*. Springer London, 2007, ISBN: 1846284929.
- [13] Bianchi, F.D., R. J. Mantz, and C. F. Christiansen, "Control of variable-speed wind turbines by LPV gain scheduling", *Wind Energy*, v 7, n 1, January/February, 2004, p 1-8.
- [14] Bianchi, F.D., R. J. Mantz, C. F. Christiansen, "Gain scheduling control of variable-speed wind energy conversion systems using quasi-LPV models", *Control Engineering Practice*, v 13, n 2, February, 2005, p 247-255.
- [15] Boukhezzar B., and H. Siguerdidjane, "Nonlinear Control of Variable Wind Turbines Without Wind Speed Measurement", *Proceedings of the 44th IEEE Conference on Decision and Control, and the European Control Conference, CDC-ECC '05*, 2005, p 3456-3461.
- [16] Bratcu, A. I., I. Munteanu, and E. Ceanga, "Optimal control of wind energy conversion systems: From energy optimization to multi-purpose criteria - A short

- survey”, *Mediterranean Conference on Control and Automation - Conference Proceedings, MED'08*, 2008, p 759-766.
- [17] Bratcu, A. I., I. Munteanu, and E. Ceanga, *Optimal Control of Wind Energy Systems: Towards a Global Approach*. London: Springer London, 2008, ISBN: 9781848000797.
- [18] Bruzelius, F., *Linear Parameter-Varying System: an approach to gain scheduling*, Doctor of Philosophy thesis, Department of Signals and Systems, Chalmers University of Technology, Göteborg, Sweden, 2004.
- [19] Caselitz, P., and J. Giebhardt, (2008, Nov.) “Condition Monitoring and Fault Prediction for Marine Current Turbines”, [Online]. Available: http://www.iset.uni-kassel.de/abt/FB-E/papers/Paper_CM4MCT_dl.pdf
- [20] Clean Current Power Systems Incorporated, 405 - 750 West Pender Street, Vancouver, British Columbia, Canada V6C 2T7. (2008, Nov.). [Online]. Available: <http://www.cleancurrent.com/>
- [21] Connor, B., and W. Leithead, “Investigation of a fundamental tradeoff in tracking the C_{pmax} curve of a variable speed wind turbine”, *Proceedings of the British Wind Energy Association Conference*, 1993.
- [22] Dambrosio, L., B. Fortunato, “One step ahead adaptive control technique for a wind turbine-synchronous generator system”, *Proceedings of the Thirty-Second Intersociety Energy Conversion Engineering Conference, (Cat. No.97CH36203)*, 1997, p 1970-5 vol.3.

- [23] Datta R., V. T. Ranganathan, "A method of tracking the peak power points for a variable speed wind energy conversion system", *IEEE Transactions on Energy Conversion*, 2003, 18(1):163-168.
- [24] Davis, B. V., "Water turbine model trials to demonstrate the feasibility of extracting kinetic energy from river and tidal currents," *Nova Energy Limited Report for National Research Council of Canada, Tech. Rep. NEL-002*, 1980.
- [25] Davis, B., D. H. Swan, and K. A. Jeffers, "Ultra Low Head Hydroelectric Power Generation Using Ducted Vertical Axis Water Turbines", *Report No.: NEL-022 prepared for the National Research Council of Canada Hydraulics Laboratory*, 1982.
- [26] De Battista H., P. F. Puleston, R. J. Mantz, and C.F. Christiansen, "Sliding mode control of wind systems with DOIG – Power efficiency and torsional dynamics optimization", *IEEE Transactions on Power Systems*, 2000a, 15(2):728-734
- [27] Dengying and Zhoujie, "LPV H-infinity Controller Design for a Wind Power Generator", *2008 IEEE International Conference on Robotics, Automation and Mechatronics, RAM 2008*, 2008, p 873-878
- [28] Ekelund, T., *Modelling and Linear Quadratic Optimal Control of Wind Turbines*, PhD. Thesis, Chalmers University of Technology, 1997.
- [29] Faure, T. D., "Experimental Results of a Darrieus Type Vertical Axis Rotor in a Water Current", *Technical Report for the National Research Council of Canada, Tech. Rep. TR-HY-005, NRC No. 23192*, 1980.
- [30] Fraser, R., C. Deschenes, C.O'Neil, and M. Leclerc, "VLH: Development of a New Turbine for Very Low Head Sites", conference proceedings, *Waterpower XV*, 2007, paper number 157.

- [31] Freeman, F. B., and M. J. Balas, Direct Model-Reference Adaptive Control of Variable Speed Horizontal-Axis Wind Turbines”, *Wind Engineering*, 1998, v 22, p 209-218.
- [32] Gahinet, P., A. Nemirovski, A. J. Laub, and M. Chilali, “LMI control toolbox”, *The Mathworks, Inc.*, 1995.
- [33] Gretton, G. I., and T. Bruce, “Aspects of Mathematical Modelling of a Prototype Scale Vertical-Axis Turbine”, *Proceedings of the 7th European Wave and Tidal Energy Conference, Porto, Portugal, 2007*
- [34] Gu, D. –W., P. Hr. Petkov, and M. M. Konstantinov, *Robust Control Design with MATLAB*. Springer London, 2005, ISBN: 978-1-85233-983-8.
- [35] Hassen, S. Z. Sayed, *Robust and Gain-Scheduled Control Using Linear Matrix Inequalities*, Master of Engineering thesis, Electrical and Computer Systems Engineering, Monash University Australia, 2001.
- [36] Heier, H., *Grid Integration of Wind Energy Conversion Systems*. West Sussex, London, England: Wiley and Sons Ltd, 2006, ISBN: 0470868996.
- [37] Hilloowala R.M., A. F. Sharaf, “A utility interactive wind energy conversion scheme with an asynchronous DC link using a supplementary control loop”, *IEEE Transactions on Energy Conversion*, 1994, 9(3):558-563.
- [38] Johnson, K. E., “Adaptive Torque Control of Variable Speed Wind Turbines”, *Technical Report NREL/TP-500-36265, National Renewable Energy Laboratory, Colorado, U.S.A.*, 2005
- [39] Kalantar, M., Sedighizadeh, M., “Adaptive-neural PID control of wind energy conversion systems using wavenets”, *Proceedings of the 20th IEEE International*

- Symposium on Intelligent Control, ISIC '05 and the 13th Mediterranean Conference on Control and Automation, 2005, p 219-224.*
- [40] Kar, N.C., and H. M. Jabr, “A novel PI gain scheduler for a vector controlled doubly-fed wind driven induction generator”, *Proceedings of the Eighth International Conference on Electrical Machines and Systems* (IEEE Cat. No. 05EX1137), 2005, 948-53 Vol. 2.
- [41] Kassel, G., and J. Kesterman, “SeaFlow: Worlds first pilot project for the exploitation of marine currents at a commercial scale”, *Report for the European Commission #:21616*, 2005, ISBN: 92-894-4593-9.
- [42] Khan, M. J., personal communication, June 2007.
- [43] Khan, M. J., M. T. Iqbal, and J.E. Quaicoe, “A Technology Review and Simulation based Performance Analysis of River Current Turbine Systems”, *2006 Canadian Conference on Electrical and Computer Engineering, 2007*
- [44] Khan, M. J., M. T. Iqbal, and J.E. Quaicoe, “Design Considerations of a Straight Bladed Darrieus Rotor for River Current Turbines”, *IEEE International Symposium on Industrial Electronics, v 3, International Symposium on Industrial Electronics, 2006.*
- [45] Kirke, B. (2008, Nov.) “Developments in ducted water current turbines”, tidal paper 16-08-03 1. [Online]. Available: <http://www.cyberiad.net/tide.htm>
- [46] Klimas, P. C., J. F. Jr. Sladky, “Vertical Axis Wind Turbine Power Regulation Through Centrifugally Pumped Lift Spoiling”, Pergamon Press, v 4, 1986, p 2142-2146.

- [47] Köse, I. E., *Robust H_∞ Control of Linear Parameter Varying Systems*, Doctor of Philosophy thesis, Mechanical and Aerospace Engineering, University of California at Irving, 1997.
- [48] Lautier, P., H. J. Ndjana, M. Leclerc, and C. O'Neil, "Improved Operation and Power Production of a Very Low Head Hydraulic Turbine", conference proceedings, *Waterpower XV*, paper number 161
- [49] Lavoie, L., P. Lautier, "Nonlinear predictive power controller with constraint for a wind turbine system", *IEEE International Symposium on Industrial Electronics*, 2006, p 124-9.
- [50] Leith, D.J., W. E. Leithead, "Performance enhancement of wind turbine power regulation by switched linear control", *International Journal of Control*, v 65, n 4, 10 1996, p 555-72.
- [51] Leith, D. J., and W. E. Leithead, "Appropriate realization of gain-scheduled controllers with application to wind turbine regulation", *International Journal of Control*, 1996, 65:2, 223 – 248.
- [52] Leithead, W. E., and B. Connor, "Control of Variable Speed Wind Turbines: Design Task", *International Journal of Control*, 2000, 73:13, 1189 – 1212.
- [53] Leithead, W.E., M. J. Grimble, S. A. De La Salle, and D. Reardon, "Wind turbine modeling and control", *Industrial Control Unit, University of Strathclyde, Report prepared for UK Department of Energy*, 1989.
- [54] Leithead, W. E., D. J. Leith, F. Hardan, H. Markou, "Global gain-scheduling control for variable speed wind turbines", *Proceedings of European Wind Energy Conference, EWEC '99*, 1999.

- [55] Leithead, W.E., S. de la Salle, D. Reardon, "Role and objectives of control for wind turbines", *IEE Proceedings, Part C: Generation, Transmission and Distribution*, v 138, n 2, 1991, p 135-148
- [56] Lescher, F., J. Zhao, and P. Borne, "Robust gain scheduling controller for pitch regulated variable speed wind turbine", *Studies in Informatics and Control*, v 14, n 4, 2005, p 299-315.
- [57] Lescher, F., H. Camblong, O. Curea, and R. Briand, "LPV Control of Wind Turbines for Fatigue Loads Reduction using Intelligent Micro Sensors", *Proceedings of the 2007 American Control Conference*, New York City, USA, July 11-13, 2007.
- [58] Ma, X., *Adaptive Extremum Control and Wind Turbine Control*, Doctor of Philosophy Thesis, Technical University of Denmark, Lyngby Denmark, 1997.
- [59] Marine Current Turbines Ltd, The Court, The Green Stoke Gifford, Bristol, BS34 8PD, UK. (2008, Nov.). [Online]. Available: <http://www.marineturbines.com/>
- [60] Mattarolo, G., J. Bard, P. Caselitz, and J. Giebhardt, "Control and Operation of Variable Speed Marine Current Turbines. Results from a Project funded by the German Ministry for the Environment", in *Proc Owemes*, 2006.
- [61] McIntosh, S.C., H. Babinsky, T. Bertenyi, "Optimizing the energy output of vertical axis wind turbines for fluctuating wind conditions", *Collection of Technical Papers - 45th AIAA Aerospace Sciences Meeting*, v 23, 2007, p 16202-16214
- [62] Muhando, E. B., T. Senjyu, N. Urasaki, A. Yona, H. Kinjo, T. Funabashi, "Gain scheduling control of variable speed WTG under widely varying turbulence loading", *Renewable Energy*, v 32, n 14, November, 2007, p 2407-2423.

- [63] Muljadi, E., K. Pierce, and P. Migliore, "Control Strategy for Variable-Speed, Stall-Regulated Wind Turbines", *National Renewable Energy Laboratory*, Technical Report NREL/CP-500-24791, April 1998.
- [64] Munteanu, I., A. I. Bratcu, and E. Ceanga, "Wind turbulence used as searching signal for MPPT in variable-speed wind energy conversion systems", *Renewable Energy*, Jan 2009, p322-326.
- [65] New Energy Corporation Inc. (NECI), Suite 473, 3553 31 Street NW, Calgary, Alberta, T2L 2K7. (2008, Nov.). [Online]. Available: <http://www.newenergycorp.ca>
- [66] Novak, P., and T. Ekelund, "Modelling, Identification and Control of a Variable Speed HAWT", *Proceedings of the European Wind Energy Association Conference*, Thessaloniki, Greece, 1994, p 441- 446.
- [67] Ohtsubo, K., H. Kajiwara, "LPV technique for rotational speed control of wind turbines using measured wind speed", *Oceans '04 MTS/IEEE Techno-Ocean '04* (IEEE Cat. No.04CH37600), 2004, p 1847-53 Vol.4.
- [68] Østergaard K. Z., P. Brath, and J. Stoustrup, "Gain-scheduled Linear Quadratic Control of Wind Turbines Operating at High Wind Speed", *16th IEEE International Conference on Control Applications Part of IEEE Multi-conference on Systems and Control Singapore*, October 2007, p 1-3.
- [69] Østergaard K. Z., P. Brath, and J. Stoustrup, "Linear Parameter Varying Control of Wind Turbines Covering Both Partial Load and Full Load Conditions", *International Journal of Robust and Nonlinear Control*, v 19, n 1, 2009, *Wind turbines: New challenges and advanced control solutions*, p 92-116

- [70] Pierce, K. G., P. G. Migliore, “Maximizing Energy Capture of Fixed-Pitch Variable-Speed Wind Turbines”, presented at the *38th AIAA Aerospace Sciences Meeting and Exhibit*, Reno, Nevada, 2000.
- [71] Ponta, F., and G. S. Dutt, “An Improved Vertical-axis Water-Current Turbine Incorporating a Channelling Device”, *Renewable Energy*, v 20, Issue 2, June 2000, p 223-241.
- [72] Power One Inc., 740 Calle Plano Camarillo, California, CA 93012, USA. (2008 Nov.). [Online]. Available: <http://www.power-one.com/>.
- [73] Rocha, R., L.S. Martins Filho and M. V. Bortolus, “Optimal Multivariable Control for Wind Energy Conversion System – A comparison between H₂ and H_∞ controllers”, *Proceedings of the 44th IEEE Conference on Decision and Control*, and *the European Control Conference 2005 Seville, Spain*, 2005, p 7906 – 7911.
- [74] Rugh, W. J., “Analytical framework for gain scheduling”, *Control Systems Magazine*, IEEE Volume 11, Issue 1, Jan. 1991 Page(s):79 – 84.
- [75] Schiemenz, I., M. Stiebler, “Control of a permanent magnet synchronous generator used in a variable speed wind energy system”, *IEEE International Electric Machines and Drives Conference*, 2001, pp 872-877.
- [76] Schonborn, A., and M. Chantzidakis, “Development of a hydraulic control mechanism for cyclic pitch marine current turbines”, *Renewable Energy*, 2007, p 662–679.
- [77] Setoguchi, T., N. Shiomi, and K. Kaneko, “Development of a Two-Way Diffuser for Fluid Energy Conversion System”, *Renewable Energy*, v 29, n 10, 2004.

- [78] Sharkh, S. M., D. Morris, S. R. Turnock, L. Meyers, and A. S. Bahaj, "Performance of an Integrated Water a Turbine PM Generator", *International Conference on Power Electronics, Machines and Drives (IEE Conf. Publ. No.487)*, 2002, 486-91.
- [79] Sheldahl, R. E., and P. C., Klimas, "Aerodynamic Characteristics of Seven Symmetrical Airfoil Sections Through 180-Degree Angle of Attack for Use in Aerodynamic Analysis of Vertical Axis Wind Turbines", *Sandia National Laboratories*, Albuquerque, NM, Report #: SAND80-2114 RS-8232-2/ 55556, 1981.
- [80] Shi, K.L., H. Li, "A novel control of a small wind turbine driven generator based on neural networks ", *IEEE Power Engineering Society General Meeting*, (IEEE Cat. No.04CH37567), 2004, 1999-2005 Vol.2.
- [81] Shiono , M., K. Suzuki, and S. Kiho, "An Experimental Study of the Characteristics of a Darrieus Turbine for Tidal Power Generation", *Electrical Engineering in Japan*, v 132, n 3, 2000.
- [82] Shiono, N., K. Suzuki, and S. Kiho, "Comparison of water turbine characteristics using different blades in Darrieus water Turbines used for Tidal Current Generations", *Transactions of the Institute of Electrical Engineers of Japan, Part B*, v 123-B, n 1, 2003, p 76-82.
- [83] Shiqian Wu, Joo Er Meng , Ni Maolin, and W. E. Leithead, "Fast approach for automatic generation of fuzzy rules by generalized dynamic fuzzy neural networks", *Proceedings of the 2000 American Control Conference*, 2000, 2453-7 vol.4.

- [84] Simoes M.G., B. K. Bose, and R. J. Spiegel, "Fuzzy logic based intelligent control of a variable speed cage machine wind generation system", *IEEE Transactions on Power Electronics*, 1997, 12(1):87-95.
- [85] SMA America Inc., 4031 Alvis Court Rocklin, California, CA 95677, USA. (2008 Nov.). [Online]. Available: http://www.sma-america.com/en_US.html.
- [86] Taylor, J., "Crossflow Turbine Developments & Testing Ultra-low Head Hydro Applications", *Highquest Engineering Inc. Technical Report*, DDS Contract File No.: 51SZ.23216-6-6156, 1987.
- [87] Thake, J.,(2005, Oct.) "Development, Installation and Testing of a Large-Scale Tidal Current Turbine", [Online]. Available: <http://www.berr.gov.uk/files/file18130.pdf>.
- [88] Tuckey, A. M., D.J. Patterson, and J. Swenson, "A Kinetic Energy Tidal Generator in the Northern Territory – Results", in *Proc. IECON, IEEE*, vol. 2. 1997, p 937-942
- [89] Vachon, W. A., "Effects of Control Algorithms on Fatigue Life and Energy Production of Vertical Axis Wind Turbines", *American Society of Mechanical Engineers, Solar Energy Division (Publication) SED*, v 5, 1988, p 149-158.
- [90] Valenciaga, F., P. F. Puleston, P. E. Battaiotto and R. J. Mantz, "An adaptive feedback linearization strategy for variable speed wind energy conversion systems", *International Journal of Research Int. J. Energy Res*, 2000; 24:151-161.
- [91] Verdant Power, LLC, 4640 13th Street, North, Arlington, VA 22207, USA. (2008, Nov.). [Online]. Available: <http://www.verdantpower.com/>.

- [92] Verdant Power LLC (RITE Project), 4640 13th Street, North, Arlington, VA 22207, USA. (2009, Feb.). [Online]. Available: <http://www.verdantpower.com/what-initiative>
- [93] Wang, L. B., L. Zhang, and N. D. Zeng, "A Potential Flow 2-D Vortex Panel Model: Applications to Vertical Axis Straight Blade Tidal Turbine", *Energy Conversion and Management*, v 48, n 2, 2007, 454-61.
- [94] Wang, Q., L. Chang, "An independent maximum power extraction strategy for wind energy conversion systems", *Proceedings of the 1999 IEEE Canadian Conference on Electrical and Computer Engineering*, 1999, pp 1142-1147.
- [95] Wang Q., L. Chang, "An intelligent maximum power extraction algorithm for inverter based variable speed wind turbine systems", *IEEE Transactions on Power Electronics*, 2004, 19(5):1242-1249.
- [96] Wu, F., X. Yang, A. Packard and G. Becker, "Induced \mathcal{L}_2 -norm control for LPV systems with bounded parameter variation rates", *International Journal of Control*, 1996, 6(9-10), p 983-998.
- [97] Wu, F., X. Yang, and A. Packard, "A generalized LPV system analysis and control synthesis framework", *International Journal of Control*, 2001, 74(7), 745-759.
- [98] Xantrex Technology Inc., 8999 Nelson Way Burnaby, British Columbia, Canada V5A 4B5. (2008 Nov.). [Online]. Available: <http://www.xantrex.com/index.asp>
- [99] Xue, D., Y. Chen, and D. P. Atherton, *Linear Feedback Control: Analysis and Design with MATLAB*. Philadelphia, Society for Industrial and Applied Mathematics, 2007, ISBN: 978-0-898716-38-2.

- [100] Yin, Ming, Gengyin, Li, Ming Zhou, Chengyong Zhao, “Modeling of the wind turbine with a permanent magnet synchronous generator for integration”, *2007 IEEE Power Engineering Society General Meeting*, 2007, p 4275748.
- [101] Zhang, X., Z. Hou, and Z. Xiao, “PID Control With Fuzzy Compensation for Hydroelectric Generating Unit”, *PowerCon 2002, International Conference on Power System Technology Proceedings*, 2002.
- [102] Zhang Xin-Fang, Xu Da-Ping; Liu Yi-Bing, “Adaptive optimal fuzzy control for variable speed fixed pitch wind turbines”, *Fifth World Congress on Intelligent Control and Automation* (IEEE Cat. No.04EX788), 2004, 2481-5 Vol.3.
- [103] Zhou, K., J.C. Doyle, K. and K. Glover, *Robust and Optimal Control*. Upper Saddle River, New Jersey, Prentice Hall, 1996, ISBN: 0-13-456567-3.
- [104] Zhou, K., and J.C. Doyle, *Essentials of Robust Control*. Upper Saddle River, New Jersey, Prentice Hall, 1998, ISBN: 0-13-525833-2.